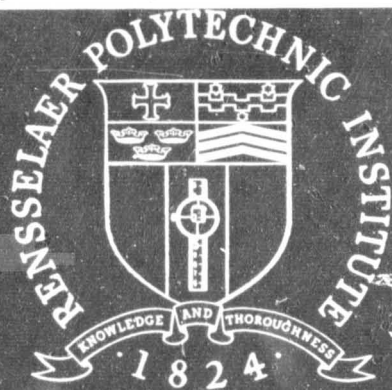


(NASA-CR-163613) A LINEAR PHOTODIODE ARRAY
EMPLOYED IN A SHORT RANGE LASER
TRIANGULATION OBSTACLE AVOIDANCE SENSOR
M.S. Thesis (Rensselaer Polytechnic Inst.,
Troy, N. Y.) 129 p HC A07/MF A01 CSCL 20E G3/37

N80-33747

Unclass
28943



Rensselaer Polytechnic Institute

Troy, New York 12181

RPI TECHNICAL REPORT MP-74

A LINEAR PHOTODIODE ARRAY EMPLOYED IN A
SHORT RANGE LASER TRIANGULATION
OBSTACLE AVOIDANCE SENSOR

by

James Paul Odenthal

A Study Supported by the
NATIONAL AERONAUTICS AND SPACE ADMINISTRATION

under

Grant NSG-7369

and by the

JET PROPULSION LABORATORY

under

Contract 954880

JPL -

School of Engineering
Rensselaer Polytechnic Institute
Troy, New York

December 1980

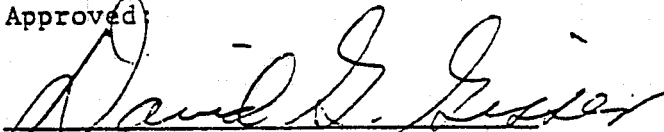
A LINEAR PHOTODIODE ARRAY EMPLOYED IN A
SHORT RANGE LASER TRIANGULATION
OBSTACLE AVOIDANCE SENSOR

by

James Paul Odenthal

A Project Submitted to the Graduate
Faculty of Rensselaer Polytechnic Institute
in Partial Fulfillment of the
Requirements for the Degree of
MASTER OF ENGINEERING

Approved:



David G. Gisser, Project Advisor

Rensselaer Polytechnic Institute
Troy, New York

December 1980

CONTENTS

	page
LIST OF FIGURES	v
ABSTRACT.	vii
1. INTRODUCTION.	1
2. DETECTOR SELECTION.	18
2.1 Detector Criteria.	18
2.2 Discrete	23
2.3 Area Arrays.	25
2.4 Linear Arrays.	28
3. 20 ELEMENT RECEIVER	33
3.1 General Description.	33
3.2 Optics	33
3.3 Array and Preamplifier Board	40
3.4 Comparator Card.	44
3.5 Digital Board.	48
4. ALIGNMENT/CALIBRATION	53
4.1 Pointing Angle, Focus, Aperture, Thresholds, Time-Window .	53
5. 20 ELEMENT RECEIVER CONCLUSION.	59
5.1 Secondary Returns.	59
5.2 Missing Returns.	59
5.3 Field of View.	62
5.4 Reliability.	62
5.5 Resolution	63
6. 1024 ELEMENT CHARGE COUPLED PHOTODIODE RECEIVER	64
6.1 General Description.	64
6.2 Optics	64
6.3 1024 Element Charge Coupled Photodiode Array	68
7. ADDITIONS/MODIFICATIONS TO RETICON DEMONSTRATION BOARD.	73
7.1 Preamp Aboard Array Board.	73
7.2 Anti-Blooming Gate	73
7.3 Peak Detectors	75
7.4 Synchronization with Mast Controller and Dark Current Limiting	75
7.5 Latches Interface to Mast FIFOs.	78
7.6 Display.	79

	page
8. 1024 CCPD RECEIVER CONCLUSION.	80
8.1 360° Vision Around Vehicle.	80
8.2 Buried Channel Charge Coupled Array	80
8.3 Improved Rangefinder.	81
9. LITERATURE CITED	86
APPENDIX A	87
APPENDIX B	93
APPENDIX C	113

LIST OF FIGURES

		page
Figure 1	Rensselaer Autonomous Roving Vehicle.	3
Figure 2a	Elevation Scanning Mast - Front View.	4
Figure 2b	Elevation Scanning Mast - Side View	5
Figure 3	Relationship between (α, β) , (Z, R)	7
Figure 4	Discrete Detectors Aboard Proposed 1984 Rover	9
Figure 5	Single Laser/Single Detector System	11
Figure 6	Vehicle Pitch, Sensor Field of View, Resolution	13
Figure 7	Laser Direction and Ranging Mast.	15
Figure 8	Multi-Laser/Multi-Detector Mast Controller.	16
Figure 9	Detector Speed, Scan Time and Angular Resolution.	20
Figure 10	Discrete Detector Scheme.	24
Figure 11	2-Dimensional Area Array Implementation	27
Figure 12	Linear Array Implementation	29
Figure 13	Detector on Mast.	34
Figure 14	Exploded View of Detector	35
Figure 15	Detector Functional Block Diagram	36
Figure 16	Geometric Optics.	38
Figure 17a	Detector Preamplifier Board	41
Figure 17b	Detector Head Layout.	42
Figure 18	Amplified Return vs. Range.	43
Figure 19	Comparator and Threshold Board.	45
Figure 19b	Comparator Board Layout and Test Point Location	46
Figure 20a	Digital Timing and Display Board.	49
Figure 20b	Digital Board Layout.	50

	page
Figure 21	Detector System Timing Diagram. 51
Figure 22	Signal Return vs. Elevation Angle of Source 57
Figure 23	Secondary Returns Terrain Ambiguity 60
Figure 24	Missing Return Problem. 61
Figure 25	1024 Element Receiver Construction. 65
Figure 26	1024 CCPD Array Block Diagram 66
Figure 27	Block Diagram of 1024 CCPD Receiver 67
Figure 28	Relative Response of Silicon Photodiode and Wraatten Filter. 69
Figure 29	Preamplifier Aboard Array Board 74
Figure 30	Peak Detector with Blanking Reset 76
Figure 31	Timing Diagram Reticon Modifications. 77
Figure 32	Improved Rangefinder. 82
Figure 33	Optics for Improved Rangefinder 85

ABSTRACT

An opto-electronic receiver incorporating a multi-element linear photodiode array as a component of a laser-triangulation rangefinder is described. Developed as an obstacle avoidance sensor for the Rensselaer Polytechnic Institute's Martian Roving Vehicle, the detector can resolve the angle of laser return in 1.5° increments within a field of view of 30° and a range of five meters. A second receiver with a 1024 elements over 60° and a 3 meter range is also documented. Included is a discussion of design criteria, circuit operation, schematics, experimental results and calibration procedures.

ACKNOWLEDGEMENT

I would like to recognize some of the people who have contributed to this effort:

To Nan, my complement;

Dr Yerazunis for his vigor and insight

Drs. Frederick and Gisser for their patience an efforts on my behalf;

To Mssrs. William Meshach and John Craig, the prime movers of the elevation scanner;

To Paul Dunn and Tahm Sadegi, for the summer it worked;

And to Dave Cipolle and Bill Kennedy, for letting me help.

PART 1

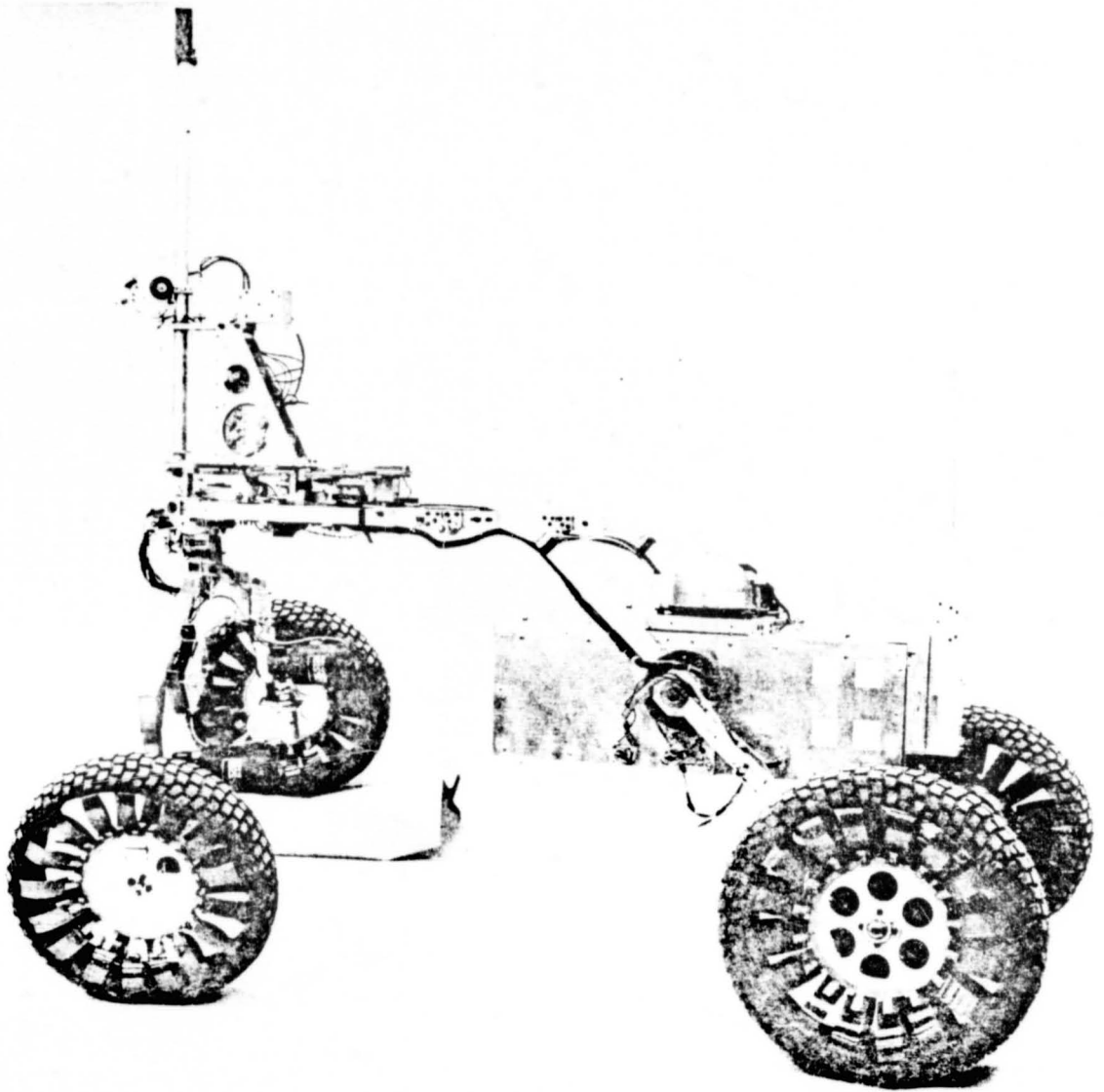
INTRODUCTION

An autonomous robot vehicle has been suggested¹ as a component of a scientific triad of orbiter, rover and penetrators devised to continue the investigation of the planet Mars. "The global reconnaissance carried out by the orbiters, the network science and limited characterization of otherwise inaccessible environments carried out by the penetrators, and the detailed study of local environments conducted by the rover,"¹ comprise the three elements of a post-Viking, pre-sample return mission.

Speaking specifically of rover operations, early mission studies¹ envisioned a two-year, 100 km survey of the Martian surface. These studies indicated that in order to survey such a significant portion of the planet's surface while still enjoying the option of intensive investigation of selected scientifically interesting sites, the machine would be obliged to travel at relatively high speeds, in excess of 1.5 meters/min, between sites. Round trip radio communication between earthbound mission control and a Martian rover (142 million mile orbit) would involve from ten to 40 minutes. Clearly, with such a loop time, real-time human control could not achieve the desired speed. However, an autonomous vehicle, capable of independently avoiding obstacles, could proceed rapidly, maneuvering through its hazardous environment with only intermittent human guidance. Such an independent operation demands a sophisticated terrain-sensing and decision-making facility on the part of the machine.

Information about surface topography, obtained for the purpose of obstacle negotiation would, as envisaged, be gathered from a triple hierarchy of sensors; orbiters overhead, stereo cameras/laser rangefinders aboard the rover, and a short-range hazard detection system. At the highest level, the orbiter, equipped with a radio altimeter and high resolution imagers, would provide the operators at JPL mission control with the requisite data to identify macro-obstacles and science goals for the next 24 hours. Coupling this information with the most recent stereo images taken by the rover's cameras, a list of traverse coordinates linking the desired science goals by a best perceivable path can be generated and transmitted to the rover.

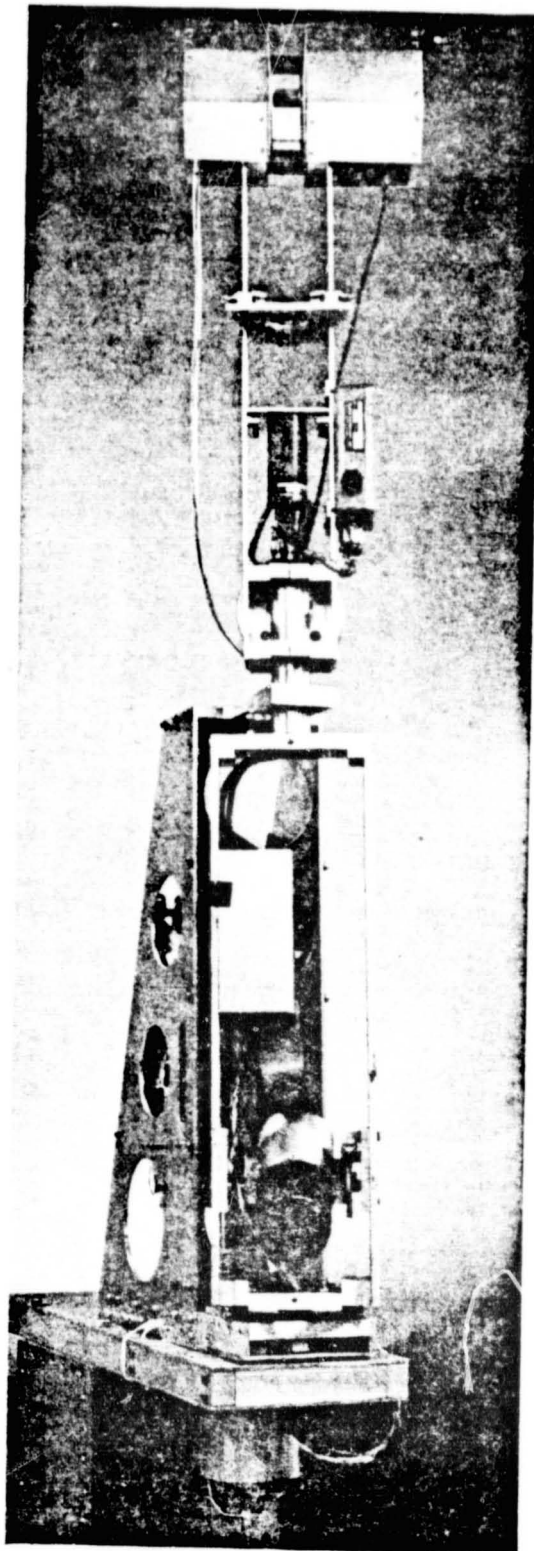
Upon receipt of the transverse link coordinates and the location of science sequences selected by JPL, the vehicle, utilizing on-board logic and hazard avoidance equipment, begins its advance across the Martian terrain. Operating in a 50 minute "halt-sense-think-travel" cycle the machine employs its mid-range (30-40 meter) sensors, stereo cameras and laser rangefinder to perform the required obstacle detection and path planning during the 25 minute "halt" portion of the cycle. In the "travel" segment the rover, travelling at a rate of 1.5 meters/min, then pursues the course plotted in the mid-range analysis, depending solely on its short-range hazard detection system. Functioning in the 1-5 meter range, the short-range system is responsible for rapidly recognizing and evading those obstacles (± 25 cm. step, ± 30 deg. slopes) which may have eluded the mid-range examination. It is the short-range problem; terrain sensing, obstacle identification and path selection,



RENSELAER AUTONOMOUS ROVING VEHICLE

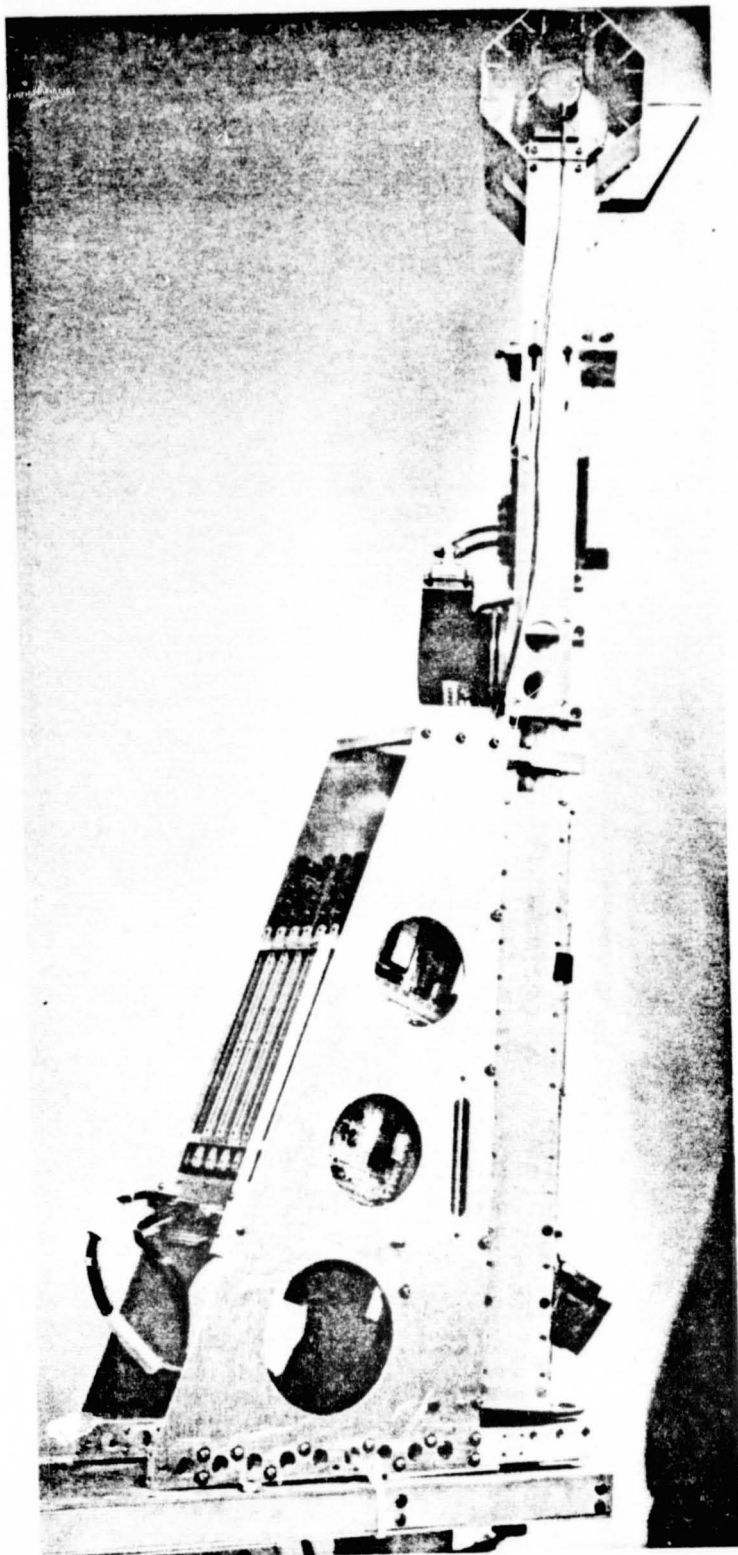
FIGURE 1

ORIGINAL PAGE IS
OF POOR QUALITY



ELEVATION SCANNING MAST - FRONT VIEW

FIGURE 2a



ELEVATION SCANNING MAST - SIDE VIEW

FIGURE 2b

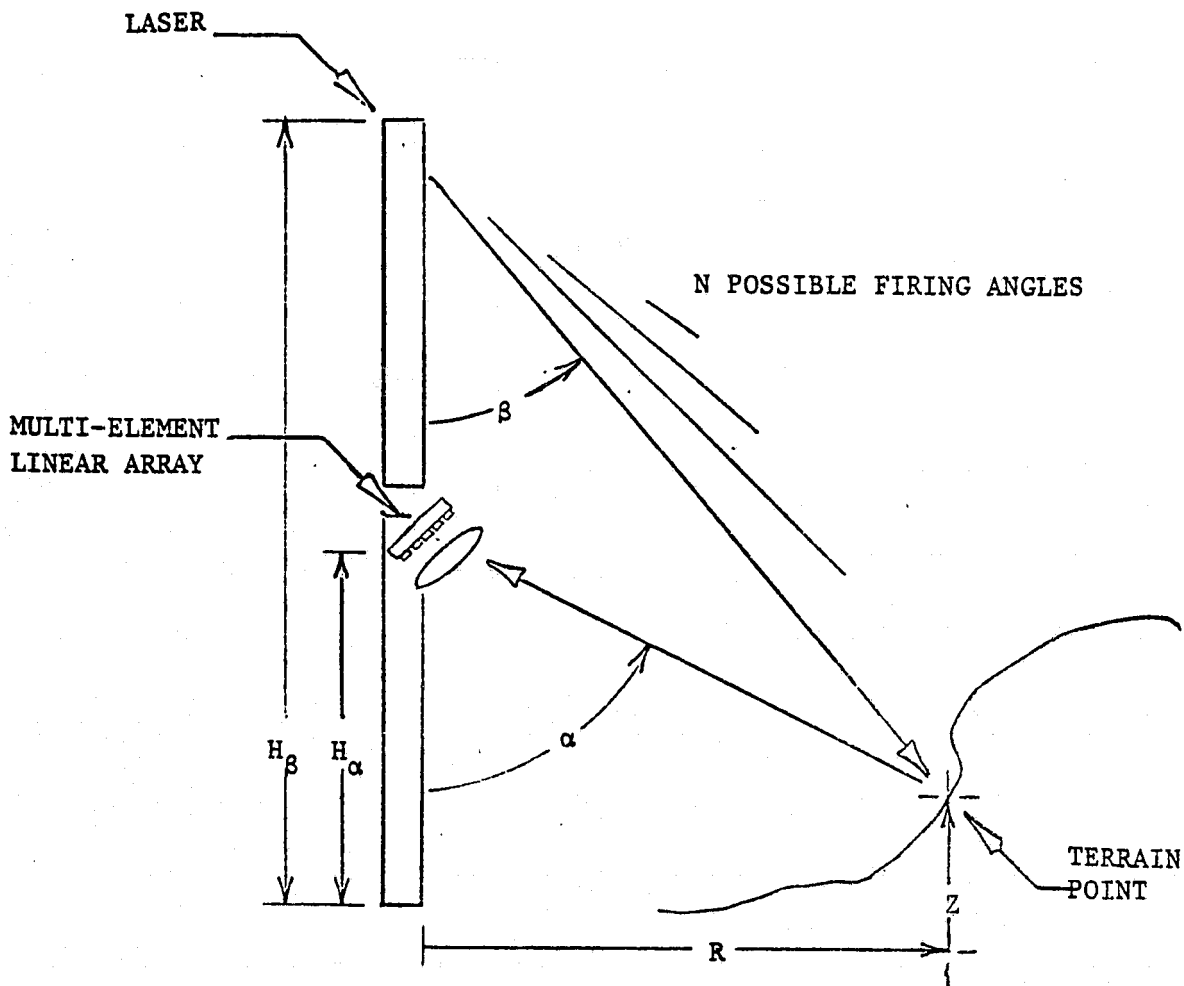
ORIGINAL PAGE IS
OF POOR QUALITY

which has been investigated at RPI in recent years.

To this end a four-wheeled, remotely-controlled vehicle has been constructed, complete with terrain sensors, control electronics, rough terrain capability and radio links to an off-board computer, to serve as a test bed and demonstration tool for hardware and algorithms, Fig. 1. Research has been conducted in the areas of packaging/deployment, vehicle stability and performance, terrain modelling, navigation and path selection as well as obstacle detection employing the laser triangulation ranger described herein.

Evaluation of the robot's performance carried out in the laboratory and at an outdoor test site involves placing the rover in an environment consisting of many arbitrary obstacles (rocks, walls, craters, etc.). The machine, equipped with a directional gyro, tachometers and terrain sensor is charged with the task of negotiating the obstacle field under autonomous control to an operator-designated goal (specified as an x-y target or vector heading).

The terrain sensor, located in the front of the vehicle and embodied in the laser/detector mast, Fig. 2, gathers direction and range information from terrain points in the vehicle's vicinity. Employing the principle of triangulation in the Laser Direction and Ranging system (ladar) scans about the vehicle firing the laser at predetermined angles, Fig. 3. At each firing the light energy is reflected from the terrain back to an array of photodiodes which resolve the angle of return. The information from this process, when sampled at a suitable spatial frequency and coupled with the vehicle roll and pitch state,



β - ANGLE OF LASER RAY

α - ANGLE OF LASER RETURN

$$Z = \frac{H_\beta \tan \beta - H_\alpha \tan \alpha}{\tan \beta - \tan \alpha}$$

$$R = \frac{\tan \alpha \tan \beta (H_\beta - H_\alpha)}{\tan \beta - \tan \alpha}$$

FIGURE 3 RELATIONSHIP BETWEEN (α, β) , (Z, R)

enables an off-board computer to perform the necessary obstacle detection and path planning.

Aboard the RPI Mars Roving Vehicle (MRV), the short-range terrain sensing has been accomplished through application of a pulsed laser/photodiode triangulation technique, but not without first considering other alternatives. Radar, for instance, used extensively in direction and range finding, offers itself as a well developed technology but suffers from a lack of resolution in the short range and large physical size of its antennae. Sonar, with shorter wavelengths, has the needed range accuracy, but can be dismissed because of the tenuous Martian atmosphere. Mechanical feelers, although suitable as the last line of defense in the form of bumpers, cannot achieve both the range needed for rapid movement and ruggedness for long service. A laser rangefinder measuring the time of flight of terrain echoes can, by appropriate averaging of many returns, estimate the range of terrain points to an accuracy of several centimeters through the use of sophisticated picosecond circuitry. Yet, though such precision may be acceptable for mid-range slope and obstacle estimation, the need for finer discrimination and higher speed in the short-range case points toward the pulsed laser triangulation scheme.

The sensitivity of a triangulation scheme increases rapidly with shorter distance and computer simulations² have demonstrated that for a laser-to-receiver distance of one meter, and an angular resolution of one degree in both laser and detector, step obstacles of 25 cm and slopes exceeding ± 30 degrees can be reliably located in the one-three

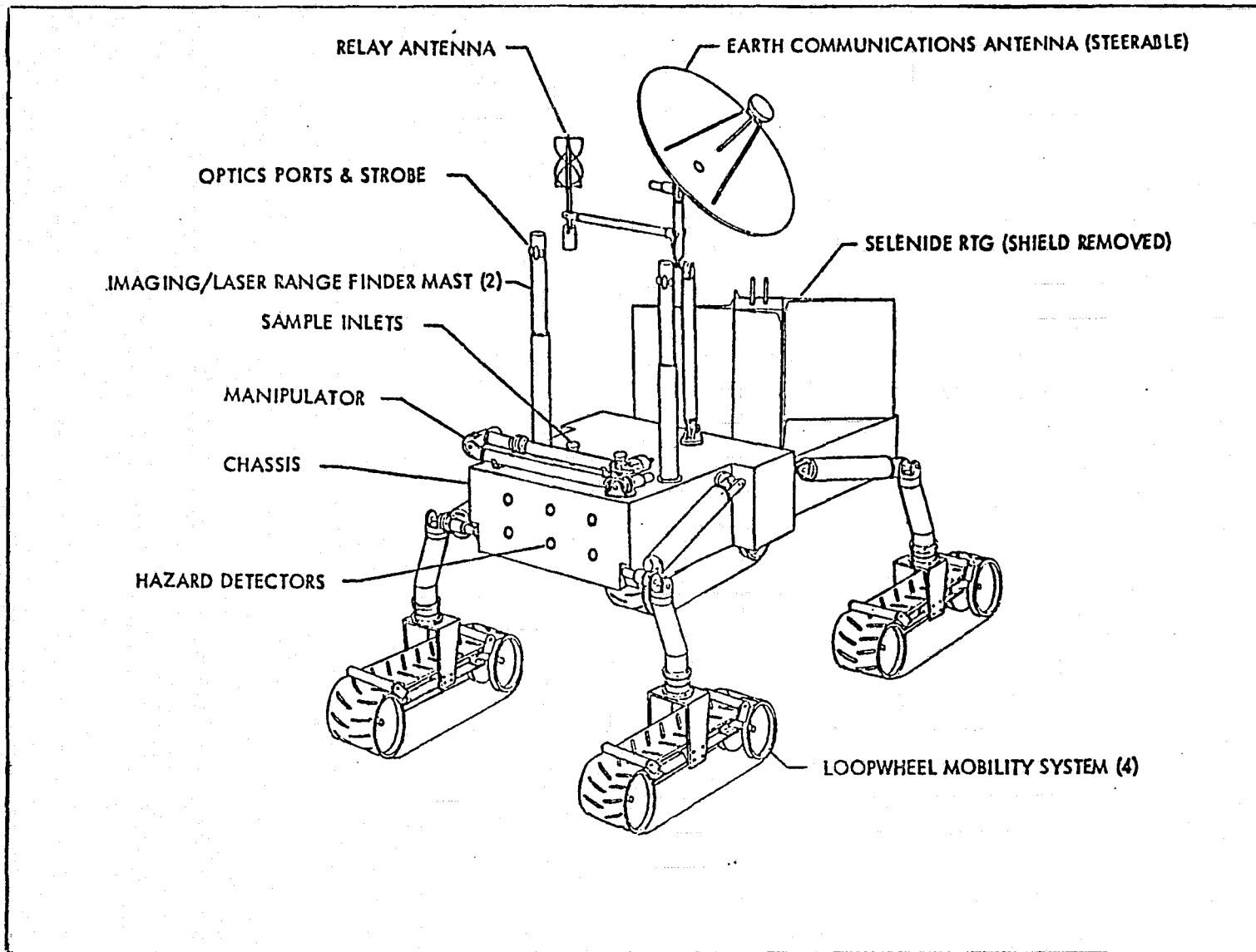
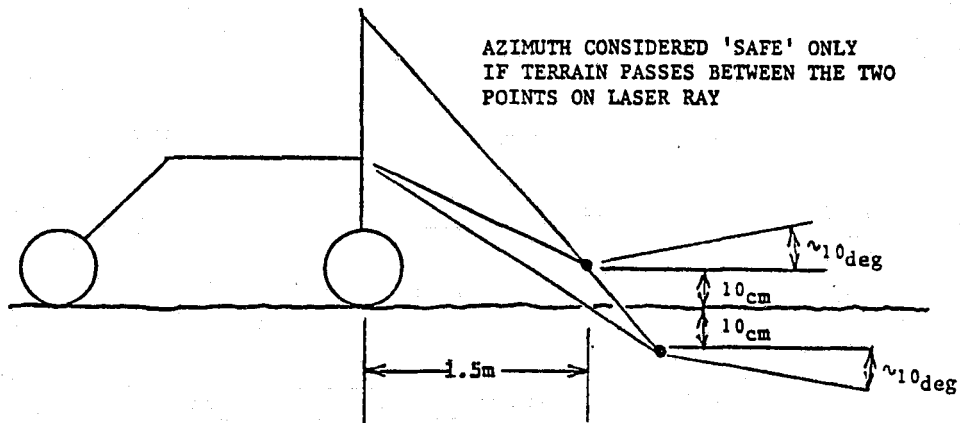


FIGURE 4 DISCRETE DETECTORS ABOARD PROPOSED 1984 ROVER

meter range. Also the triangulation system, by avoiding the averaging demanded in the time-of-flight ranger and unencumbered by the computational load of the stereo correlation approach, permits the rapid sampling over the wide field of view imposed by the short-range problem. Furthermore, because of the active nature of the laser ranger, it can be utilized at night without the artificial illumination requirement of the passive stereo camera sensor, a feature which increases available traveling time while minimizing power expenditure. Another advantage of the triangulation scheme is that laser sources and photo-receptive receivers can be easily proliferated around the machine fixed in appropriate directions, thereby eliminating the need for mechanical scanning, Fig. 4. For these reasons and others, including low cost, silicon reliability and conceptual ease, the terrain sensors in service aboard the RPI MRV have been of the pulsed laser triangulation variety.

The first terrain sensor employed aboard the RPI MRV was the single-laser/single-detector system depicted in Figs. 1, 5. The laser and detector were both fixed in elevation aboard a vertical mast which oscillated through 140° of azimuth. In principle only laser reflections within the detector cone of vision were considered as evidence of possible terrain. If in any azimuth a missing return occurred, an entry was made into the path selection terrain map indicating the presence of a hazard in that azimuth at a range of 1.5 meters.

By adjusting the field of view of the detector, by means of an iris in the photo-sensitive image plane, step obstacles of 25 cm, positive and negative, as well as slopes exceeding $\pm 10^\circ$, could be



BY CONTROLLING DETECTOR FIELD OF VIEW STEP OBSTACLES OF ± 25 CM.
(WHEEL RADIUS) CAN BE PERCEIVED

HOWEVER THIS RESTRICTS SLOPE CAPABILITY TO ± 10 DEG.

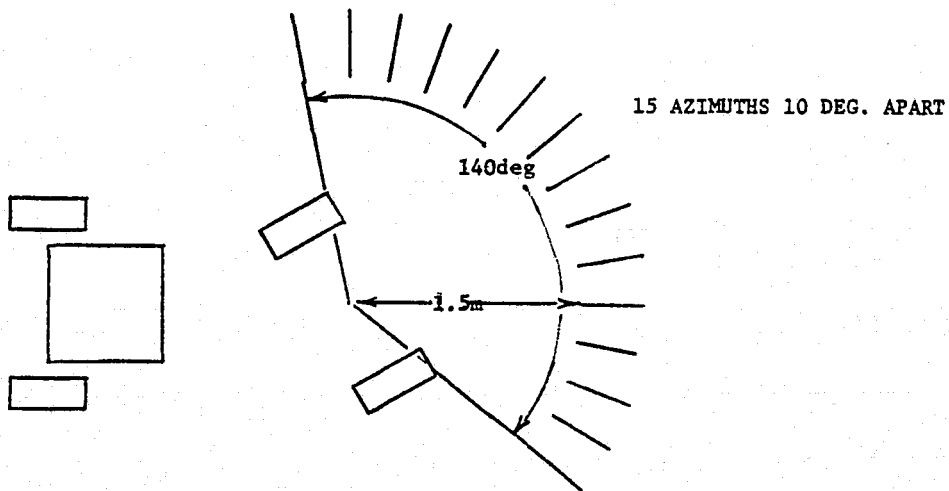
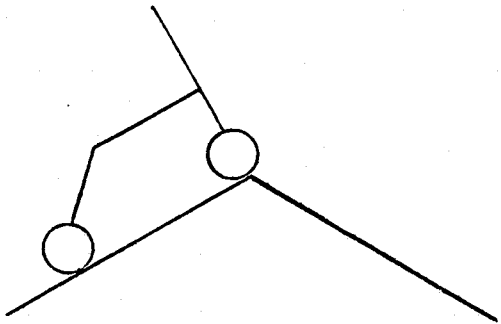


FIGURE 5 SINGLE LASER -SINGLE DETECTOR SYSTEM

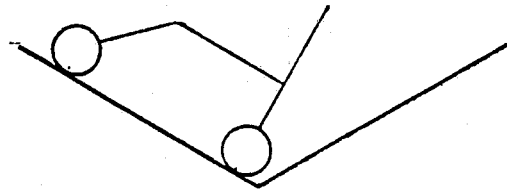
distinguished. Yet the vehicle was designed to climb $\pm 30^\circ$ slopes. Furthermore since there was no indication of range, the range was estimated conservatively at 1.5 meters thereby foregoing a good deal of maneuvering room, particularly in the case of negative obstacles. The inability of the single-laser/single-detector scheme to detect both step obstacles and $\pm 30^\circ$ slopes as well as its range ambiguity restricted its realm of operation to relatively level terrain ($\pm 10^\circ$ roll and pitch) populated by discrete obstacles several vehicle widths apart.

Although the single-laser/single-detector system was limited in terms of scene interpretation by its geometry it did demonstrate the feasibility of the hardware, namely that a pulsed (10 watt, 200 ns) laser and a silicon photodiode could function reliably over the wide range of reflectivities, ranges and ambient light conditions encountered in its environment. Given the confirmed viability of the laser/photodiode combination it remained to improve the perceptual performance of the terrain sensor to include the capability for detection of step obstacles embedded in $\pm 30^\circ$ hillsides.

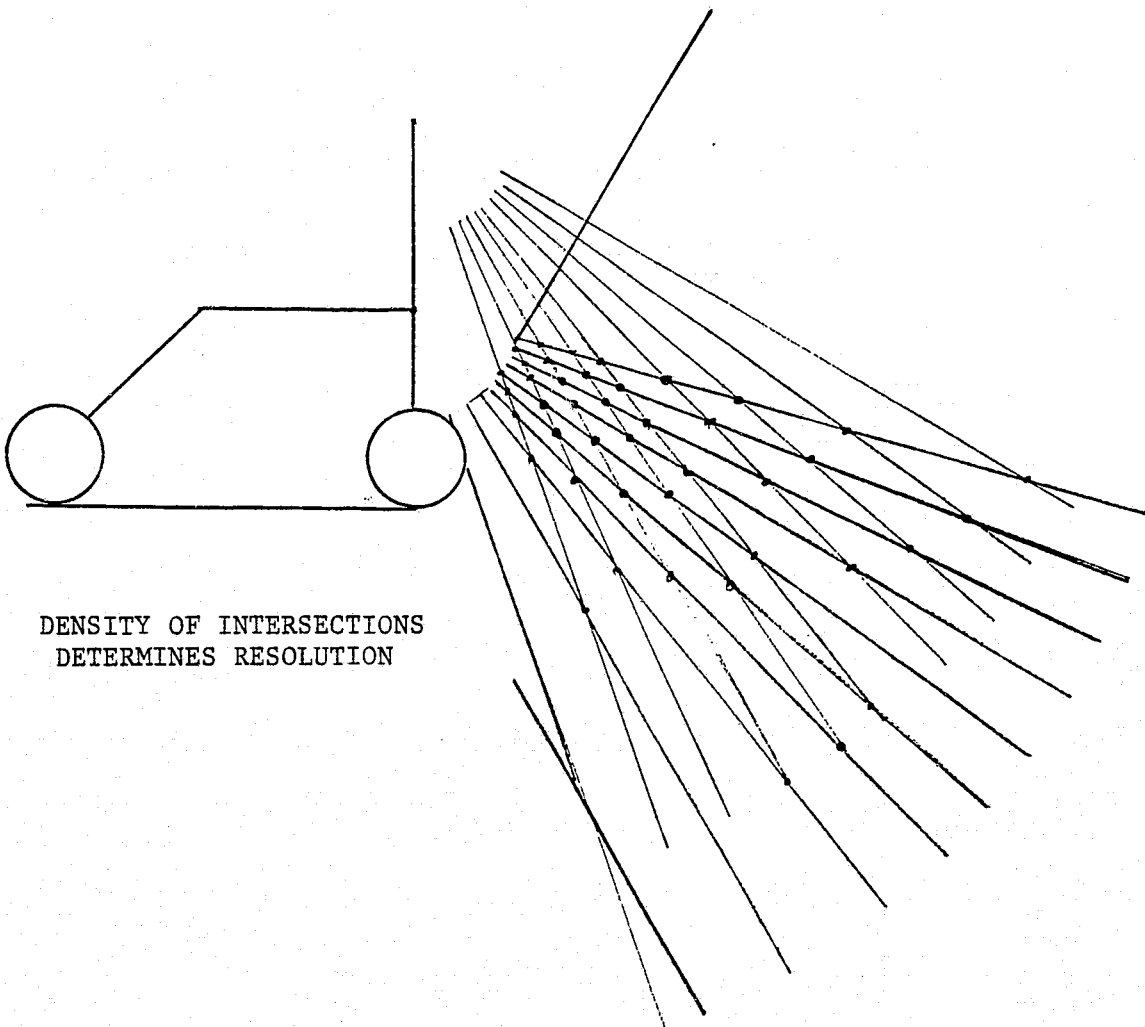
The multi-laser/multi-detector's concept was to increase the number of laser and detector rays so that the density of their intersections would be sufficient to distinguish a 25 cm step obstacle anywhere within the volume defined by worst-case slope constraints. Figure 6 illustrates how the $\pm 30^\circ$ slope limit of the rover defines the volume within which passable terrain must be sampled ($\pm 60^\circ$ with respect to vehicle) and the distribution of the source/sensor intersections



-60 DEG. w.r.t. VEHICLE



+60 DEG W.R.T. VEHICLE



DENSITY OF INTERSECTIONS
DETERMINES RESOLUTION

FIGURE 6 VEHICLE PITCH, SENSOR FIELD OF VIEW, RESOLUTION

generated in the elevation scanning scheme. The field of view of laser and detectors required to encompass this volume can be estimated from this illustration to be approximately 45° and 60° respectively. The angular resolution of the laser and detector can be estimated from the elevation cross-section of the 25 cm obstacle at the maximum range of four meters. Simply,

$$\tan \Delta\beta = 25 \text{ cm}/4.0 \text{ meters} \rightarrow \Delta\beta \sim 4^\circ$$

To sample at twice this frequency with an extra 100% margin of error, a resolution of 1-2 degrees was set as a goal for both laser and detector. Subsequent computer simulations² using 1° resolution and 40° field of view for both laser and detector have since confirmed the validity of this choice.

The hardware needed to scan the laser/detector through azimuth and elevation was designed^{3,4,5} in the 1977-78 academic year and is shown in Figs. 2 and 7. The system allows 1024 laser shots fired in a 32×32 pattern with a resolution of 1.05° in a 90° elevation field and 2.8° resolution in a 360° azimuth scan.

The two primary components of the mast controller are the elevation and azimuth encoders, Fig. 8. As the eight-sided mirror rotates the elevation encoder outputs 2048 pulses per revolution (every 0.18°). Likewise the azimuth encoder produces 256 pulses (every 1.4°) in its revolution. In the controller, the counts from these two encoders are compared to a firing pattern stored in the azimuth and elevation

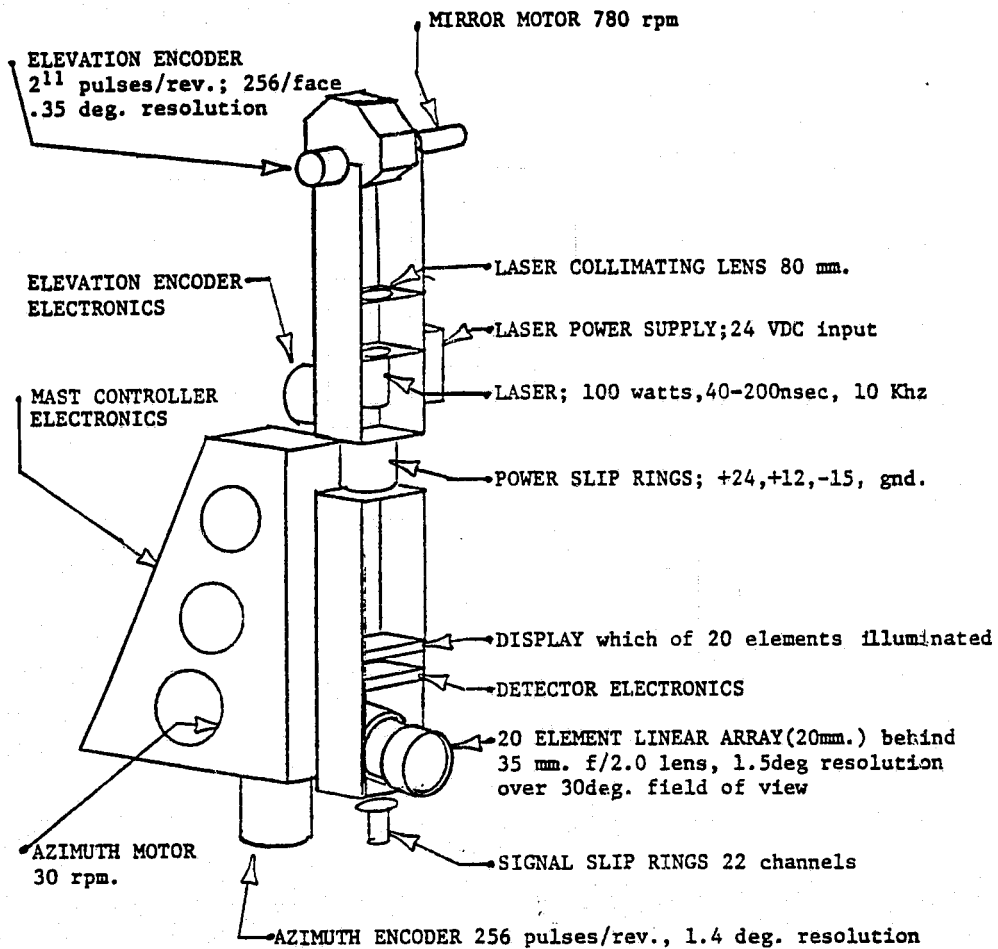


FIGURE 7 LASER DIRECTION AND RANGING MAST

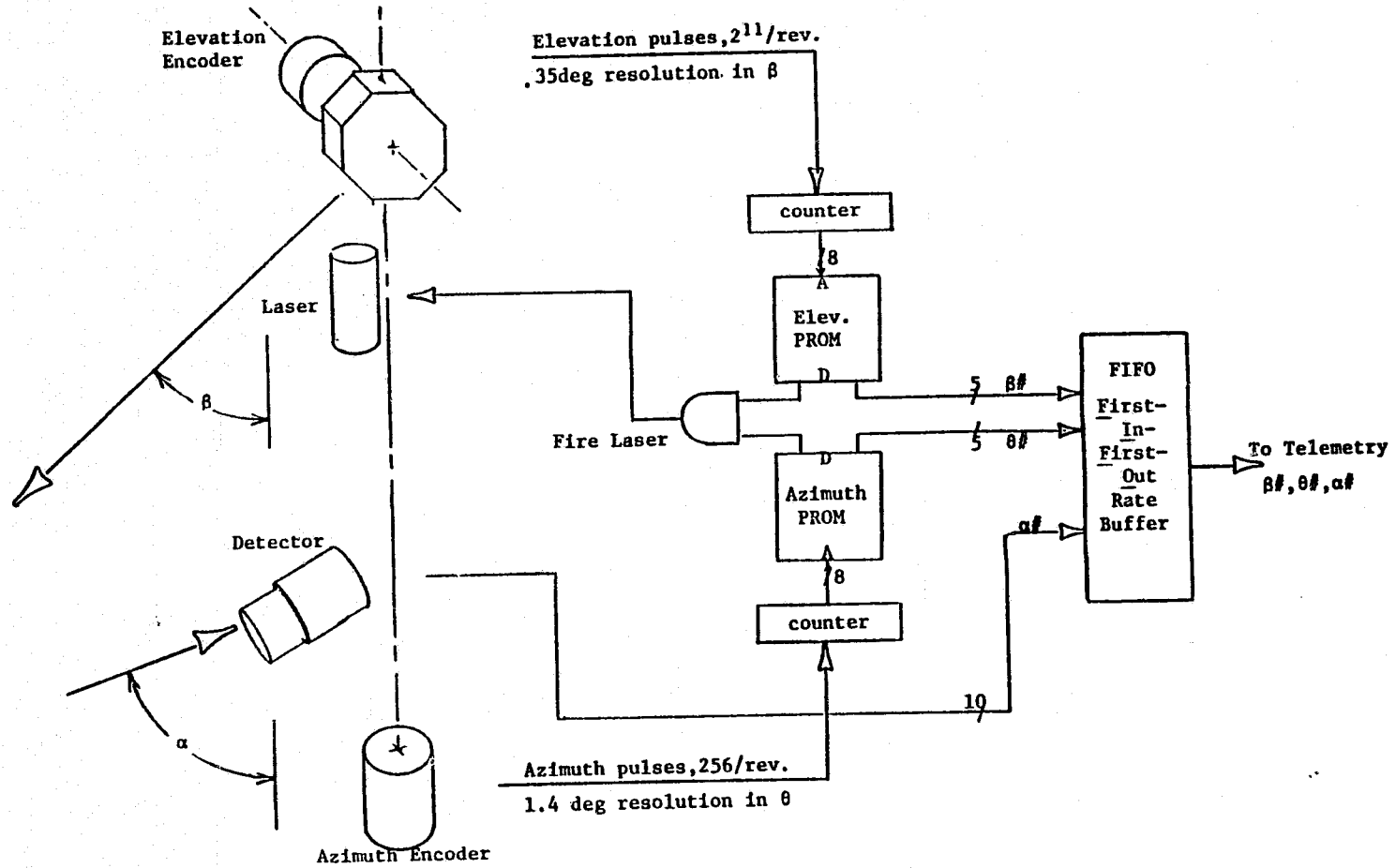


FIGURE 8 MULTI-LASER MULTI-DETECTOR MAST CONTROLLER

PROM (Programmable Read Only Memory). When a match occurs the laser is fired and the detector output is loaded into the telemetry FIFO (First-In-First-Out buffer) along with two five-bit words, $\beta\#$ and $\theta\#$, which identify at which elevation and azimuth angle the laser was fired. This process can be repeated at a 10 kHz rate allowing a complete azimuth scan to be completed in as little as 1.65 seconds. With the laser scanner designed it remained to select a detector compatible with the elevation scanning scheme.

PART 2

DETECTOR SELECTION

2.1 Detector Criteria

In any triangulation scheme the location of an unknown point is determined by measurement of angles from two known points. In the laser ranger used aboard the RPI Martian Rover the unknown points are the laser spots on the terrain and the known points are the laser atop the rotating mast and the detector situated below. The angle from the laser, β , is measured by the mirror shaft encoder and constrains the terrain point to lie along the indicated laser ray, Fig. 3. The function of the detector is to measure α , the elevation angle of the intersecting image ray. Three schemes for resolving α were considered: discrete receivers, linear arrays and two-dimensional arrays. Below is a discussion of the considerations involved in the detector selection.

Practical factors such as cost, size, weight and safety being equal, four criteria pertinent to this analysis have been isolated: resolution, speed, scope and sensitivity.

The resolution of the receiver is its ability to discriminate differences in the position of the laser reflection upon the ground. Measured in terms of angular accuracy, it is obvious that an increased number of photo-receptive elements within a given angle serves to enhance the resolution of the detector. A large number of detectors also affords the researcher the flexibility necessary to examine a wide variety of possible detector geometries. Computer simulations² have indicated that a detector resolution of 1° - 2° is adequate to perceive

the 25 cm threshold obstacle.

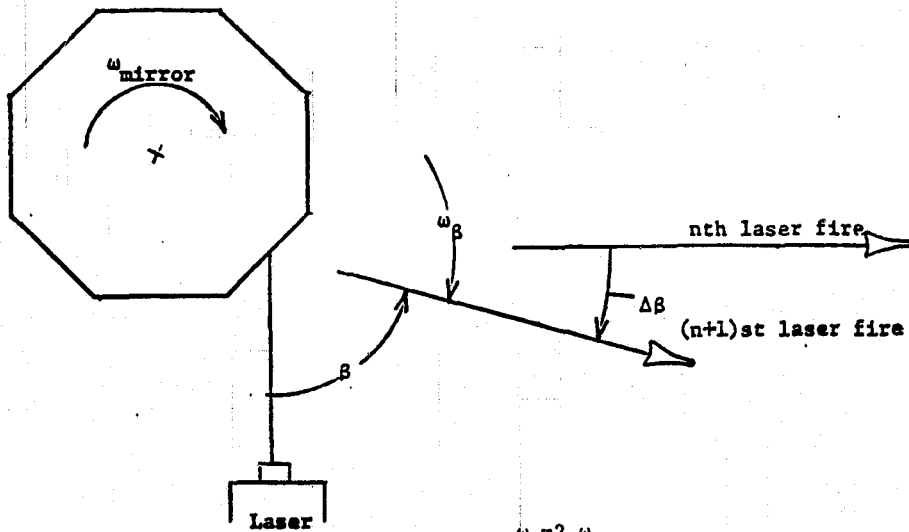
Also of prime concern in detector selection is the speed at which it can function. Since the vehicle travels in a continuous fashion, it is imperative that the laser/detector system operate at a rate sufficient to ensure that any terrain has been scanned several times before the machine rolls over it. Specifically, if the vehicle velocity is 1 km/hr (approximately $\frac{1}{4}$ meters/sec), the sensor's range 4 meters, and the time between successive scans of the terrain is 4 sec, then the terrain passing beneath the vehicle will have been sampled four times. As a further example, at the mission study speed of 1.5 meters/min, to scan the terrain ten times, a detector with a range of three meters has as long as 12 seconds to complete its azimuth rotation. In general,

$$\frac{\text{Sensor Range}}{\Delta t_{\text{scan}} \cdot \text{Vehicle Velocity}} = \# \text{ times terrain scanned.}$$

Given the rate at which the terrain must be scanned, the relationship between the mast/mirror rotation and the desired angular resolution of the laser determine the detector's operating speed. Assuming an n-sided mirror spinning continuously through 360° in both azimuth and elevation, the time between laser shots and scan time can be related, Fig. 9.

$$\omega_{\text{mast}} = 2\pi / \Delta t_{\text{scan}}$$

$$\Delta\theta = \omega_{\text{mast}} \left| \frac{2\pi}{N} / \omega_{\text{mirror}} \right|$$



$$\omega_{\beta} = 2 \omega_{\text{mirror}}$$

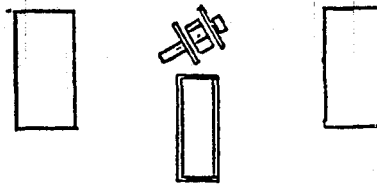
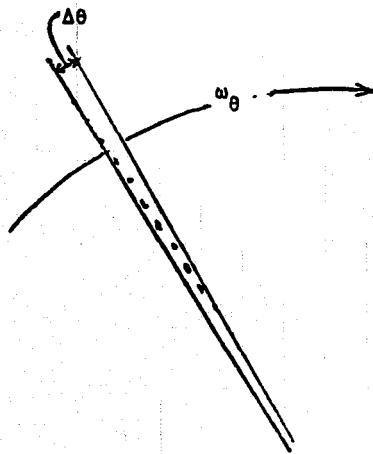
$$\Delta\beta = \omega_{\beta} \Delta t_{\text{det.}}$$

$$\Delta t_{\text{face}} = \frac{2\pi}{N/\omega_{\text{mirror}}}$$

$$\Delta\theta = \omega_{\theta} \Delta t_{\text{face}}$$

$$\Delta t_{\text{scan}} = 2\pi/\omega_{\theta}$$

$$= \frac{8\pi^2 \Delta t_{\text{det}}}{\Delta\theta \Delta\beta N}$$



Top View of Laser Mast

FIGURE 9 DETECTOR SPEED, SCAN TIME, and ANGULAR RESOLUTION

$$\Delta\beta = \Delta t_{\text{det}} \omega_{\beta} = \Delta t_{\text{det}} 2\omega_{\text{mirror}}$$

$$\Delta t_{\text{det}} = \frac{\Delta\beta \Delta\theta N}{8\pi^2} \Delta t_{\text{scan}}$$

where

t_{det} = time allotted for detector operation, also time between closest consecutive laser firings

$\Delta\beta$ = minimum elevation angle between successive laser shots (rad)

$\Delta\theta$ = azimuth angle within which elevation sweep occurs (rad)

N = number of faces on polygonal mirror

Δt_{scan} = time between successive scans of terrain

For example, the 4 sec. scan, with a laser resolution of 1° in elevation, an azimuth error of $\pm 1^\circ$ ($\Delta\theta = 2^\circ$), and using an eight-sided mirror, constrains the receiver to 246 μsec (~ 4 kHz) or faster. The dependency of Δt_{det} , $\Delta\beta$ and vehicle velocity illustrates the trade-offs between spatial and temporal data density inherent in the rotating mast-mirror scheme. If it were possible to scan the laser at electronic frequencies, instead of employing rotating mechanical components, then the tradeoffs would be remarkably improved. Investigation into other means of laser deflection (such as acousto-optical crystals (Glen Herb '73)⁵) showed that the combination of large deflection (50°) and high speeds was not feasible.

Another criterion applying to the detector is its scope.

What is meant here is the volume, defined by the detector's field of view and range, within which the laser spot on the terrain can be seen.

Terrain which falls outside this envelope cannot be measured and must be assumed to be hazardous. Ideally the scope or envelope would encompass all possible terrain, slopes of $\pm 60^\circ$ and a range long enough to perceive hazards outside the vehicle's turning radius (~2 meters). This implies that the detector's scope should be 60° in elevation, 180° in azimuth and in excess of 3 meters in range.

The detector must respond reliably to any laser spot which falls within its volume of perception. The detector must be sensitive to the wavelength of the laser (904 nm.) as well as the low light level of the terrain reflection. The amount of energy that can be expected to return can be calculated by considering the amount of energy released by the laser, account for path losses and then arrive at the energy impinging on the detector.

The laser (Meshach '78) generates 100 watts for 40 ns. The collimating lens transmittance and mirror reflectance are assumed to be 85% and 90% respectively. Ground reflectance is assumed to be as low as 10%. Assuming further that the energy reflected from the ground radiates in all directions equally (a reasonable assumption considering the diffuse nature of the terrain the rover should encounter), the ratio of the energy entering the detector to that radiated away is:

$$\frac{\text{Area Lens Aperture}}{\text{Area of Hemisphere with Radius = Range}}$$

If the transmission of the detector lens and filter are included

$$\begin{aligned}
 \text{Energy} &= (100 \text{ watts}) (40\text{ns}) (\text{lens trans}) (\text{mirror reflect}) \\
 \text{def} & \quad (\text{ground reflect}) \left(\frac{r^2}{2 R^2}\right) (\text{filter trans}) (\text{lens trans}) \\
 & (100 \text{ watts}) (40 \text{ ns}) (.85) (.90) (.10) \frac{1}{2} \left(\frac{r}{R}\right)^2 .8 (.85) \\
 & = 10^{-7} \left(\frac{r}{R}\right)^2 \text{ joules}
 \end{aligned}$$

Assuming the ratio of the lens radius (on the order of millimeters) and the range (1-5 meters) can be approximated by 1/1000, then the amount of energy passing through the detector's lens could be presumed to be

0.1 picojoules or 2.5 μ watts peak

Now that the criteria for the detector have been enumerated it is possible to evaluate the three proposed receiver candidates, i.e., discrete arrays, linear arrays and area arrays.

2.2 Discrete

A discrete receiver approach calls for n individual detectors, each with its own lens, photosensor and amplifier. Each detector would have both variable attitude and field of view. A single detector of this sort is presently functioning reliably aboard the RPI MRV.

The resolution of this system is limited by the number of receivers that can be mounted aboard the rotating mast. Since only 25 to 30 discrete detectors could realistically be mounted, the potential resolution is limited. Although the detector cones could be overlapped to increase the effective resolution potential errors due to vibration and misalignment appear likely.

The speed of the discrete detector's alternative is the

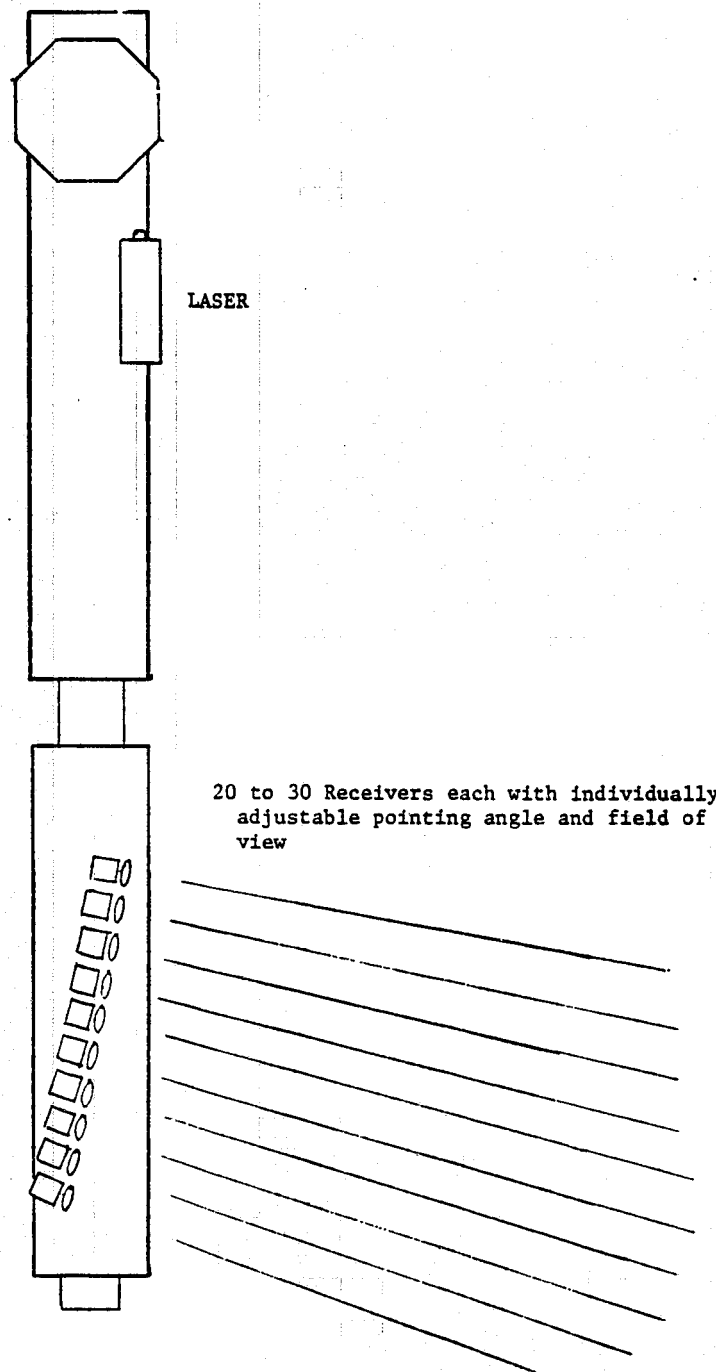


FIGURE 10. DISCRETE DETECTOR SCHEME

fastest of any of the three approaches. Since each detector measures returning power and has individual amplifiers, its speed, constrained only by the rise and fall time of a single detector, can approach the megahertz range.

The scope of the discrete detector scheme is the most versatile. Since each detector can be pointed in any desired direction any conceivable detector geometry can be generated. Range measurements taken under laboratory conditions show that this laser/detector combination has a reliable range in excess of five meters.

Sensitivity of the discrete approach is confirmed by the successful operation in rough terrain environment of the current single-laser/single-detector system. It has operated reliably throughout its desired range and in bright sunlight.

With its high speed, flexible scope and proven sensitivity a discrete detector approach could have readily been achieved by replicating the single-laser/single-detector receiver. Yet this system's disadvantages, including low resolution, large size and very difficult alignment problems, did not seem to make it the most attractive proposal.

2.3 Area Arrays

Two-dimensional detectors, as opposed to discrete and linear arrays, have also been suggested for use as receivers. Devices such as vidicons and solid state matrix arrays offer very high resolution with typically 100 elements per dimension, and the sensitivity, particularly of silicon-intensified-vidicons, is quite good. Yet for most

area arrays, excluding the CID random-access imagers, the speed of area arrays is limited by the need to sample the entire frame at rates near 30-60 Hz. This disadvantage could be circumvented if the laser were scanned rapidly in a direction perpendicular to the line between the laser and receiver. Specifically if the laser is located above the receiver it should be scanned rapidly in azimuth while the elevation angle is held constant, Fig. 11. Then the image of the laser would be a single-valued function of the horizontal dimension of the array. A striking advantage of this scheme is that only the mirror must be rotated, not the receiver, obviating the need for slip-rings. Furthermore the measurement of the azimuth angle is derived directly from the horizontal position in the array, thereby eliminating the need of an azimuth encoder. Yet although the resolution is high, the speed not a strong disadvantage and the mechanical scanning greatly simplified, matrix arrays not only have a limited field of view in elevation but in azimuth as well. To achieve a 180° azimuth field of view in front of the vehicle might require three or four cameras. Each camera would have to be aligned separately and devoted exclusively to short-range hazard detection. Although it is a simple matter to proliferate cameras aboard the vehicle, and it may be advantageous to have redundant cameras, the costs of the cameras exceed the project budget and it was felt that a single dedicated unit contained on the mast fits more with the spirit of the proposal for a short-range hazard detection system.

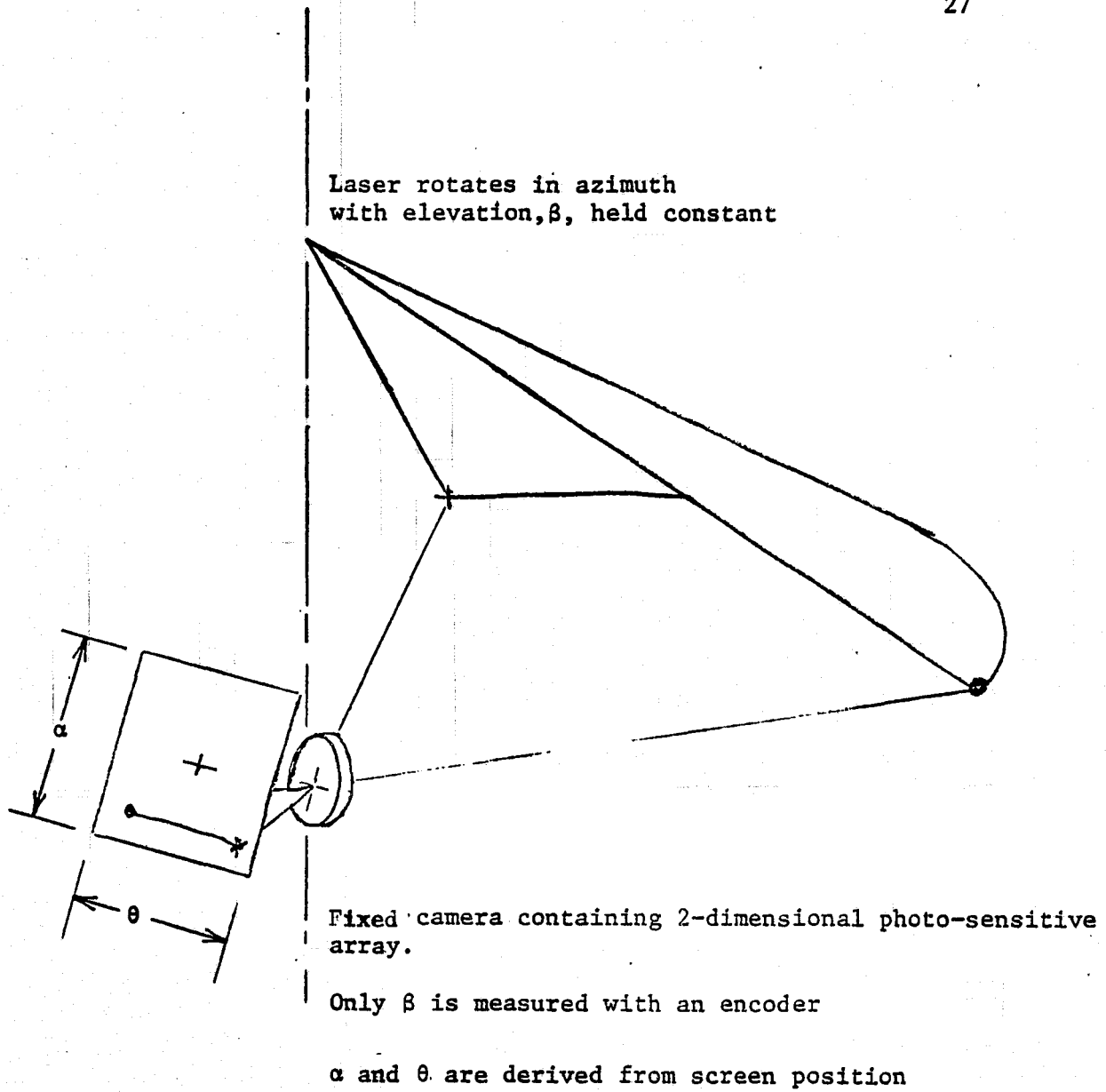


FIGURE 11. 2-DIMENSIONAL AREA ARRAY IMPLEMENTATION

2.4 Linear Arrays

A detector incorporating a linear array of precisely manufactured photo-diodes behind a single lens avoids the severe alignment problems of n discrete receivers. With a single lens, only the pointing angle of the camera and the distance from lens to array need be adjusted. Fig. 12

The resolution of the linear array is a function of the number of elements along its length, and the field of view chosen. Linear arrays are available with from 16 to 1728 elements, which with a field of view of 60° gives a resolution of 3.75° and 2 min 5 sec respectively.

The speed of the linear array receiver depends strongly on the number of elements involved. Arrays with 20 or less elements can provide separate outputs for each of their photodiodes in a single dual-in-line-package. These arrays are as fast as diode receivers since each photosensor is used in parallel with its own amplifier. When more than 20 elements are involved it becomes difficult to offer a separate output for each diode and some form of on-chip scanning or multiplexing is required. This either takes the form of analog multiplexors (C.I.D.s) or of analog shift registers as in the case of CCD imagers. In both cases the time for array operation increases linearly with the number of elements. Typically the maximum scanning frequency is from 1 to 5 Mhz so that for 1024 elements the detector time is from 1 msec to 200 μ sec. Using the expression relating detector time, Δt_{det} , to the time required for a scan, Δt_{scan} :

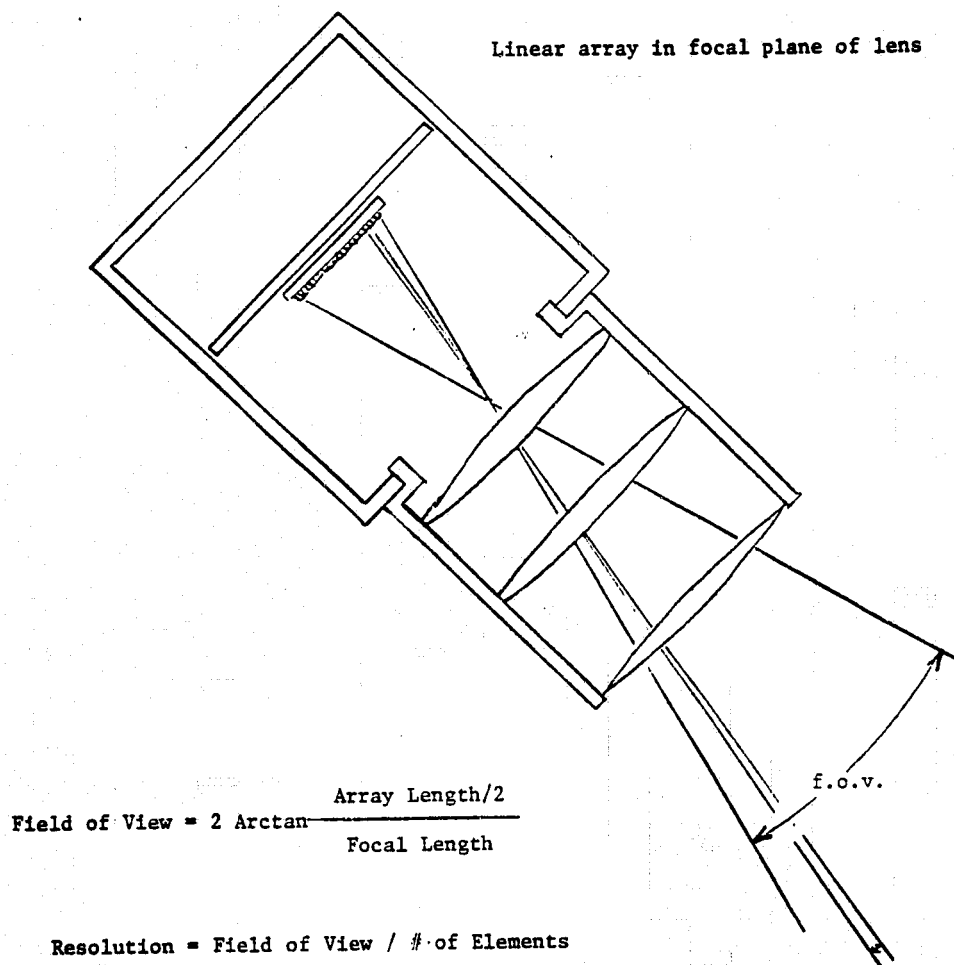


FIGURE 12. LINEAR ARRAY IMPLEMENTATION

$$\Delta t_{\text{scan}} = \frac{\pi^2}{\Delta\beta\Delta\theta} t_{\text{det}}$$

$\Delta\beta$ = resolution in β $\sim 1^\circ$

$\Delta\theta$ = error in azimuth $\sim 2^\circ$

For 1 μsec and 204 μsec detector time, the 1024 element linear array limits the scan time to greater than 16.5 or 3.3 sec respectively.

The scope of the linear array is a function of the lens' focal length and is a trade-off between field of view and resolution. For a given number of elements, say 20, the requirement for at least 1.5° resolution limits the receiver's field of view to 30° . A linear array with 1024 elements enjoys such a high resolution that even at the maximum desired field of view of 60° there is only 3 min 30 sec of arc between diodes.

The sensitivity of the linear array receiver also varies with the number of elements. For a 20 element array with parallel outputs the sensitivity is similar to that of the discrete approach with the important advantage of the single lens. In the discrete detector system each receiver has its own lens which, for 20-30 detectors must be relatively small. However in the linear array receiver each photodiode receives an image from the entire large lens providing substantial gain and thus reducing the amplification needed. The sensitivity of self-scanned linear arrays is more complicated to analyze. Although the longer arrays also benefit from the single lens they suffer from disadvantages peculiar to the scanning mechanism which permits their long length. First of all the switching noise and

capacitance of the multiplexors degrade the signal-to-noise ratio. Secondly, since the photodiodes must hold their photo charge until scanned by the multiplexers, they are susceptible to leakage and dark currents. To hold their photo current the photodiodes must integrate the light intensity falling on them, thereby measuring the energy falling on them between samples. Yet the energy released by the laser (100 watts, 40 ns = 4 μ joules) when averaged over t_{det} (204 sec) gives an effective power of $\frac{4 \mu\text{joules}}{204 \mu\text{sec}} = 20 \text{ mw}$. Hence the advantage of a high power (100 watt) laser exploited by the discrete and short linear schemes is dissipated by the integrating nature of the long self-scanned arrays.

In summary, the three candidates for the multi-detector system, discrete, area and linear methods, were compared in terms of their resolution, speed, scope and sensitivity. The discrete receivers, while having the highest speed, most versatile scope and proven sensitivity, were hampered by relatively low resolution and very difficult alignment. Area arrays such as vidicons and solid state matrices obviate the need for azimuth encoders, but the cost of several cameras to cover 180° in azimuth exceeds the project budget.

Hence linear arrays with the alignment simplicity and increased sensitivity granted by the single lens appeared as a compromise between the complexity of the discrete detectors and the high cost of the multiple area arrays. Two linear arrays were purchased. A 20-element array with parallel outputs promised proven sensitivity, 10 kHz speed and 1.5° resolution over 30° field of view. In addition, due to

the prospect of very high resolution a self-scanned 1024 element array was acquired in the hope that its relatively slow speed and questionable sensitivity could be overcome.

PART 3

20 ELEMENT RECEIVER

3.1 General Description

The 20-element detector system is divided into two main packages, Fig. 14. The detector head holds a 35 mm/f/2.0 lens, the 20-element array, and 20 amplifiers in a $2 \frac{1}{4}$ inch diameter cylinder. The pointing angle of the detector head is adjustable by means of a worm gear ($3^\circ/\text{turn}$) through 90° . A 26 conductor ribbon cable connects the detector head to the $2 \frac{1}{4} \times 3 \times 4 \frac{1}{2}$ " signal conditioner and display unit. Contained in this second package are the threshold adjust/comparator board and the digital timing and display board, Fig. 15. The sensitivity of each of the photodiodes can be adjusted with one of the 20 threshold potentiometers; and the 20 LEDs (Light Emitting Diodes) display which of the photodiodes have been illuminated. Digital detector output as well as power (+24, 15, 5, -15) and Laser Fire Signal pass through a 16 conductor ribbon cable between the digital board and the slip rings.

The entire system offers 1.5° resolution over 30° field of view and is able to operate at well over 10 kHz

3.2 Optics

The lens, specified in terms of its focal length and f-number, determines the field of view, range and indirectly, the resolution of the detector system. Figure 16 illustrates how the focal length of the lens and the length of the photodiode array constrain the field of view. Given that the 20 elements of the linear array cover 20 mm and

ORIGINAL PAGE IS
OF POOR QUALITY

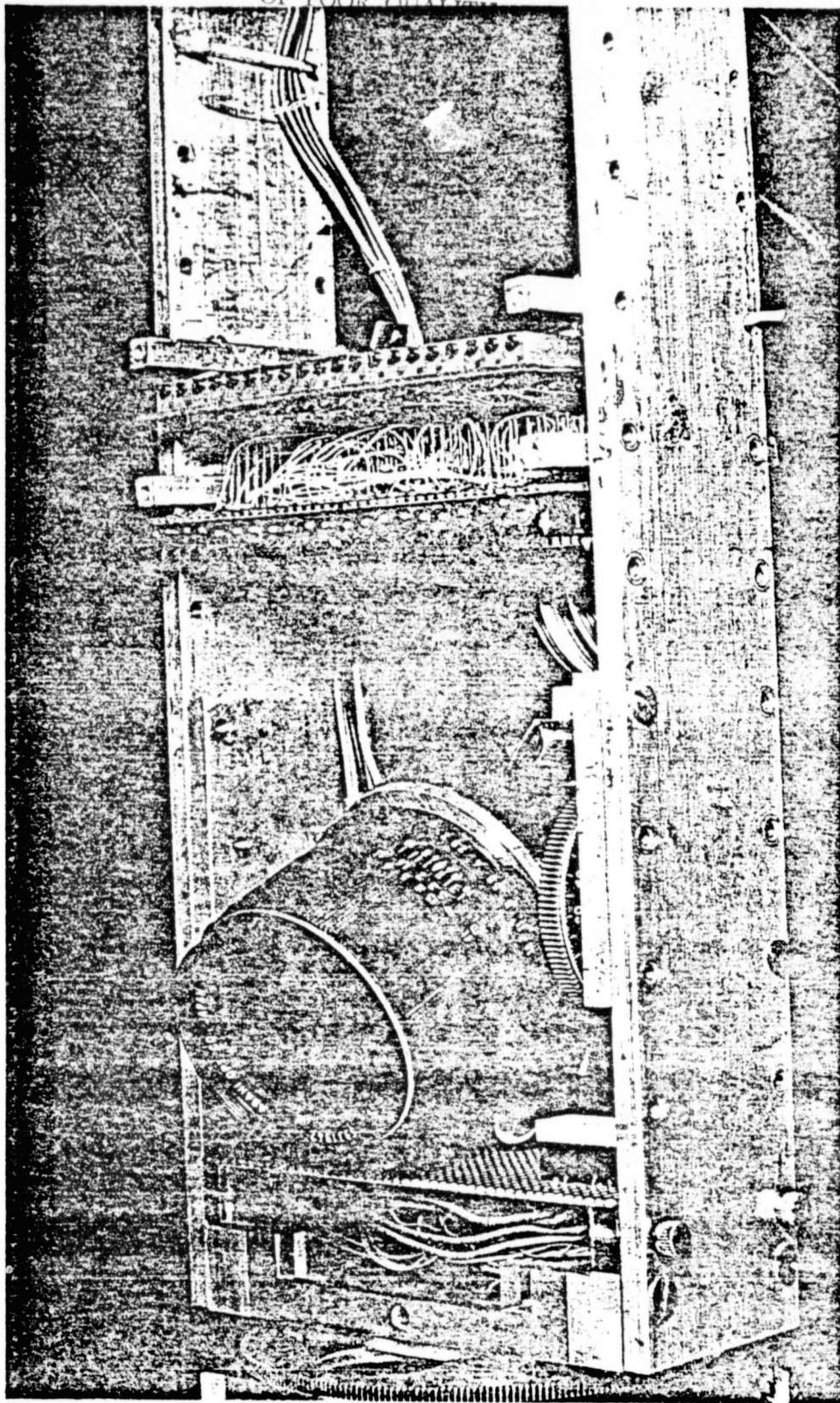


FIGURE 13. DETECTOR ON MAST

ORIGINAL PAGE IS
OF POOR QUALITY

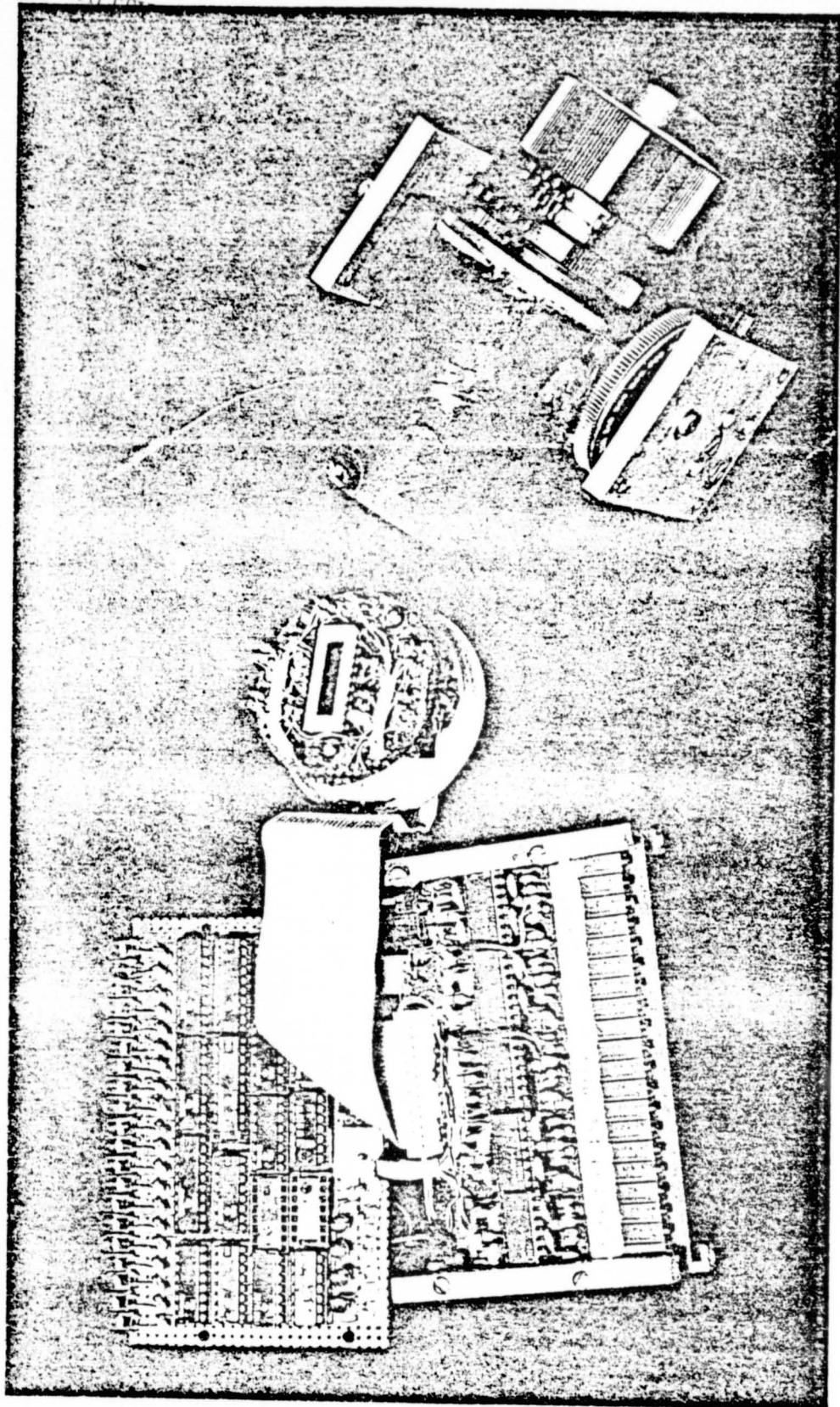


FIGURE 14. EXPLODED VIEW OF DETECTOR

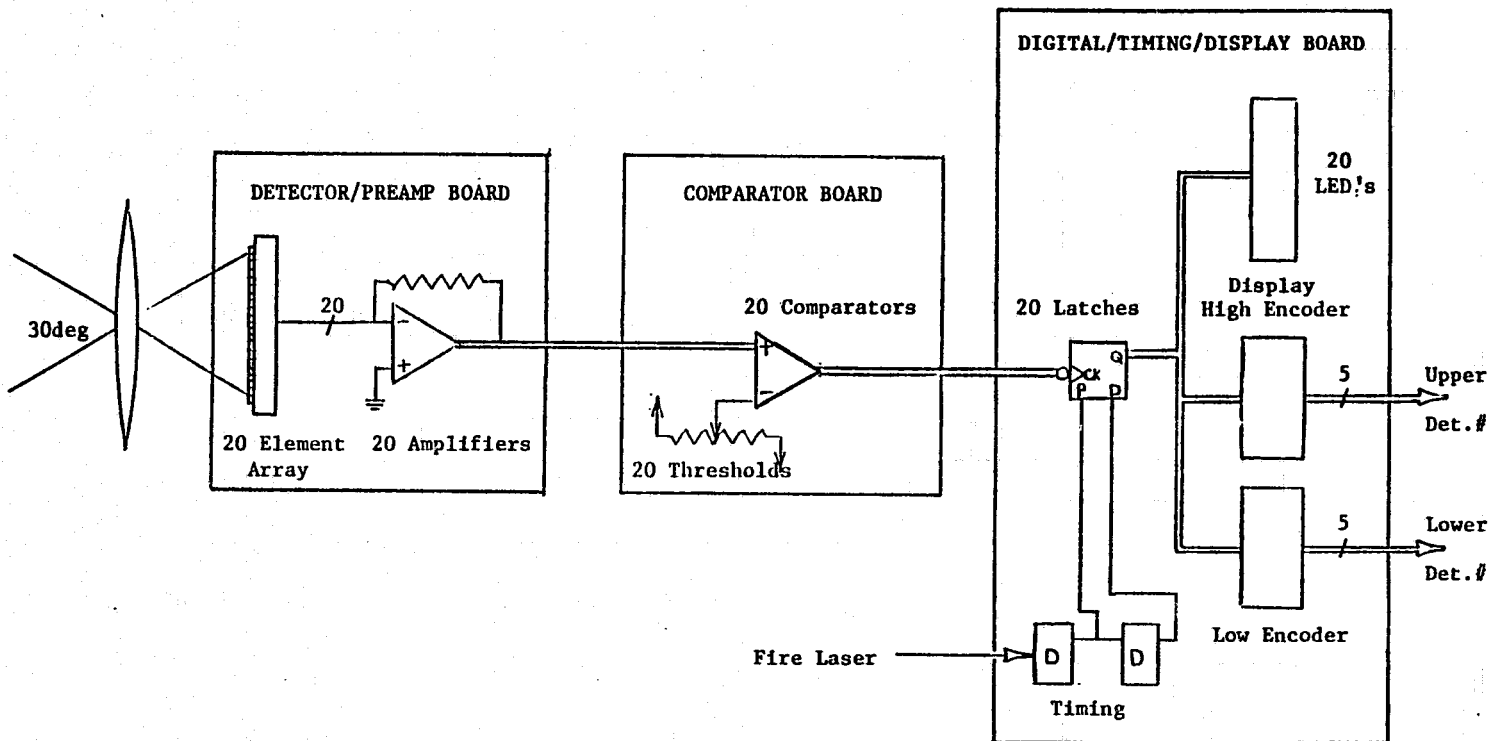


FIGURE 15. DETECTOR FUNCTIONAL BLOCK DIAGRAM

that the field of view of the receiver is desired to be 30° one can calculate a suitable focal length

$$\text{Detector lens focal length} = \frac{20 \text{ mm}}{2} / \tan 15^\circ = 37.32 \text{ mm}$$

35 mm is a readily available standard photographic focal length which allows a field of view of

$$\tan \left[\frac{\text{f.o.v.}}{2} \right] = 10 \text{ mm} / 35 \text{ mm}$$

$$\text{f.o.v.} = 31.89 \text{ degrees}$$

Measurements taken with 35 mm/f2.0 lens confirmed this analysis.

The range and sensitivity of the detector are directly related to the intensity of the laser image formed upon the photodiode array. The f-number of the lens, defined as the ratio of focal length to aperture diameter, should be chosen as small as possible to maximize the aperture to image size ratio. The lens that was purchased has a minimum f-number of 2.0. At this setting the lens has an effective aperture of

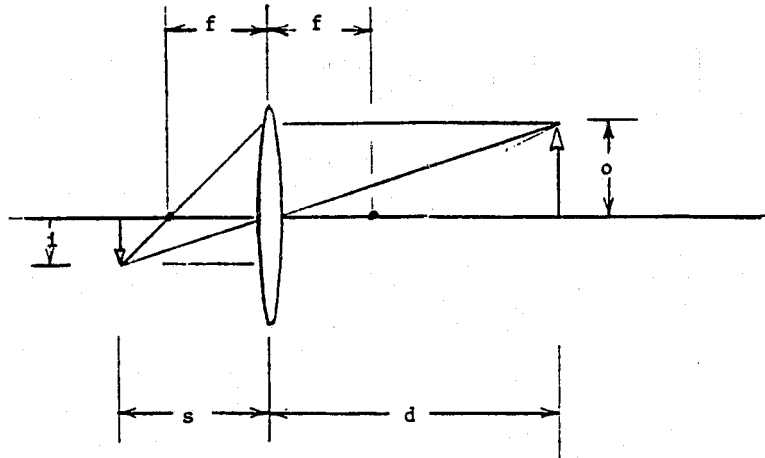
$$\text{f-number} = \frac{\text{focal length}}{\text{aperture diameter}} \rightarrow \text{diameter} = \frac{35}{2.0} = 17.5 \text{ mm}$$

For an effective area of

$$\pi(9 \text{ mm})^2 = 2.54 \text{ cm}^2$$

Since the lens' f-number can be varied from 2 to 16, its light-gathering power can be varied over a range from 1 to 64, a feature which is used to control the sensitivity of the receiver.

The effect of the focal length upon the resolution of the detector can be readily seen by dividing the 20 photodiodes into the



Lens Makers Equation : $\frac{1}{f} = \frac{1}{s} + \frac{1}{d}$

Magnification : $\frac{i}{o} = \frac{d}{s}$

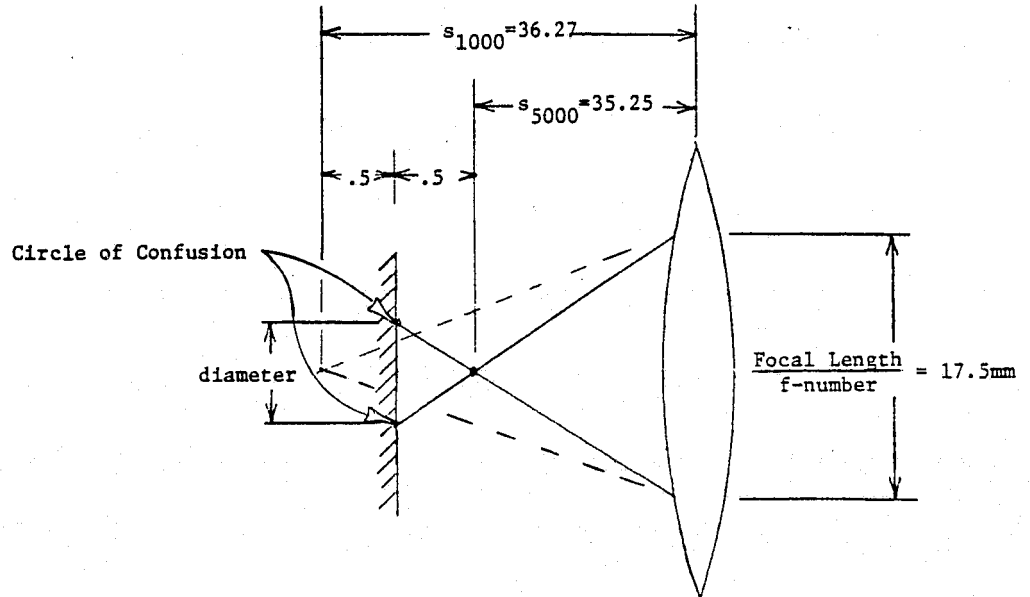


FIGURE 16. GEOMETRIC OPTICS

field of view

$$\frac{32 \text{ degrees}}{20} = 1.65^\circ \text{ per element}$$

The resolution of the detector is also dependent upon the f-number of the lens. From the "lens-makers-equation,"⁸ the distance of the image from the lens, s, can be related to the object distance, d.

$$\frac{1}{p} = \frac{1}{s} + \frac{1}{d} \text{ lens-makers-equation}$$

This equation shows that a laser spot from 1 meter will be focused at 36.27 mm and a 5 meter laser return image at 35.25 mm. If the array is placed halfway between these extremes, at 35.76 mm, so that 1.6 meters is in perfect focus, it remains to be seen the degree of defocus present over the 1 to 5 meter depth of field.

As was said before, a point source on the lens axis at 1000 mm will form a point image at 35.25 mm. All the rays entering the lens aperture are bent to pass through this point. However the detector, placed at 35.76 mm, will not observe a point image but a blurred image termed a "circle of confusion."⁸ The diameter of this circle can be calculated by similar triangles from the axial distances and the lens diameter.

$$\frac{\text{diameter of circle of confusion}}{\text{distance array from focus pt}} = \frac{\text{lens diameter}}{\text{lens to focus pt}}$$

$$\text{diameter circle} = .25 \text{ mm}$$

Since the laser spot on the terrain is not a point source but has a diameter of approximately 5 cm of 5 meters the laser image formed without blurring effects is

$$\frac{i}{5 \text{ cm}} = \frac{35.25 \text{ mm}}{5.0 \text{ meter}} \rightarrow i = .35 \text{ mm}$$

Combining the blurring effects with the unblurred image the composite image can be expected to be 0.6 mm in diameter. Although the blurring effects are appreciable, considering that the photo receptive elements are on 1 mm centers, it is the diode array itself which constrains the detector's resolution.

3.3 Array and Preamplifier Board

Housed within the cylindrical detector head a single 2 inch diameter circuit board holds the 20 element linear array, biasing circuit and 20 operational amplifiers configured as current-to-voltage converters, Fig. 17.

The 20 element array purchased from Centronics, New Jersey, consists of 20 photodiodes each, .9 mm x 4 mm on 1 mm centers in a single 22 pin dual-in-line-package. Located in the center of the analog board on the optical axis of the receiving lens, the photodiodes convert the incident laser radiation into current at the 20 individual diode outputs. The sensitivity of the photodiodes are .43 amps/watt incident.

The biasing and supply circuits provide filtered ± 15 volts for the op-amps and 24 volts used to back-bias the photodiodes. The diodes in the supply lines were included to "idiot proof" the power inputs.

The current pulses from the photodiodes are transformed into negative going voltage waveforms by the 20 operational amplifiers

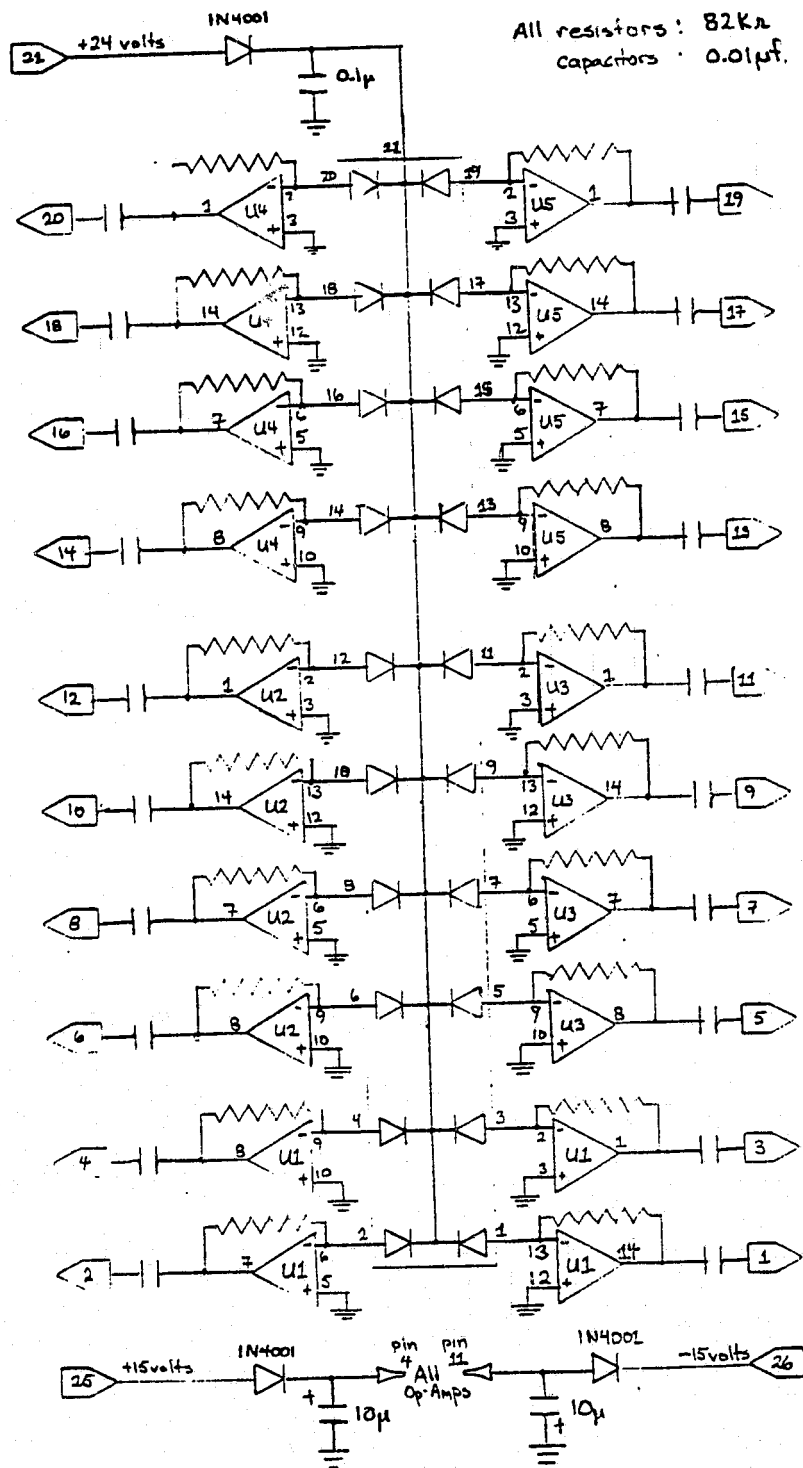
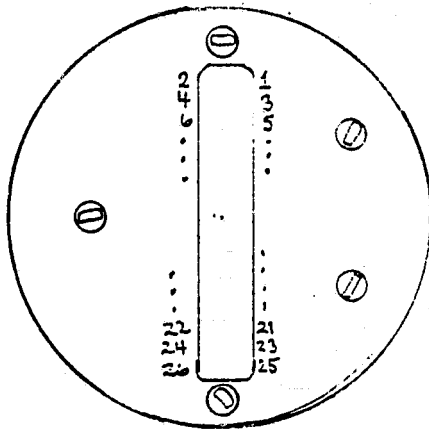
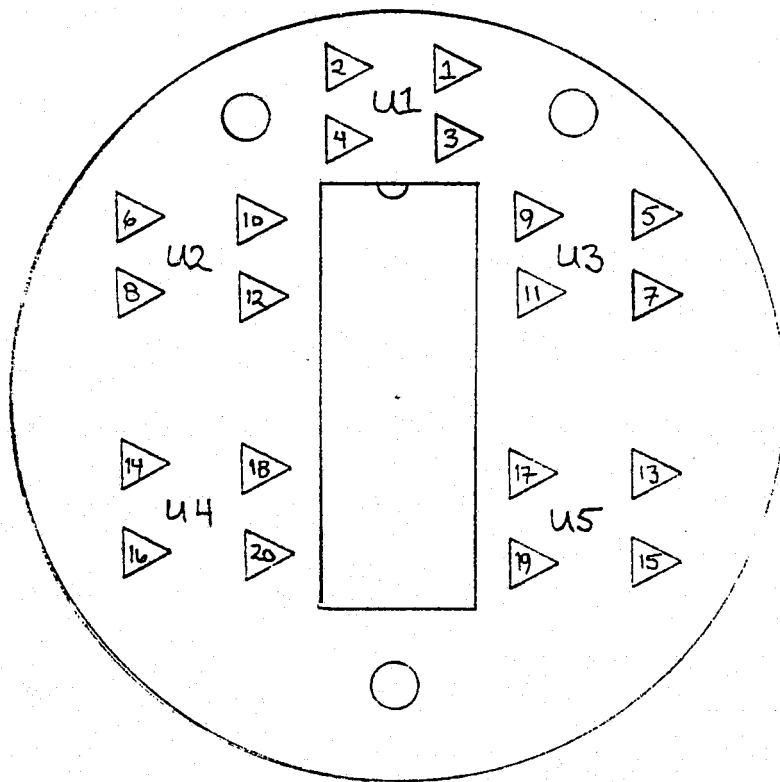


FIGURE 17a. DETECTOR PREAMPLIFIER BOARD



Rear of Detector Head



Array Side of Preamp Board

FIGURE 17b. DETECTOR HEAD LAYOUT

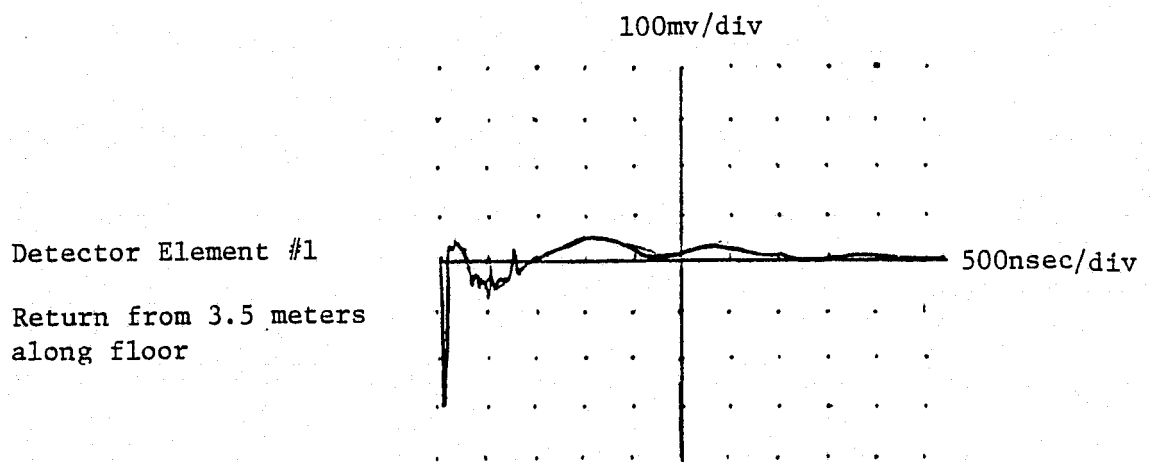
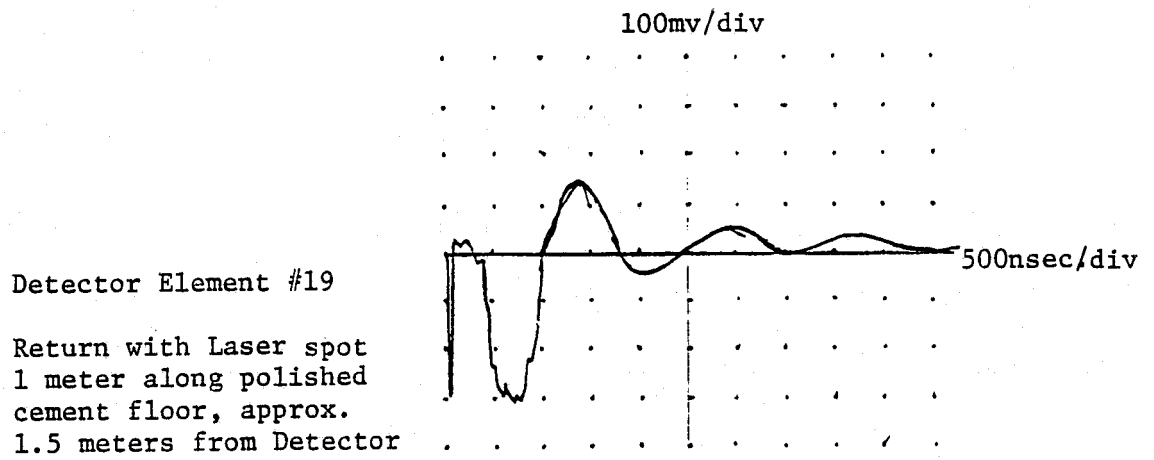
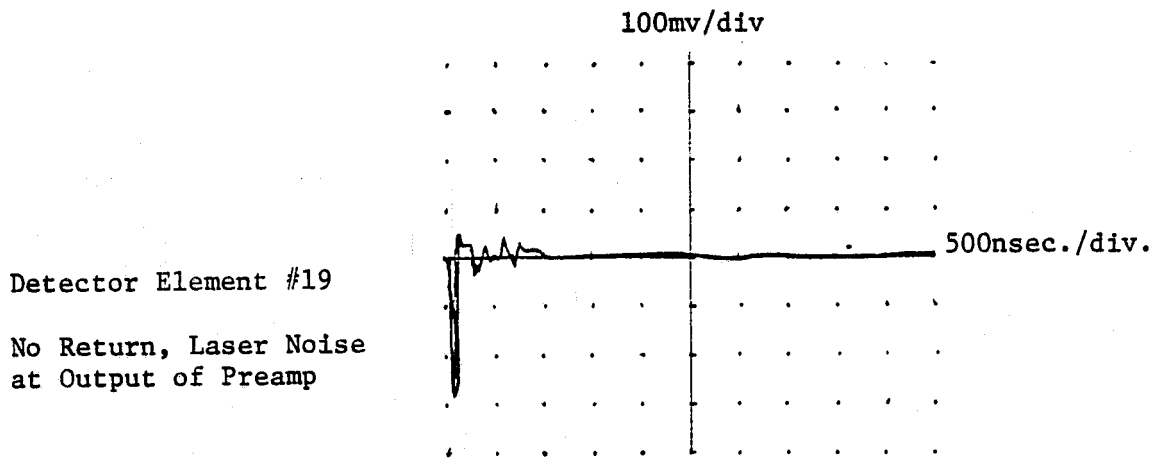


FIGURE 18. AMPLIFIED RETURN vs. RANGE

configured as inverting current to voltage converters. The 82 k Ω resistors were chosen as a compromise between the high gain and the needed amplifier stability. The expected signal from these converters can be estimated by recalling the amount of power entering lens (2.5 μ watts) multiplied by the array's photosensitivity (.43 amps/watt) and the feedback resistance (82 k Ω).

$$2.5 \mu\text{watts} \times .43 \text{ amps/watt} \times 82 \text{ k}\Omega = 88 \text{ mv.}$$

Measured returns from poor reflectors at three meters exceeded 50 mv with an acceptable level of oscillation at the amplifier output, Fig. 18.

The Harris HA 4905 was selected because the quad operational amplifiers in a single dual-in-line-package were easy to service, offered high packing density, while still providing an 8 MHz gain-bandwidth product. The five packages have been socketed for easy replacement. Finally the coupling capacitors between the amplifiers and the comparators block any d.c. offsets which may vary with temperature and device age. Overall, the analog board provides the conversion from the lens' spatial filter to the 20 voltage pulses in a simple, serviceable package while still meeting the physical constraints of the rotating mast.

3.4 Comparator Card

The comparator card, Fig. 19, receives the 20 amplified photodiode signals from the analog board through the 26 cond cable. The pulses it receives are negative going with an amplitude of from

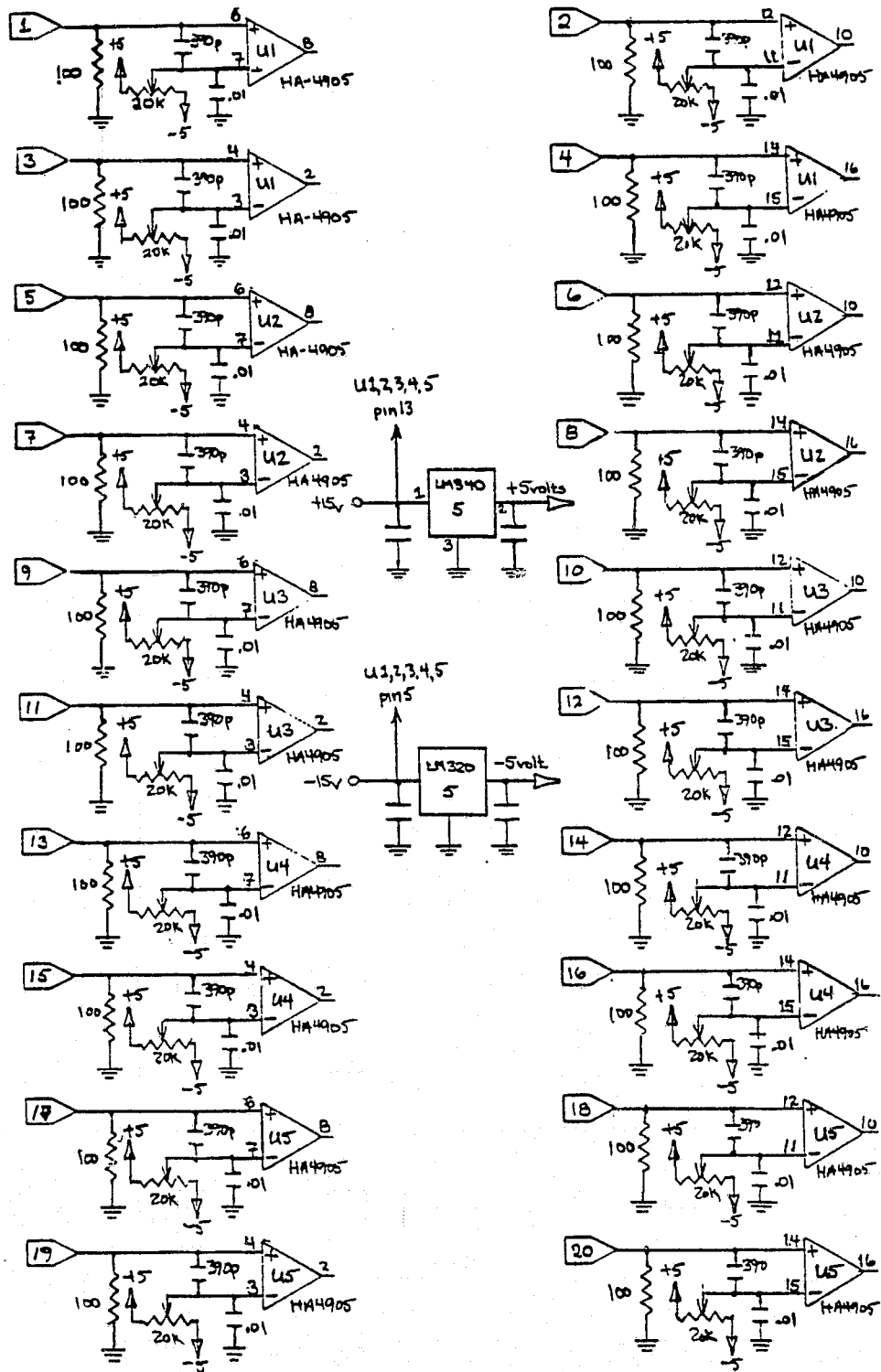


FIGURE 19. COMPARATOR AND THRESHOLD BOARD

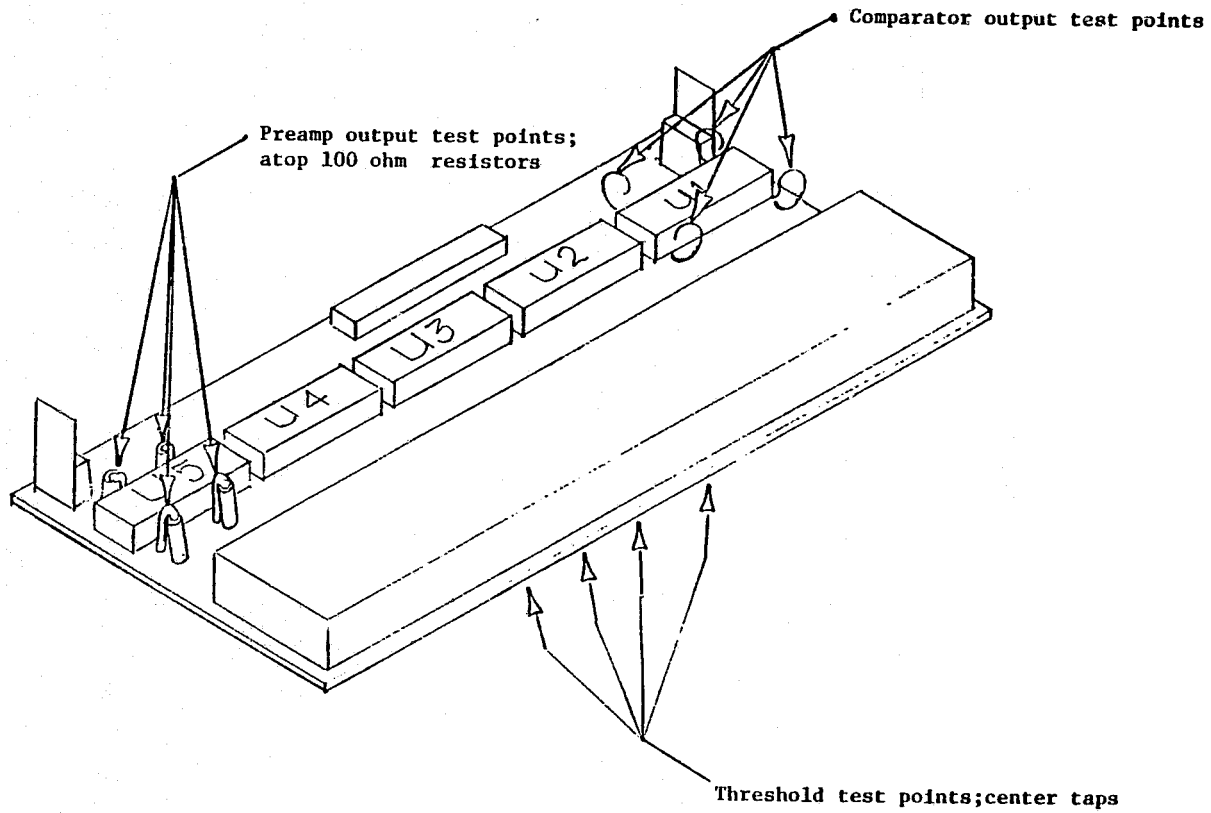


FIGURE 19b. COMPARATOR BOARD LAYOUT AND TEST POINT LOCATION

ten to 500 mv, Fig. 18, Also superimposed on each line is noise generated primarily by the laser firing. The 390 pf capacitor and the 100 ohm resistor form a filter which is used to prevent the laser noise from triggering the comparators.

The comparators selected are HARRIS HA-4605. Again the quad comparators offer the advantage of high packing density, easy replacement and fast (130 ns) fall time. The amplified photodiode pulses are fed into the positive inputs of the comparators and cause a lowgoing TTL-level at the comparator output whenever the pulse amplitude goes below the threshold set on the negative inputs.

The thresholds are adjusted by the voltage-dividing action of the 20 threshold potentiometers. The reason 20 individual thresholds are necessary is in part so that d.c. offsets can be nulled out. Also the individual adjustments allow for a correction of the lens roll-off or vignetting, whereby the image received on the edges of the field of view are less intense than images closer to the optical axis. By lowering the thresholds of the channels associated with the off-axis elements they can be made more sensitive than the center photo receptors, thereby fattening the lens roll-off. Furthermore the separate thresholds allow that the lower detectors, which normally operate at farther ranges, can be adjusted to be more sensitive than the higher elements. Thus each channel can be tuned to the expected signal level providing a large dynamic range over the array while minimizing the possibility of false returns. The plus and minus supplies to the potentiometers are regulated down from ± 15 volts to increase the

discrimination of the threshold adjustment as well as isolate the thresholds from the ± 15 volt supplies.

3.5 Digital Board

The digital board, Fig. 20, accepts the 20 digitized channels from the comparators along with the Laser Fire Signal. The Laser Fire Signal, generated by the Mast Controller, causes the laser to fire and is used by the receiver to synchronize itself with the incoming laser energy, Timing Diagram, Fig. 21. Upon receipt of the Laser Fire Signal the 20 j-k flip-flops are reset clearing the stored channels from the last laser shot. The two one-shots then form a time window during which the j-k flip-flops are allowed to change state if their clock inputs experience a falling transition. By this window mechanism only channels which have been illuminated during the window will be set, thereby discriminating against noise pulses which may occur at other times. In fact since the laser return trails the injected laser noise by several hundred nanoseconds (due to the relatively slow response of the photodiode, amp, comparator circuit), by delaying the beginning of the window the system effectively masks out the early laser noise pulses. Both the delay and width of window are independently variable with the ports P1 and P2 respectively.

After the window has closed one or more channels should have been latched. The question now arises of how to relay this information to the obstacle detection computer. Since the data path to the computer is only 16 bits wide this precludes the sending of all 20 bits in parallel. One could send five bits to indicate which element has

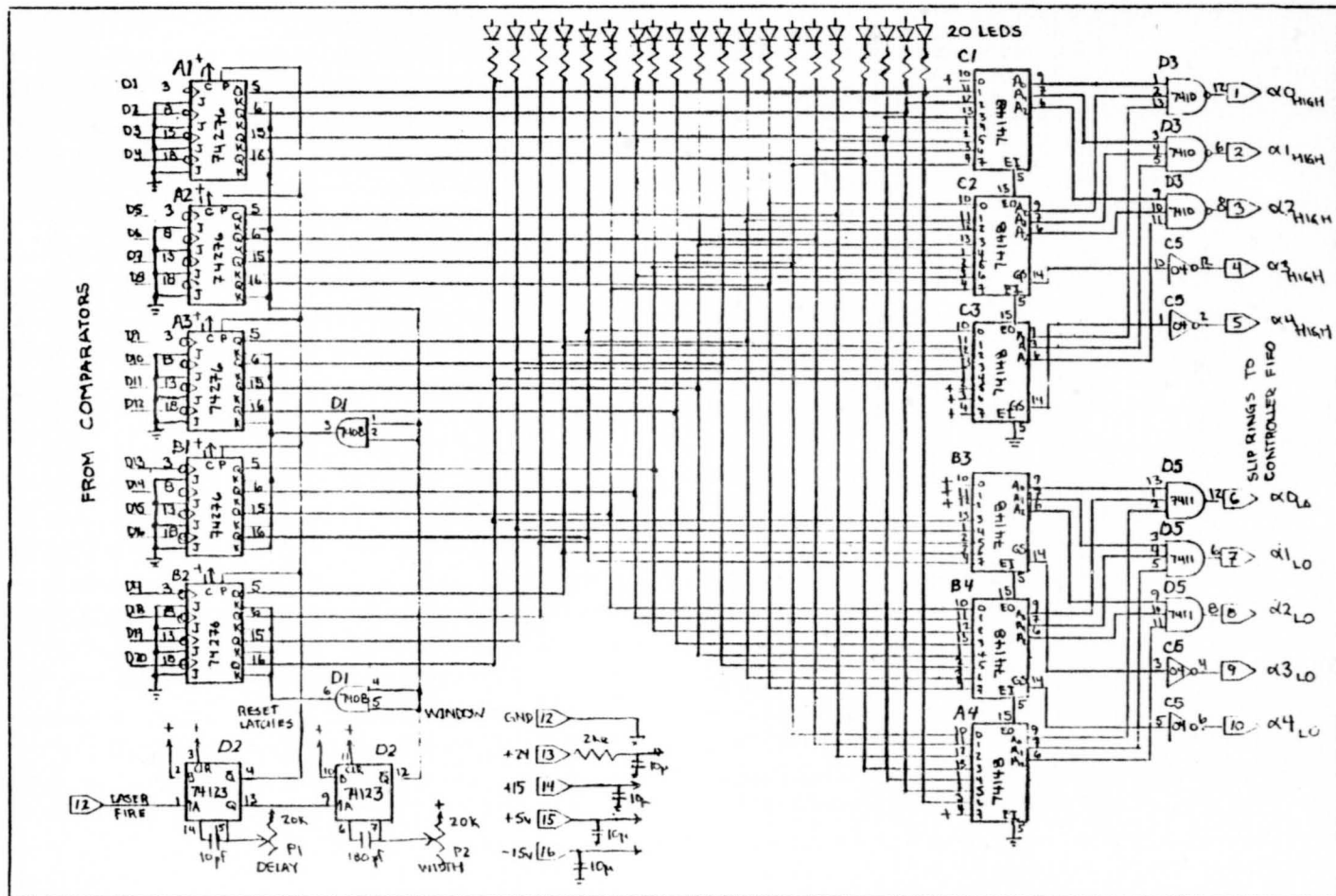


FIGURE 20a. DIGITAL TIMING AND DISPLAY BOARD

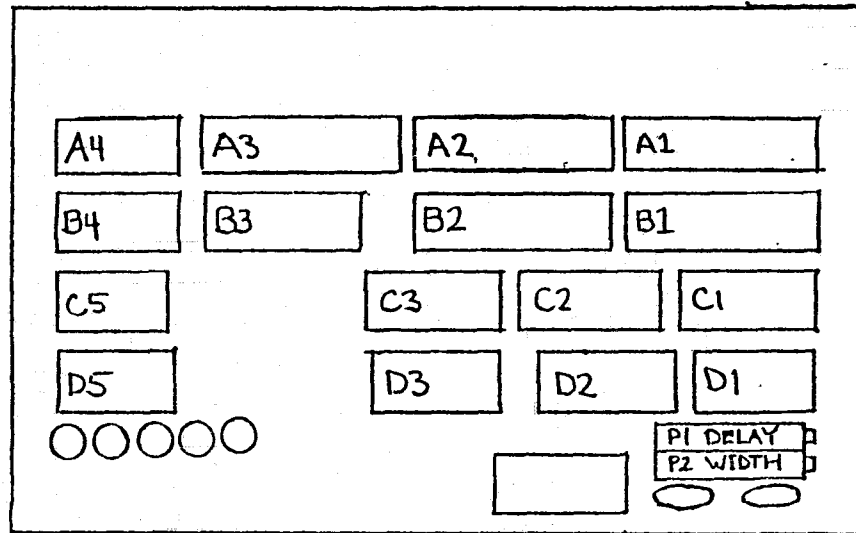


FIGURE 20b. DIGITAL BOARD LAYOUT

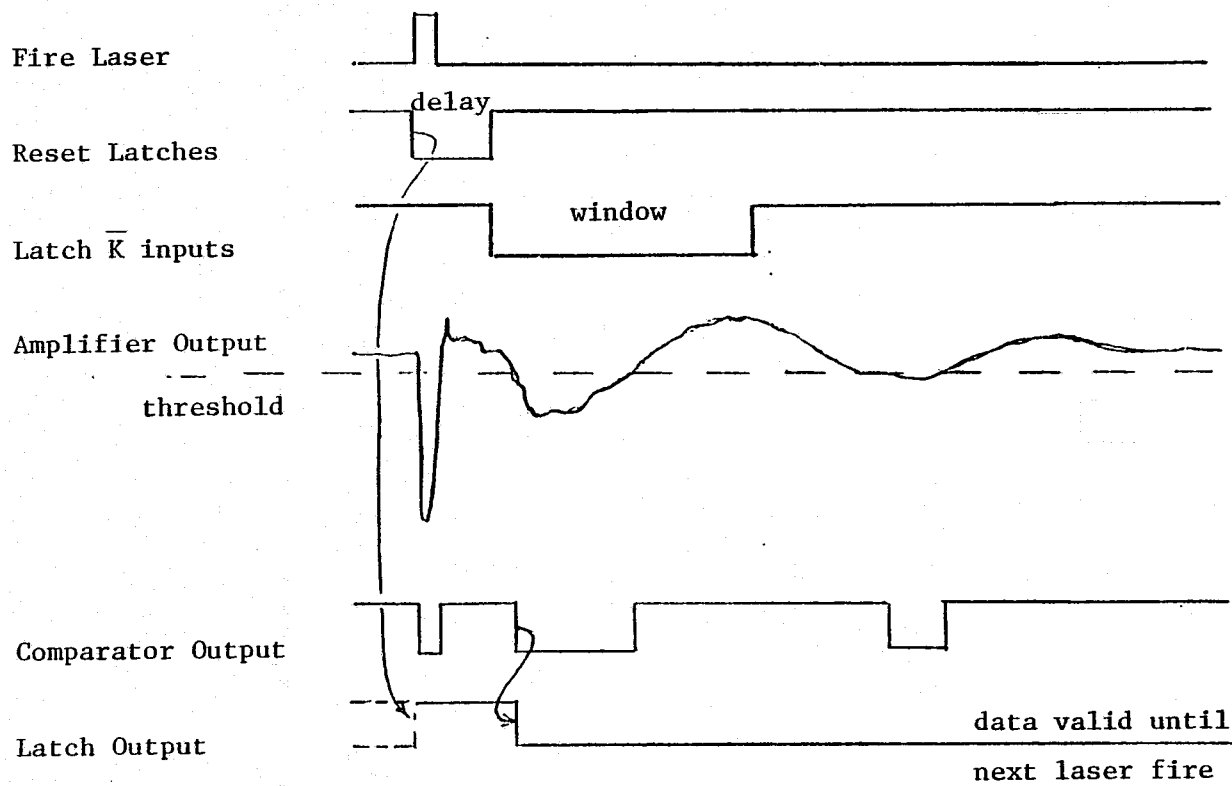


FIGURE 21. DETECTOR SYSTEM TIMING DIAGRAM

been illuminated, yet this would ignore the event of more than one return. The scheme implemented on the digital board generates five bits corresponding to the highest photodiode excited and another five bits representing the lowest illuminated element. The two five-bit words are then concatenated into a single ten-bit word to be sent in parallel to the Mast Controller FIFO (First-In-First-Out buffer).

The details of this encoding scheme can best be seen in the digital board schematic, Fig. 20. These are two sets of octal priority encoders (74148). The lower set has det #20 on its least significant input and the upper set has det #1 on its least significant input. Note that if no inputs are set then the output is uniquely $\alpha_{04}^{\#1} = 0$ $\alpha_{04}^{\#} = 7$, a result which is used in the obstacle detection algorithms to indicate a missing return.

PART 4

ALIGNMENT/CALIBRATION

4.1 Pointing Angle, Focus, Aperture, Thresholds, Time-Window

Alignment of the detector involves only five variables: pointing angle, focus, aperture, comparator thresholds and time-window. The pointing angle or attitude of the camera, defined as the angle between the mast and the center of receiver f.o.v., is adjusted by means of the worm gear connecting the camera to the mast. With 120 teeth on the gear a single turn of the worm results in a 3° change in camera attitude. The desired pointing angle must be fully determined by future evaluation of its performance in ± 30 pitch and roll, but has been estimated as 40° in early level terrain experiments.

The focus of the camera is determined by the lens to array position. Since the laser at 904 nm is outside the normal photographic range, the standard Pentax lens mount to image plane distance cannot be used. Instead the correct lens to array distance must be determined experimentally. From the lens-makers-equation $\frac{1}{f} = \frac{1}{s} + \frac{1}{d}$ the image distance, s , can be determined from the object distance, d . If the mean object distance is two meters then for a 35 mm lens the image distance is 35.62 mm, that is, if the lens is set to focus at two meters then the array should be placed at 35.62 mm from the idealized principle lens plane. But since the position of the idealized lens plane is unknown, the plane to array distance must be adjusted indirectly through field of view measurements. A 19 mm image plane, measured from the centers of 1st diode to the 20th diode, when placed from 35.62 mm from

the lens plane should provide a 29.87° field of view. Hence to align the lens focus, the lens should be set to two meters (using the infra-red scale pointer) and the position of the array board adjusted until a 29.87° f.o.v. is obtained. The field of view can be quickly determined by holding the receiver fixed and moving the laser while observing the amplified outputs of dets 20 and 1. Using the infra-red TV camera and monitor, measure the position of the laser spot when channels 1 and 20 are at their maximum. The field of view of the lens can be obtained from the laser positions.

The aperture of the lens should be made as small as possible while still allowing reliable returns over all surfaces encountered. The smaller size increases the depth-of-field, while decreasing the double returns possible with strong returns from ranges in poor focus.

The thresholds should be adjusted with the laser reflecting off a level surface of poor reflecting characteristics. In this arrangement the lower photodiodes (det #1) will be operating at longer ranges and hence receiving smaller signals. By turning the potentiometers (clockwise increases sensitivity) the element-by-element sensitivity can be tailored to the varying ranges expected. With the laser spot in the center of the n^{th} photodiode, determined by observing amplified photodiode signal, the threshold should be set so that a return is possible off the poorest reflector with only minimum overlap between adjacent elements.

The time-window as explained earlier should occur only during expected transitions from comparators. By adjusting the delay poten-

tiometer, begin the window with the earliest detector's return. The laser noise which may pass through the comparator threshold then occurs before the window and will be ignored. The window width should then be adjusted to accept all genuine detector transitions (~2 μ sec).

Calibration of the detector can be performed in the same manner as the field of view was determined in the focusing procedure. By measuring the position of the laser spot which maximizes the return to each detector their respective elevation angles can be measured. The first step in the procedure is to level the mast. A bubble level was useful here. The next step is to disconnect the mast controller (at least Motor Speed and Rate Buffer Boards) so that the mirror can be hand turned and the drive to the laser opened. By using an external trigger to fire the laser (1-3 KHz) the spot can be observed with the silicon-intensified TV camera to move as the mirror is turned manually. As the laser spot is moved in and out along the floor, the location at which each diode's return is maximized can be marked on the floor. (Note, the surface of the floor should have constant reflectivity.) Since the height (Z) of the floor can be assumed to be zero these ranges can be converted to angles for each of the detector elements.

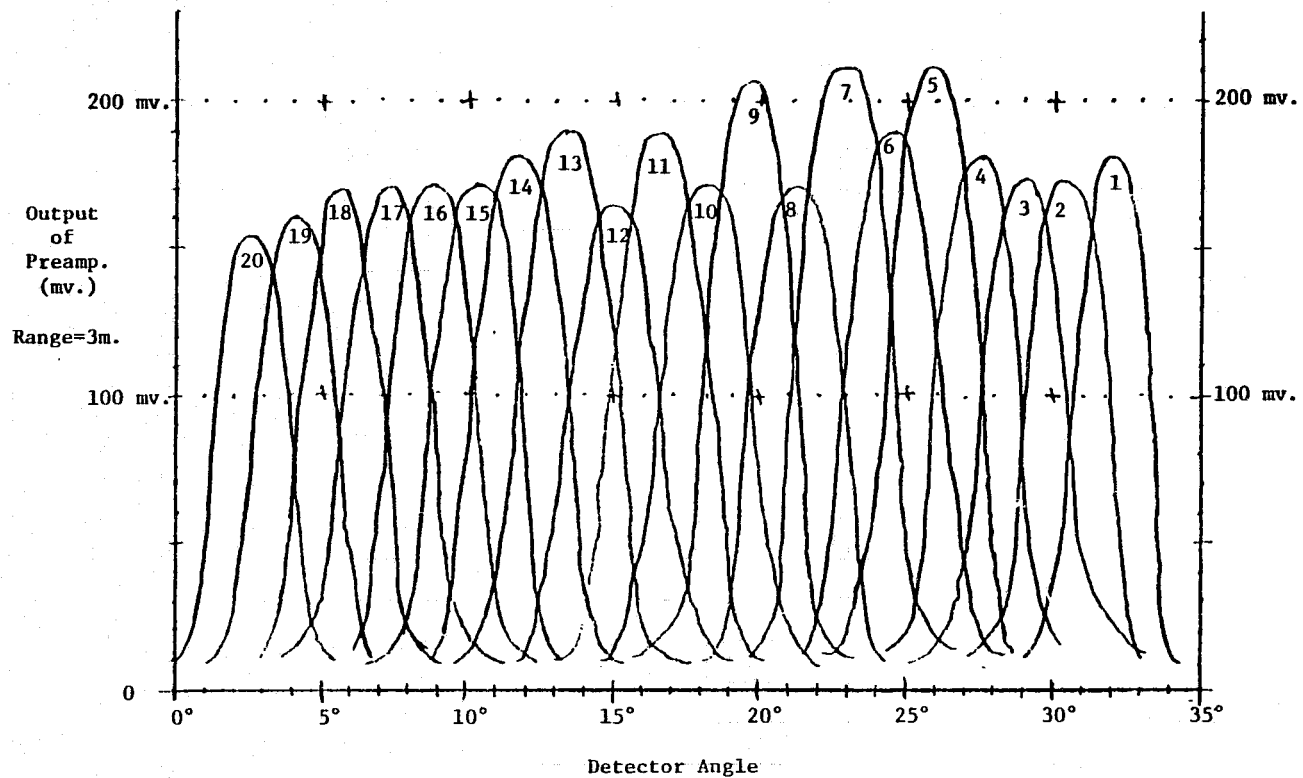
$$\alpha(\alpha\#) = \tan^{-1} R^{\#} / h_{\alpha}$$

where α = elevation angle of n^{th} detector;
 $\alpha^{\#}$ = detector number 1 through 20;
 R = range associated with n^{th} detector;
 h_{α} = height of detector above floor.

This same procedure can be used to calibrate the laser.

Another method of calibration is to hold the laser spot fixed on a surface of constant reflectivity at a constant range while the detector is rotated. Figure 22 is a graph showing the magnitude of each channel's amplifier output as the receiver was rotated. These measurements were taken with a good reflector, the aperture wide open, and at a range of three meters. The variation in peak height from channel to channel is a result of device non-uniformity. The rounding of the individual peaks is indicative of both receiver defocus and a relatively large laser spot on the reflector. There is considerable overlap between adjacent diode response curves and the thresholds must be set carefully if only a single return is desired. The problem is greatly complicated when a multiplicity of ranges and reflectivities are considered. Yet with proper adjustment of the lens aperture and the 20 thresholds, returns can be restricted to single returns and double returns from adjacent elements. It should be noted that the overlap increases the effective resolution of the detector since the number of possible returns has been increased to 39, 20 single returns and 19 double returns. The double (or triple) returns, provided for in the detector's encoders, can be exploited by the obstacle detection computer to effectively double (triple) the receiver's resolution.

In general the measurements taken thus far have shown that the angular separation between elements ($\sim 1.5^\circ$) can vary somewhat with focus but remain constant over the length of the array without the pronounced pinching that occurs with receivers with wider fields of



$$\text{Angle Det\#1} - \text{Angle Det\#20} = 32.0^\circ - 2.4^\circ = \underline{29.6^\circ}$$

$$\text{Det. to Det. Angle} = 29.6^\circ / 19 = \underline{1.55^\circ}$$

FIGURE 22. SIGNAL RETURN vs. ELEVATION ANGLE OF SOURCE

view. Since the separation can be assumed constant over the array the simplest calibration would only measure the angles between two elements, presumably det #1 and #20, and divide by the number of incremental separations between them. Thus if the focus has somehow been changed two quick measurements can re-establish the relation between detector number and angle, α , required by the obstacle detection computer.

PART 5

20 ELEMENT RECEIVER CONCLUSION

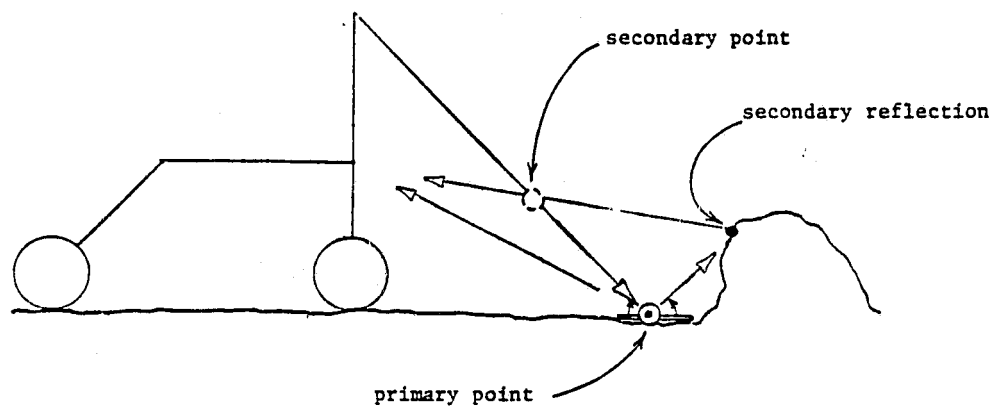
The 20 element receiver has been in operation since the fall of 1979. During this time its overall performance has been satisfactory meeting its design goals, yet some shortcomings have subsequently become apparent.

5.1 Secondary Returns

The most surprising problem was that of secondary returns. As can be seen in Fig. 23, secondary returns occur when the detector receives two returns, one from the primary laser spot and the second from the primary's reflection off a second surface. This occurs when specular reflectors, such as mirrors, polished metal or glass, either deflect the primary beam to a second surface or allow the viewing of the primary spot from a second vantage. The first attempt at a solution was to use diodes and amplifier feedthrough to the comparator's thresholds to select the channel with the maximum signal. This worked only marginally due to the low level signals involved and the fact that primary and secondary signals are often the same or even reversed with respect to their magnitudes. Although Mars may not have many specular surfaces in other applications any laser triangulation system will suffer from this malady, a problem which worsens with detector field of view.

5.2 Missing Returns

Another problem facing laser triangulation is that of missing



Primary reflection specular

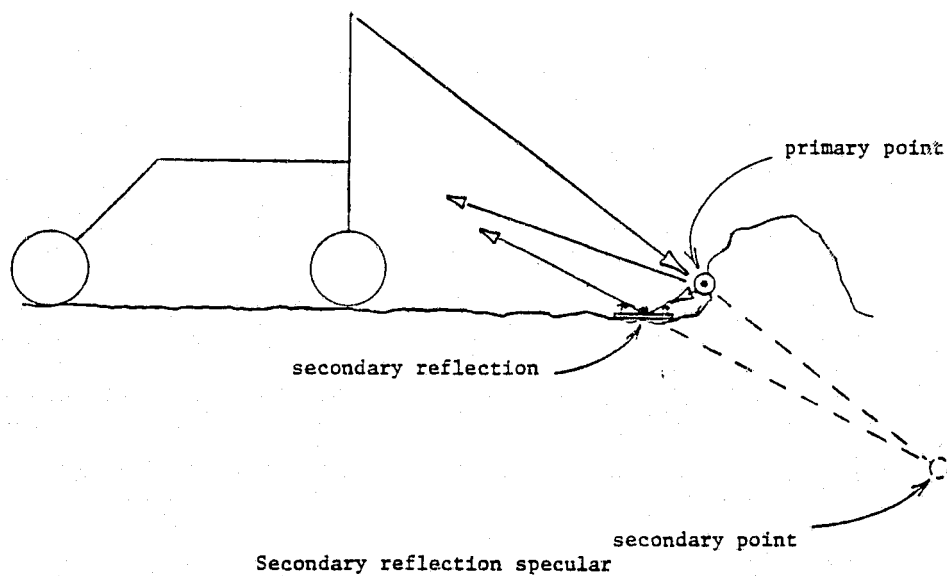


FIGURE 23. SECONDARY RETURNS TERRAIN AMBIGUITY

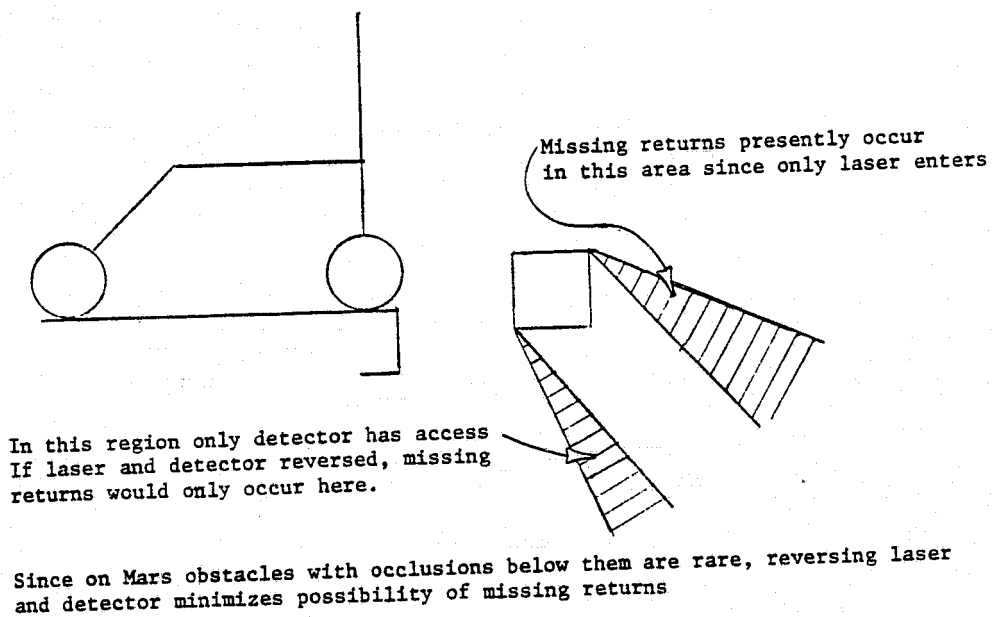
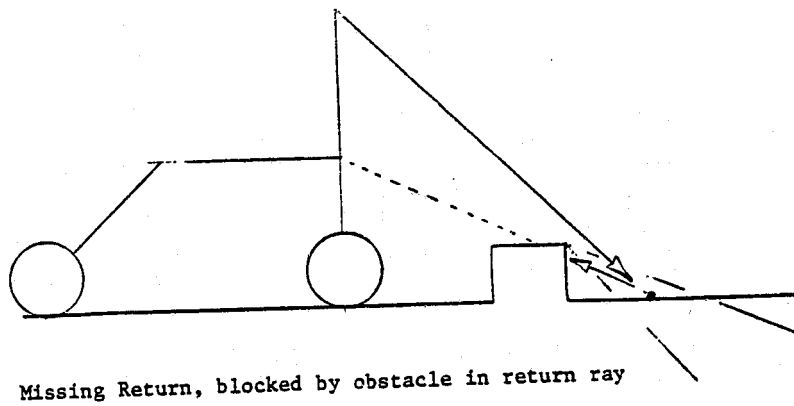


FIGURE 24. MISSING RETURN PROBLEM

returns. In this case some object blocks the path of the laser spot between the terrain and the receiver. In our application this normally happens when the laser fires over an obstacle and strikes the terrain at a point shadowed from the detector by the same obstacle, Fig. 24. On a Martian rover the fact the surface is generally a function of two variables can be exploited to minimize the number of missing returns. In particular by mounting the detector above the laser a missing return could only occur if the laser spot were beneath an obstacle and its return blocked from above. Hence, in the peculiar environment of Mars, where overhanging objects are rare, by placing the detector above the laser and bringing the two as close as possible the problem of missing returns would be minimized.

5.3 Field of View

The field of view (30°) of the 20 element detector presently limits the roll and pitch the vehicle can sustain. Although it is yet to be experimentally demonstrated it seems clear that slopes exceeding $\pm 25^\circ$ with respect to the vehicle would be outside the sensors' scope. Building a second receiver would alleviate this problem as would rotating the detector under computer control.

5.4 Reliability

The reliability of the device as presently constructed is also of some concern. The many small wires and parts under rapid acceleration or continued handling are a source of failures and difficult to locate. The use of printed circuit construction would be a

great improvement as well as an aid in developing a second detector if desired.

5.5 Resolution

The resolution of the device at 1.5° has yet to be proven sufficient. Difficulties in the Mast Controller and the PRIME computer interface have prevented the evaluation of the perception system until late August of 1980. Should it prove necessary the multiple return encoding in the detector could allow through the use of double overlap returns a two-fold increase in resolution.

PART 6

1024 ELEMENT CHARGE COUPLED PHOTODIODE RECEIVER

6.1 General Description

The 1024 element receiver is divided into two main packages: 1) the detector head, (3 3/4" x 3 3/4" x 4 3/4"), Fig. 25, housing the Array Board, a 12.5 mm/f:1.9 lens and filter, and 2) the 4 1/2 x 6 1/2" Mother Board holding the digital timing and signal processing circuits. The detector head is mounted below the laser with the optical axis of the lens, the 1024 element linear array, and the laser ray all in the same vertical plane, Fig. 3. Sampling of each of the 1024 photodiodes is accomplished by means of a parallel transfer into dual charge coupled analog shift registers aboard the array chip, Fig. 26, followed by sequential passage through a peak detection circuit, Fig. 27, on the Mother Board. Timing for the CCD registers including four phase clocks, transfer and reset strobes are generated on the Mother Board and relayed to the Array Board along a six-inch 16 cond, ribbon cable. Amplified video output then returns to the signal conditioner and peak detector along a coaxial cable. Adjustments include video sample rate (1-5 MHz) and peak threshold. A four-digit BCD display indicates which of the elements has been illuminated.

Overall the 1024 element charge coupled receiver, in conjunction with 100 watt 200 ns laser pulser operating at 2 KHz offers 3 min 30 sec resolution within 60° field of view and a three meter range.

6.2 Optics

The lens employed in the 1024 element receiver is a Cosmucar

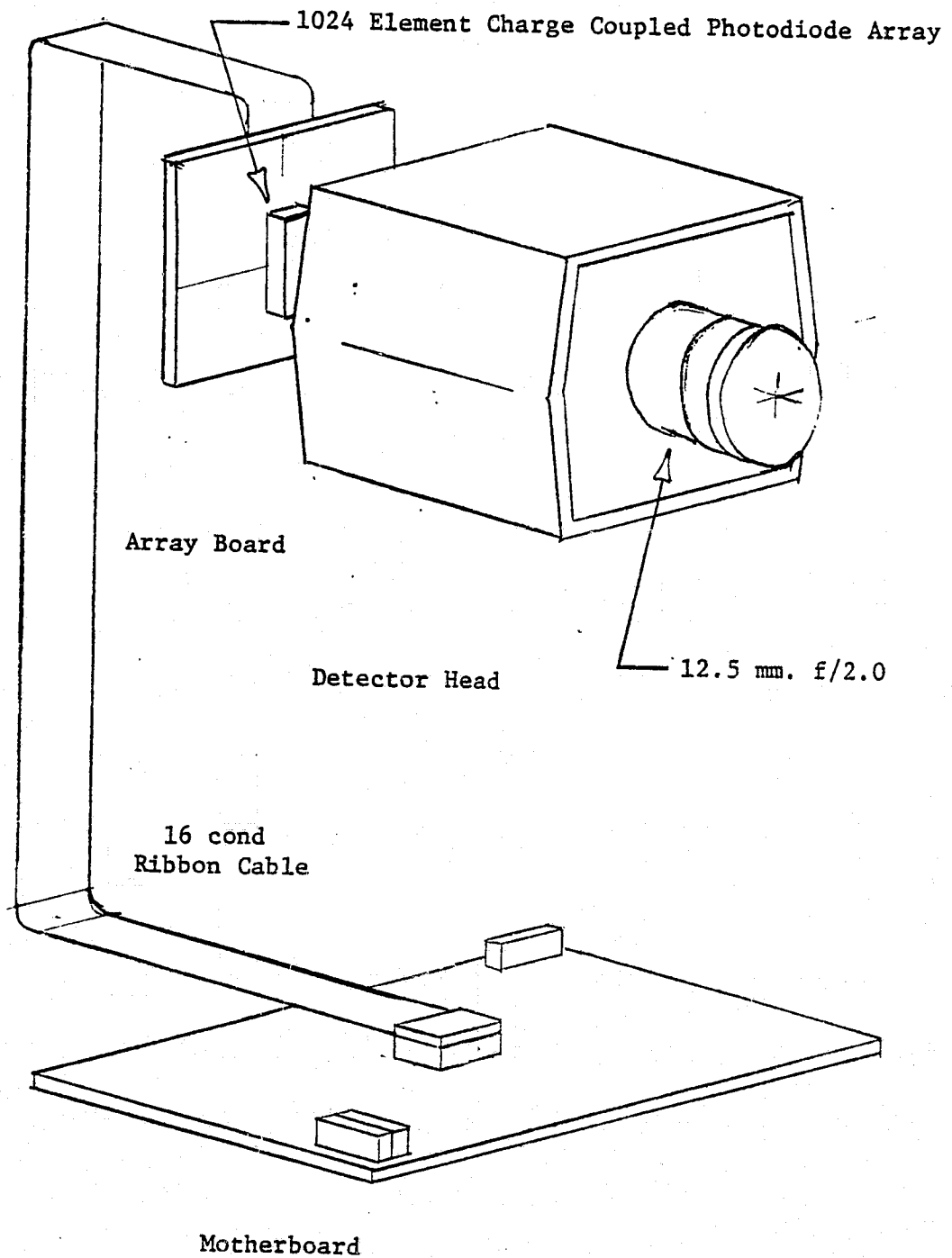


FIG. 25. 1024 ELEMENT RECEIVER CONSTRUCTION

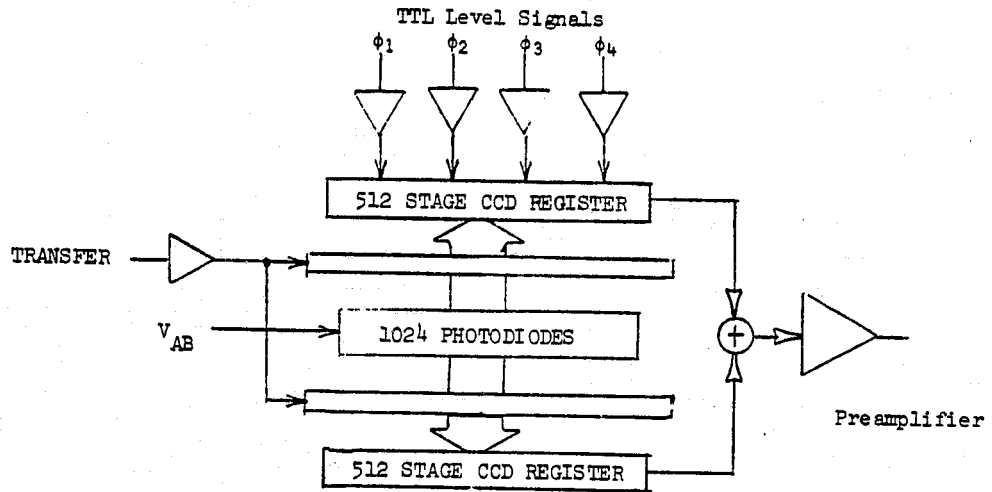


FIG. 26. 1024 CCD ARRAY BLOCK DIAGRAM

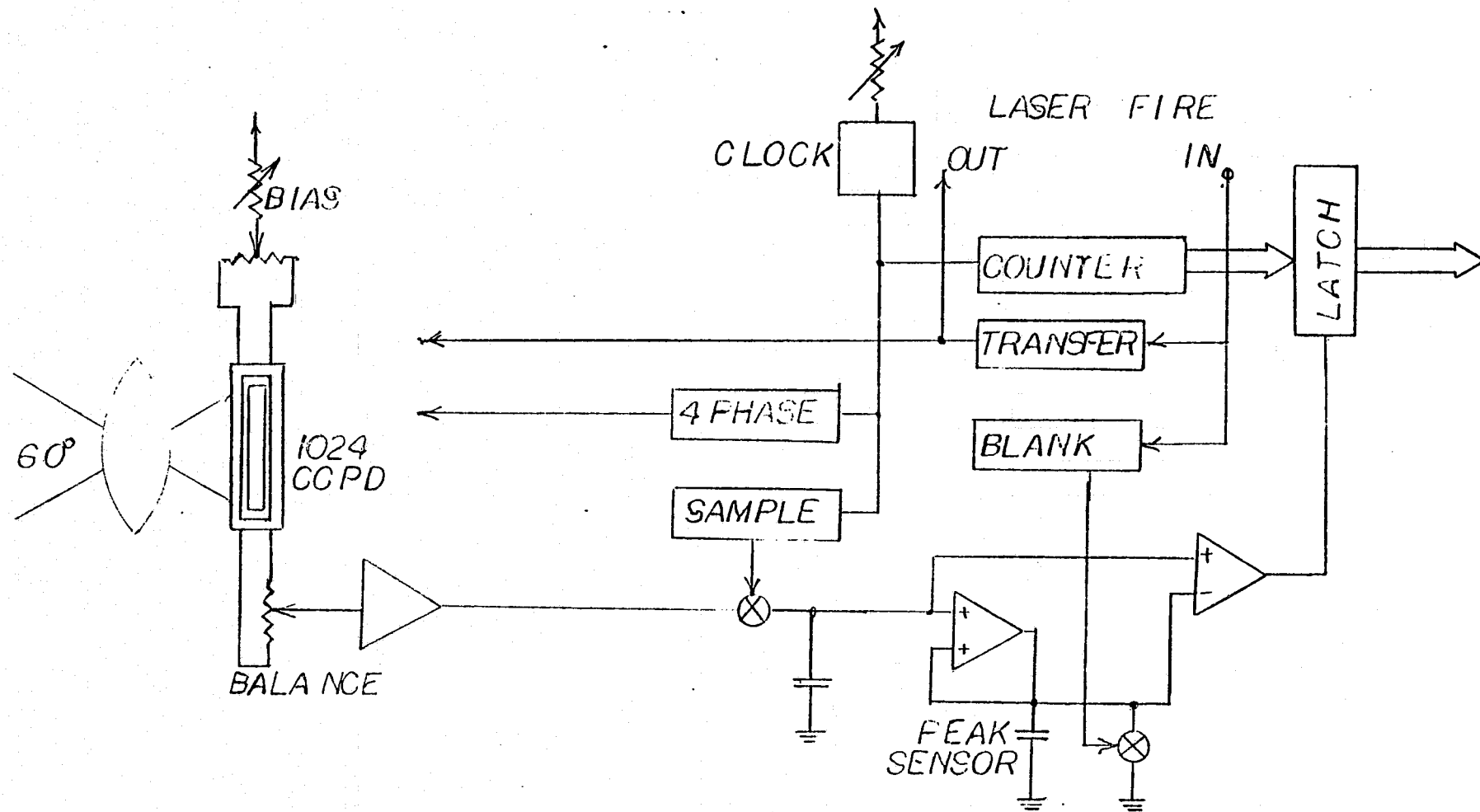


FIG. 27. BLOCK DIAGRAM OF 1024 CCD RECEIVER

B1218, with a 12.5 mm focal length and an f-number of 1.8. Designed for use with one-inch vidicon tubes its maximum field of view is given as $64^{\circ} 50'$. The 16 mm length of 1024 CCPD when combined with the 12.5 mm lens should provide a field of view of 65° . The resolution of the receiver can be estimated as $65^{\circ}/1024 \sim 3 \text{ min } 30 \text{ sec}$.

Another optical component in the 1024 element receiver is a bandpass filter used to limit the ambient light striking the array. Located between the lens and the array a Wratten 87C lowpass filter only transmits light with a wavelength exceeding 850 nanometers, Fig. 28. Since the response of a silicon photodiode begins to fall off rapidly around 950 nanometers the combination of the Wratten filter and photodiode response effectively forms a bandpass filter around the laser wavelength (904 nm).

6.3 1024 Element Charge Coupled Photodiode Array

The photosensitive window of the array is comprised of a 1024, $16\mu\text{m} \times 16 \mu\text{m}$ p-n junction photodiodes in a row 16 mm long, Appendix B. Light incident on the sensing aperture generates photocurrent which is integrated and stored as a charge on the capacitance of the reverse biased photodiodes. Pulsing of the transfer gate then simultaneously transfers the accumulated photocharge into one of two 512 stage surface channel CCD analog shift registers. The odd diodes are switched into one register and the even into another. Readout is accomplished by clocking the shift registers so that the charge packets are delivered sequentially to two on-chip charge detection diodes. The outputs of the two charge detectors are then multiplexed off-chip

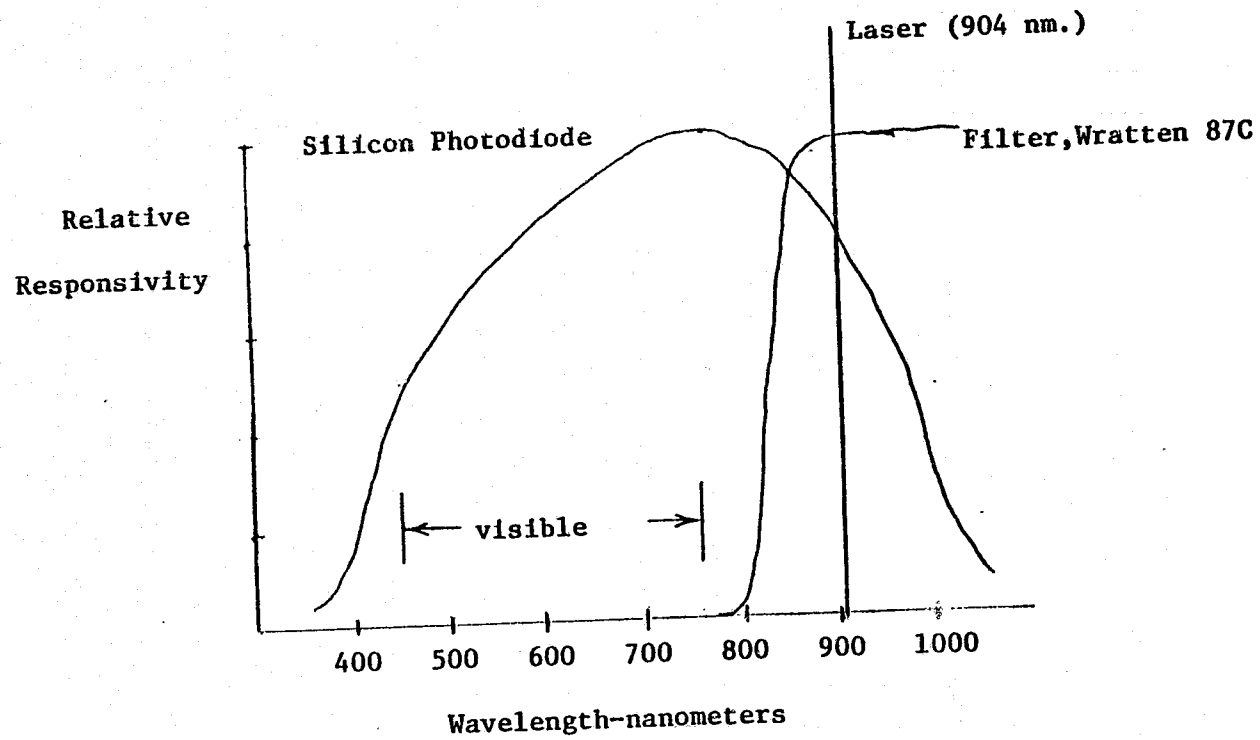


FIG. 28. RELATIVE RESPONSE OF SILICON PHOTODIODE AND WRATTEN FILTER

to obtain a step-wise continuous video signal.

The speed of the device, limited by transfer inefficiency and thermal heating considerations, is given as 5 MHz. However in this ranging application the array is operated at 2 MHz or a 2 KHz line rate. This is because the laser diode, which must be run at maximum power (100 watts) and pulse width (200 ns), in order to be sensed by the receiver, can only be run at 2 KHz if it is not to exceed its rated duty factors (.04%).

The feasibility of the receiver/laser combination was analyzed before the array was acquired assuming a 40 ns, 100 watts laser and an array noise equivalent exposure as given of 10^{-3} watts/cm².⁹ The calculations, similar to those in Part 2.1, indicated that the signal returning from three meters would be approximately 40 times the noise level and hence the array was purchased. Subsequently when the array was tested it was discovered that the signal, from a poor reflector, equalled the noise level at a two-meter range. The error in the analysis was the assumption that the laser could be collimated sufficiently to ensure that the laser spot image was concentrated on only a single element. To fall within a single element the laser spot size, x, at three meters, would have to have been

$$\frac{x}{3m} = \frac{16 \mu m}{12.5 mm} \rightarrow x = 3.7 mm$$

To collimate the .41 mm laser source to 3.7 mm at three meters would have taken a lens of more than 300 mm with an exit pupil much larger than the mirror face. The lens that was used has a focal length of 85 mm which at a range of three meters gives a spot size of

approximately 2 cm. A 2 cm spot has as much area as 25,4 mm spots and hence due to the lack of sufficient collimation the actual intensity on the array was 1/25th of the level expected, or 1.6 times noise level. It was necessary to increase the 40 n sec pulse to 200 ns and at the same time reduce operating speed from 10 KHz to 2 KHz to enable the 1024 element receiver to function in the three meter range.

A further consideration involved in the selection of this array was the anti-blooming gate feature whereby the integration period can be made shorter than the line read-out time. By pulsing the anti-blooming gate, V_{AB} , the photodiodes are reset thereby limiting the integration period to the time between the trailing edge of V_{AB} and the trailing edge of the transfer gate, ϕ_T , 1.5 μ sec minimum. By this mechanism the anti-blooming gate acts as an electronic shutter that when open accepts the pulsed laser energy but when closed reduces the ambient light noise by a factor of

$$\frac{500 \mu\text{sec}}{1.5 \mu\text{sec}} \sim 300.$$

The anti-blooming gate also allows the array to be run synchronously with the laser. Without the V_{AB} feature the charge accumulated since the last laser shot would have to be shifted out before the laser could be fired, effectively halving detector speed.

The array board is a 3 x 3 inch printed circuit board holding the 1024 CCPD array and its associated drivers, bias circuits and amplifiers, Fig. B1. The drivers (MH 0026), Fig. B2, accept the TTL level timing signals and level shift them to the necessary 15 volt swing. The

bias circuits generate the d.c. bias voltages needed; substrate, output drains, input and output gate biases. The amplifier is a CA 3127, Fig B3, configured as a common emitter current amplifier with a current mirror as base bias.¹⁰

The mother board contains the digital control/timing circuitry and the analog signal processing circuit, Appendix B, Fig. B4. The timing begins with oscillator, U1, whose frequency can be varied by P1 from 1.5 to 8 MHz giving sample rates of 750 KHz to 4 MHz. This clock frequency can be monitored at pin J1-2. The four-phase clocks, ϕ_1 , ϕ_2 , ϕ_3 , ϕ_4 , transfer pulse ϕ_T , and the sampling pulse are all derived from this clock. Scan Start on pin J1-E can be used to sync up to the line rate.

The analog circuitry consists of sample and hold circuit and a d.c. restoration circuit. The sample and hold circuit helps to isolate high frequency noise while the d.c. restoration circuit can be used to set the d.c. level of the video signal and forms a high pass filter against noise sources with wavelength longer than line time. The switch edge cancellation circuit is used to cancel clock noise coupled through the sample switch and the blanking circuit pulls the video to zero volts between the 1024th sample pulse and the next transfer pulse.

PART 7

ADDITIONS/MODIFICATIONS TO RETICON DEMONSTRATION BOARD

The array and demonstration board as purchased from Reticon Corporation was described in Part 6 and in Appendix B. Some modifications and additions were required however to incorporate the demonstration board into the elevation scanning mast controller. Among these adaptations were: increasing amplification of preamplifier; addition of resettable peak detectors; anti-blooming gate implementation; changes to timing to allow array to run synchronously with mast controller; interface to controller FIFOs; and a display of which elements were illuminated.

7.1 Preamp Aboard Array Board

An LM 318 high speed operational amplifier was inserted for U7, LM310 unity-gain buffer, on the array board, Fig. 29. Since the pin-out was almost identical this was chosen as the location to increase the gain before the sample-and-hold circuit. The increase in gain was possible because the old circuit was designed for one volt saturation signals whereas the laser returns are on the order of ten to 100 millivolts. The gain allowed the signal level to exceed the switching noise introduced in the sample-and-hold circuit and allows easier detection of laser return.

7.2 Anti-Blooming Gate

As in the device data sheet the charge on the photodiodes can be reset by pulsing V_{AB} to +5 volts for at least 1 μ sec. The integration

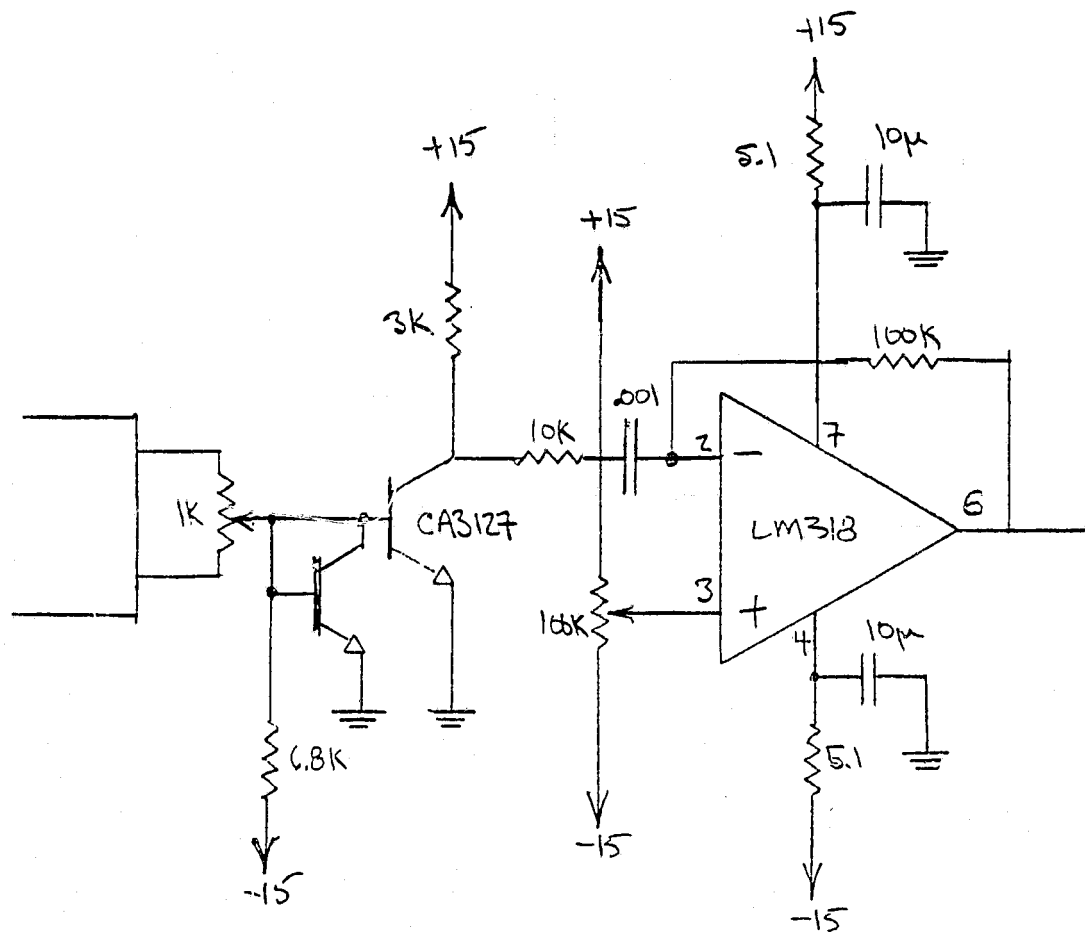


FIG. 29. PREAMPLIFIER ABOARD ARRAY BOARD

period is then the time between the trailing edge of V_{AB} and the trailing edge of next ϕ_T pulse. In this application V_{AB} is held high except when the laser is fired. This avoids a 1 μ sec time delay in firing the laser associated with holding V_{AB} high. Instead when the laser fire signal arrives V_{AB} is brought Lo and ϕ_T is applied simultaneously. In fact V_{AB} is tied directly to ϕ_T on the array board. This effectively reduces all ambient sources by a factor of approximately transfer pulse width/line scan time = 1 μ sec/500 μ sec \sim 500.

7.3 Peak Detectors

The function of the peak detector is to find the maximum signal along the line scan. U_{16} and U_{17} on the mother board were replaced with LM311 comparators, Fig. 30. The first comparator ensures that the storage capacitor is changed to the maximum level encountered while the second comparator senses where the video signal exceeds the stored peak. When the peak is exceeded the latches monitoring the array counter store the count value at the time of the peak. The blanking circuit on the mother board is used to reset the peak storage capacitor. The resetting prepares the peak detector for the next line and also forms a high pass filter discriminating against noise with periods larger than the line rate.

7.4 Synchronization with Mast Controller and Dark Current Limiting

The demonstration boards run on their own internal clock asynchronous with anything external. As described in Appendix B there are two counters, the Array Counter and Integration Counter, which

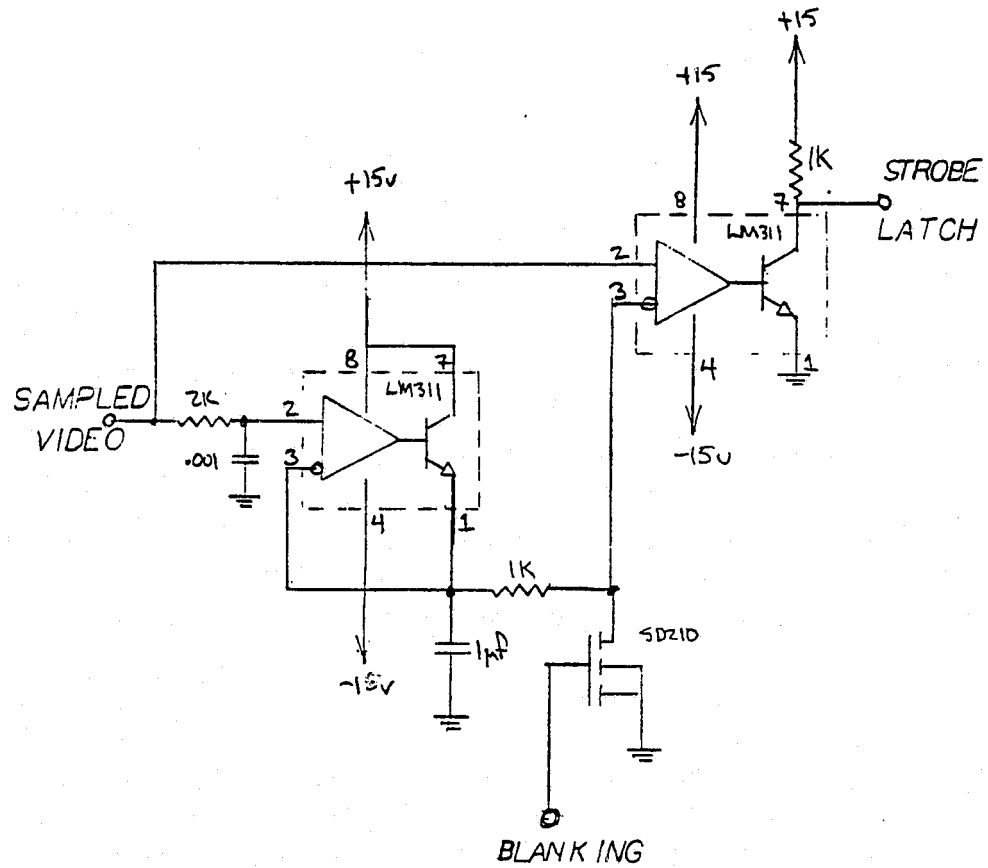


FIG. 30. PEAK DETECTOR WITH BLANKING RESET

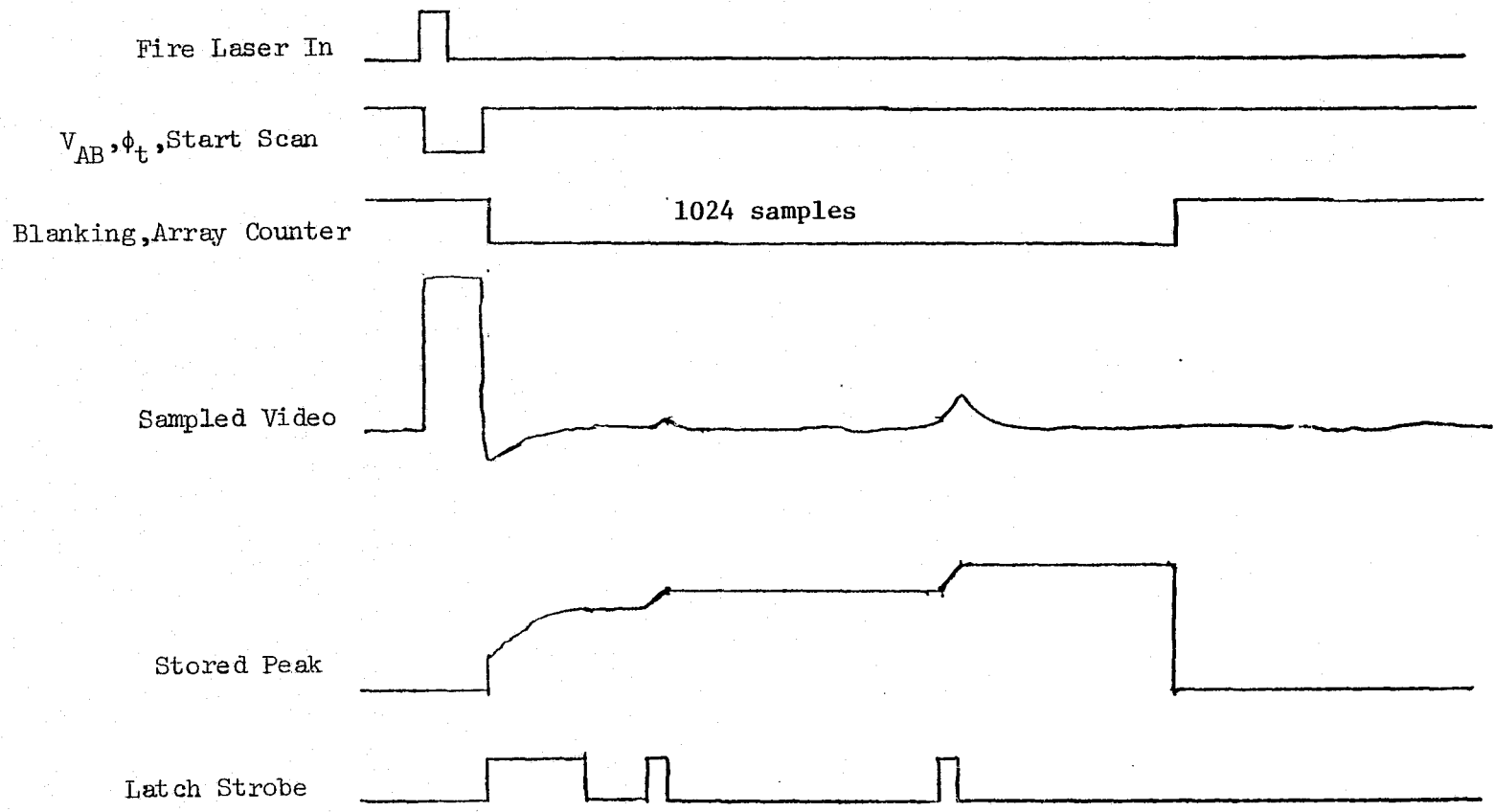


FIG. 31 TIMING DIAGRAM RETICON MODIFICATIONS

control, the time the blanking circuit is activated, and the time between transfer pulses. It is necessary that this system be modified to operate at a rate dictated by the mast controller. When the laser fire signal arrives the array must be ready to accept the reflected laser light and shift it out before the next laser pulse.

Before any laser pulse arrives the system is in the Stand By mode. In this mode the 4ϕ clocks continue running, thereby preventing the build-up of dark current in CCD shift registers. Also the ϕ_{TRANSFER} is disabled holding V_{AB} HI and keeping CCD registers free of charge. This ensures that the device will be prepared to integrate light as soon as possible after receipt of Fire Laser In.

This Stand By modification is realized by inserting Fire Laser In between the integration counter U_{12} and U_8 . Then until the arrival of FIRE LASER IN the system continues to cycle the four-phase clocks while ϕ_T and V_{AB} remain HI. Upon the arrival of FIRELASER IN, the transfer ϕ_T and V_{AB} are enabled, and the blanking generator released. Fire Laser Out (same as scan start) which is used to fire the laser, falls with ϕ_T , and V_{AB} , allowing time for the array to begin integration before the laser is fired. After the transfer is complete the 4ϕ clocks shift the video out to the signal processing circuits until the array counter counts 1024 and sets the blanking and resets the peak storage capacitor.

7.5 Latches Interface to Mast FIFOs

A pair of 74174 hex latches are used to monitor the array counter and are clocked by the peak detector output. At the end of the

line scan they contain the value of the array counter when the peak was sensed. This information is held for the FIFOs to absorb until the next laser pulse occurs and the blanking Flip-Flop is released.

7.6 Display

A display has been constructed giving the BCD count of the number of clock pulses at the time the peak was sensed. Constructed from 4-74143, counter and seven segment drivers, the counters are clocked by the clock out (J1-7) and latched by the output of the peak detector.

PART 8

1024 CCPD RECEIVER CONCLUSION

8.1 360° Vision Around Vehicle

As the CCPD receiver revolves on the mast it sweeps it's 60° field of view 360° around the vehicle. During that time 1024 shots (32 azimuth· 32 elevation) are taken with 500 μsec. allotted for each shot. With anti-blooming integration control only 1.5 μsec. are used to gather light. In a 8 to 10 second scan the remaining time could be used to interlace video information so as to gather a grey level image that completely surrounds the vehicle. What would be needed would be a mechanical shutter removing the infrared filter during the grey level line samples and a video frame store for display. Also some form of slip ring to relay the video stream from the rotating mast. The camera should of course be mounted as high as possible to enable the system to survey behind the machine as well. Moving the laser and sensor closer together, made possible by the high resolution of the 1024 CCPD array, reduces the problem of secondary returns(sec. 5.1), and placing the detector above the laser aids in the missing return case (sec. 5.2).

8.2 Buried Channel Charge Coupled Array

The use of a buried channel CCD array such as that manufactured by Fairchild Camera would offer better performance since they are inherently a lower noise device¹¹ when compared to surface channel arrays such as the Reticon CCPD product. Surface channel devices require a bias charge injected into their inputs to overcome the image smearing caused by partially filled interface states with random relaxation times. Injection of charge at the input as well as the reset required at the output ports introduce even more

noise into the video stream.

A buried channel device requires no bias charge hence no injection noise and the reset of the charge detector may be reset at the end of the line scan instead of after every pixel. This method of avoiding injection and reset noise was attempted with the Reticon array but proved unfeasible due to excessive smearing of the laser image along the array length.

Cooling of the device would also minimize noise since much of the noise is thermally generated and the array has been observed to run quite warm.

8.3 Improved Rangefinder

The ultra high resolution of the 1024 element CCPD array permits the laser and receiver to be brought much closer together than possible with the 20 element sensor. In fact if the laser and detector were brought close enough to be reflected off the same mirror then neither the laser nor the receiver need rotate, Fig. 32. Of course the mirror used would have to be larger than the 8-sided s-anner presently used.

With the laser and detector stationary no slip rings would be necessary. Furthermore the two components when so close are housed in a much smaller and practical package. Instead of a 2 meter mast rotating about a vertical axis, a small, (6 inch), mirror mounted in gimbals would scan the laser ranger only where desired through a dust tight window.

The mirror could still rotate through 360° in both azimuth and elevation but slip rings would be needed only for the elevation motor and encoder. An 8-sided mirror with 6-inch faces would be prohibitively large. It seems preferable to employ a single faced mirror foregoing the 360° scan and drive the gimbals with stepping motors. Then the time sacrificed

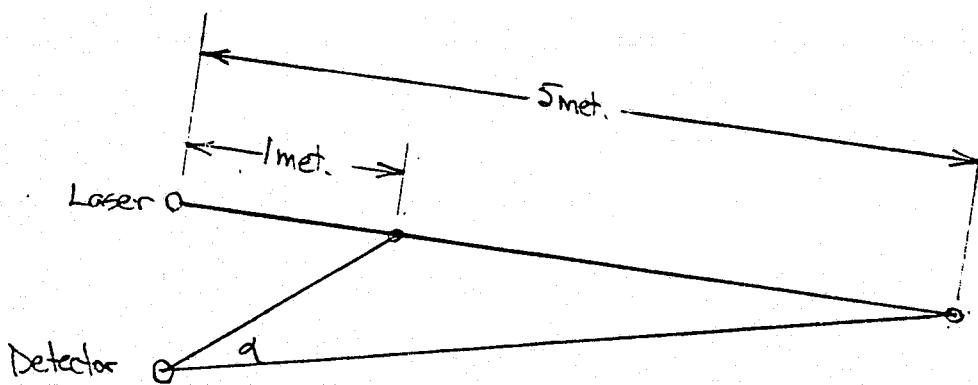
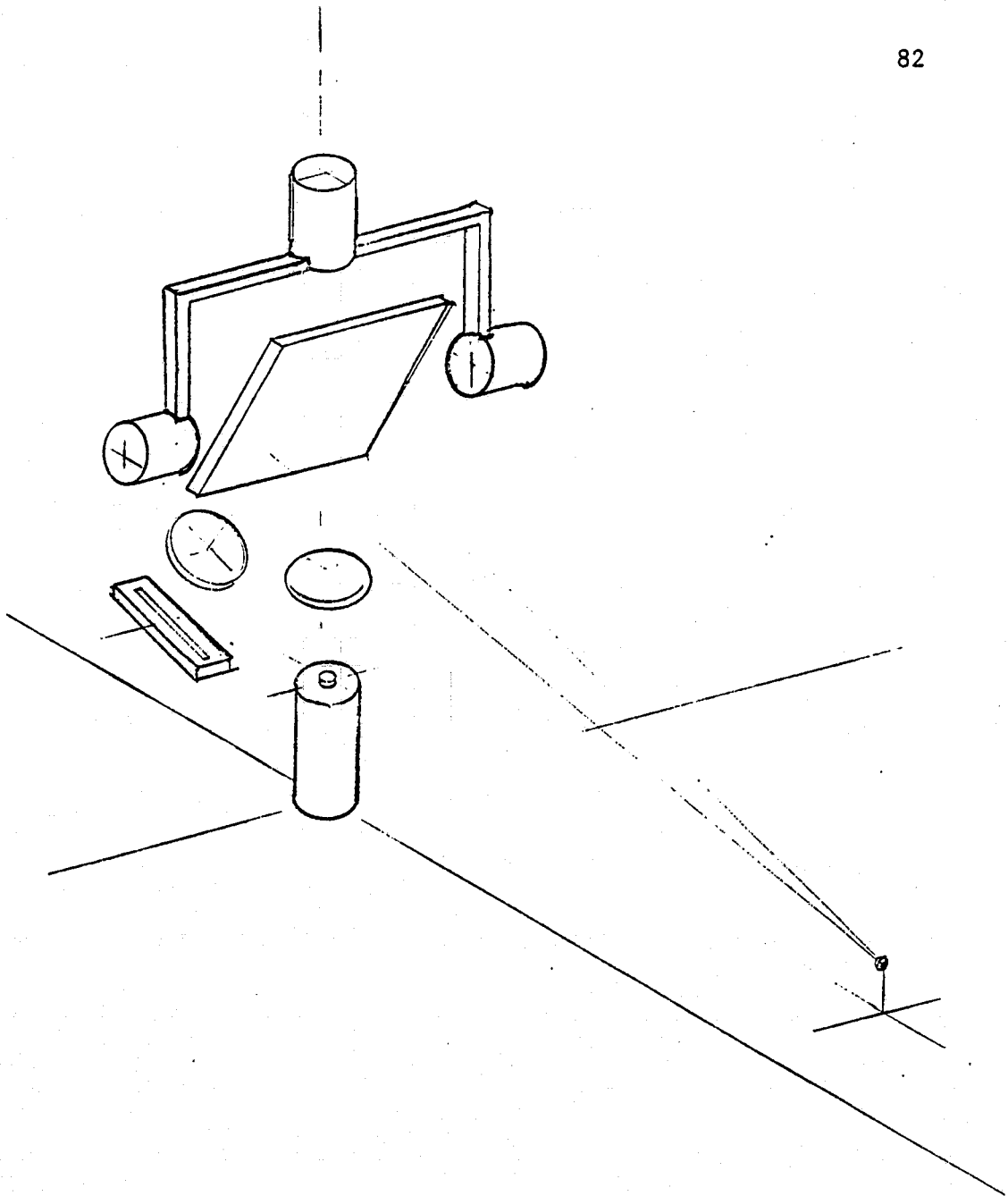


FIG. 32. IMPROVED RANGEFINDER

in using the one-sided mirror could be recovered by not scanning the raser to the rear of the machine. In this case without 360° azimuth scanning even the elevation slip rings could be eliminated.

The question of scan time can be analyzed by assuming an angular resolution, dividing it into the field of view, and multiplying by the time required per motor step. The present scanner has a resolution of 0.35° in elevation and 1.4° in azimuth. Given that the field of view is desired to be 60° in 32 elevation sweeps and 140° in azimuth:

$$\Delta t_{\text{scan}} = \left[32 \left(\frac{60^\circ}{.35^\circ} \right) + \frac{140^\circ}{1.4^\circ} \right] \Delta t_{\text{step}}$$

Stepping motors with a step frequency in excess of 1000steps/sec. are available Appendix B giving a Δt_{step} of approximately 1msec., and a Δt_{scan} of ≈ 6 seconds.

If inertial effects and others contributed a factor of two we still might assume a scan time of 12 seconds; which for a 3 meter range, 1/4 meter /sec. velocity, allows the terrain to be scanned once before the vehicle rolls over it. Or at the mission study speed of 1.5 meters/min. each portion of the surface would be sampled 10 times.

The lens used in the scheme would be of a long focal length, 100mm. or more. It should be chosen so that it's field of view encompasses the laser ray from 1 meter to five and would vary with laser/receiver separation. For example at a separation of 100mm. a receiver field of view of 4.56° would be sufficient. A focal length of 200mm. would be required to subtend 4.56° with a 16mm. array.

Another optical problem, in addition to trying to find a long focal length lens with a small f-number, is the small depth of field of such long focal length lenses. For example, with a 100mm. lens, a 1 meter spot

would focus at 111mm. and a 5 meter laser spot at 102mm. A solution is possible since a given element can be expected to operate at the same range when the laser and receiver are fixed with respect to each other, Fig.33. The array can be tilted to alleviate the depth of field allowing each element to function at or near it's optimum focal distance.

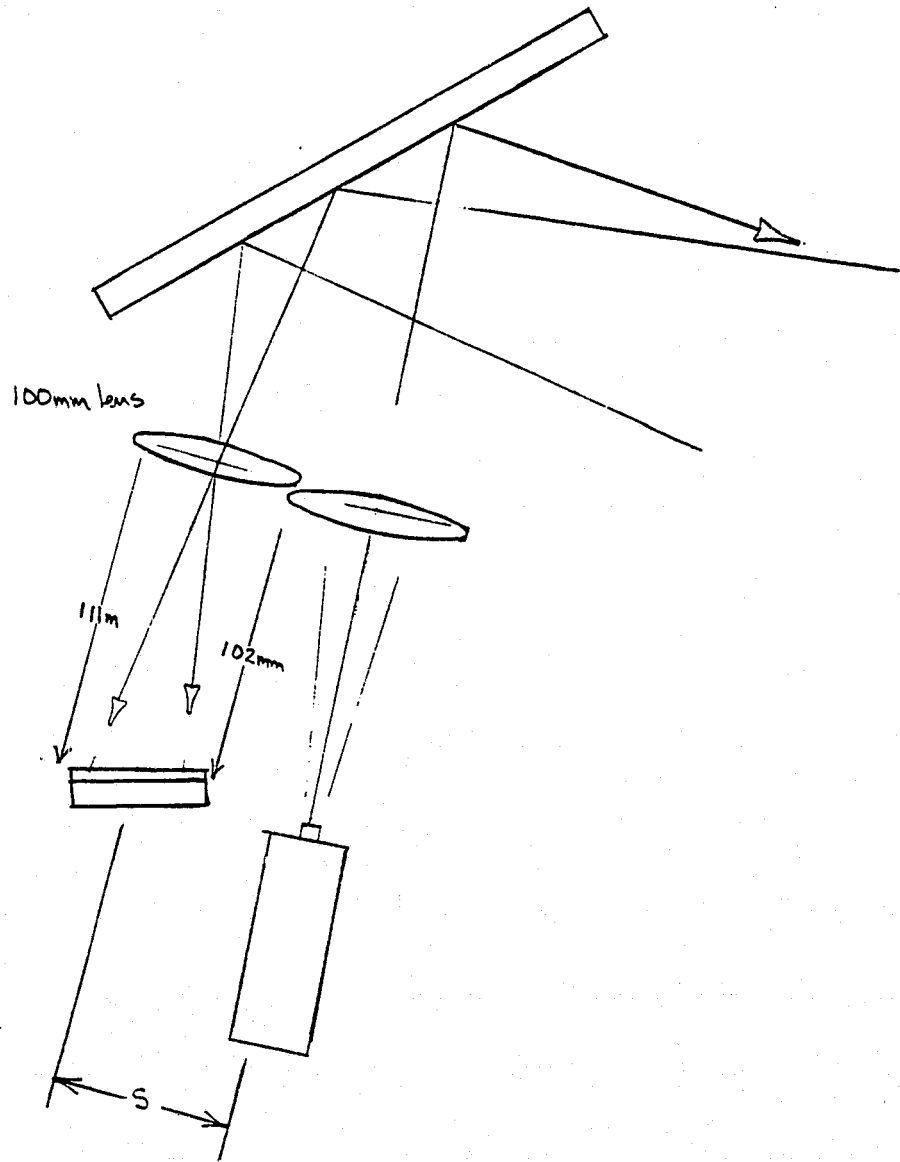


FIG. 33. OPTICS FOR IMPROVED RANGFINDER

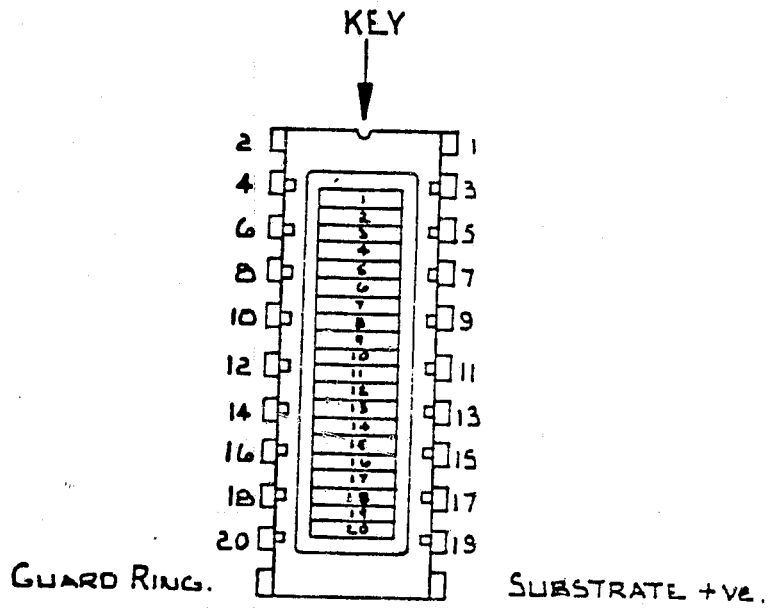
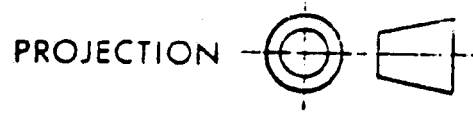
PART 9

LITERATURE CITED

1. N.A.S.A. A Mars 1984 Mission Report of the Mars Science Working Group, NASA TM-78419, July 1977
2. Messing, B., Interpretation of Laser/detector Data for Short Range Terrain Modeling and Hazard Detection, Rensselaer Polytechnic Institute, Troy, N.Y., August 1980
3. Knaub, D., Evaluation of the Propulsion Control System for a Planetary Rover and Design of an Elevation Scanning Mast, Rensselaer Polytechnic Institute, Troy, N.Y., May 1978
4. Craig, J., Design and Implementation of the Laser Scanning/Multi-Detector Controller for a Hazard Detection System, Rensselaer Polytechnic Institute, Troy, N.Y., May 1978
5. Kennedy, W., Control Electronics for a Multi-Laser/Multi-Detector Scanning System, Rensselaer Polytechnic Institute, Troy, N.Y., December 1980
6. Meshach W., Elevation Laser Scanning/Multi-Detector Hazard Detection System: Pulsed Laser and Photodetector Components, Rensselaer Polytechnic Institute, Troy, N.Y., May 1978
7. Herb, G., Laser Scanning Methods and Phase Comparison, Modulated Laser Rangefinder for Terrain Sensing on a Mars Roving Vehicle, Rensselaer Polytechnic Institute, Troy, N.Y., May 1973
8. Nussbaum, A., Geometric Optics Addison-Wesley, Reading, Ma., 1968
9. Yerazunis, S., Autonomous Control of Roving Vehicles for Unmanned Exploration of the Planets, A Progress Report, June 1, 1977 to November 30, 1977, RPI Technical Report MP-55, School of Engineering, Rensselaer Polytechnic Institute, March 1978
10. Millman & Halkias, Integrated Electronics, McGraw-Hill, 1972
11. Sequin & Tomsett, Charge Transfer Devices, Academic Press, 1975

APPENDIX A

19
A 9 5027



ACTIVE AREA OF EACH ELEMENT
4 x 0.9 mm.
SEPARATIONS 0.1 mm.

TYPE No. WD20-2
SERIAL No. 12715
MAX VOLTAGE. 60V

Johnson
31/10/77



HA-4900/4905

Precision Quad Comparator

FEATURES	DESCRIPTION
<ul style="list-style-type: none"> FAST RESPONSE TIME 130ns LOW OFFSET VOLTAGE 2.0mV LOW OFFSET CURRENT 10nA SINGLE OR DUAL-VOLTAGE SUPPLY OPERATION SELECTABLE OUTPUT LOGIC LEVELS ACTIVE PULL-UP/PULL-DOWN OUTPUT CIRCUIT - NO EXTERNAL RESISTORS REQUIRED 	<p>The HA-4900/4905 are monolithic, quad, precision comparators offering fast response time, low offset voltage, low offset current, and virtually no channel-to-channel crosstalk for applications requiring accurate, high speed, signal level detection. These comparators can sense signals at ground level while being operated from either a single +5 volt supply (digital systems) or from dual supplies (analog networks) up to ± 15 volts. The HA-4900/4905 contains a unique current driven output stage which can be connected to logic system supplies (V_{Logic+} and V_{Logic-}) to make the output levels directly compatible (no external components needed) with any standard logic or special system logic levels. In combination analog/digital systems, the design employed in the HA-4900/4905 input and output stages prevents troublesome ground coupling of signals between analog and digital portions of the system.</p> <p>These comparators' combination of features makes them ideal components for signal detection and processing in data acquisition systems, test equipment, and microprocessor/analog signal interface networks.</p> <p>Both devices are available in 16 pin dual-in-line ceramic packages. The HA-4900 operates from -55°C to $+125^{\circ}\text{C}$ and the HA-4905 operates over a 0°C to $+75^{\circ}\text{C}$ temperature range.</p>
<h3>APPLICATIONS</h3> <ul style="list-style-type: none"> THRESHOLD DETECTOR ZERO-CROSSING DETECTOR WINDOW DETECTOR ANALOG INTERFACES FOR MICROPROCESSORS HIGH STABILITY OSCILLATORS LOGIC SYSTEM INTERFACES 	
<h3>PIN OUT</h3>	<h3>SCHEMATIC</h3>
<p>Package Code 4B</p> <p>Top View</p> <p>CAUTION: These devices are sensitive to electrostatic discharge. Users should follow IC Handling Procedures specified on pg. 1-4.</p>	<p>One Fourth Only (HA-4900/4905)</p> <p>SEE PAGES 760-762 FOR PACKAGE SELECTION GUIDE</p>

C-2

ABSOLUTE MAXIMUM RATINGS (Note 1)

Voltage Between V+ and V-	33V
Voltage Between V _{Logic(+)} and V _{Logic(-)}	18V
Differential Input Voltage	±15V
Peak Output Current	±50mA
Internal Power Dissipation (Notes 7, 8)	580mW
Storage Temperature Range	-65°C ≤ T _A ≤ 150°C

ELECTRICAL CHARACTERISTICS

V₊ = +15.0V
 V₋ = -15.0V
 V_{Logic(+)} = 5.0V
 V_{Logic(-)} = GND.

PARAMETER	TEMP.	HA-4900 -55°C to +125°C			HA-4905 0°C to +75°C			Units
		MIN.	TYP.	MAX.	MIN.	TYP.	MAX.	
INPUT CHARACTERISTICS								
* Offset Voltage (Note 2)	25°C Full		2.0	3.0 4.0		4.0	7.5 10.0	mV mV
* Offset Current	25°C Full		10	25 35		25	50 70	nA nA
* Bias Current (Note 3)	25°C Full		50	75 150		100	150 300	nA nA
Input Sensitivity (Note 4)	25°C Full			3.1 4.1			7.8 10.1	mV mV
* Common Mode Range	Full	V-		V+ -2.4	V-		V+ -2.4	V
TRANSFER CHARACTERISTICS								
Large Signal Voltage Gain	25°C		400K			400K		V/V
Response Time (T _{pd0}) (Note 5)	25°C		130			130		ns
Response Time (T _{pd1}) (Note 5)	25°C		180			180		ns
OUTPUT CHARACTERISTICS								
* Output Voltage Level								
Logic "Low State" (V _{OL}) (Note 6)	Full		0.2	0.4		0.2	0.4	V
Logic "High State" (V _{OH}) (Note 6)	Full	3.5	4.2		3.5	4.2		V
Output Current								
I _{Sink}	Full	3.5			3.5			mA
I _{Source}	Full	3.0			3.0			mA
POWER SUPPLY CHARACTERISTICS								
* Supply Current, I _{DD(+)}	25°C		6.5	12		7	13	mA
* Supply Current, I _{DD(-)}	25°C		4	8		5	7	mA
* Supply Current, I _{DD(Logic)}	25°C		1.7	2.0		1.7	2.5	mA
Supply Voltage Range								
V ₊	Full	+5.0		+15.0	+5.0		+15.0	V
V ₋	Full	-15.0		0	-15.0		0	V
V _{Logic(+)} (Note 7)	Full	0		+15.0	0		+15.0	V
V _{Logic(-)} (Note 7)	Full	-15.0		0	-15.0		0	V

*100% tested for HA1-4900-8.



HARRIS
SEMICONDUCTOR
A DIVISION OF HARRIS CORPORATION

HA-4602/4605

High Performance Quad Operational Amplifier

FEATURES	DESCRIPTION
<ul style="list-style-type: none"> • LOW OFFSET VOLTAGE 0.3mV • HIGH SLEW RATE $\pm 6V/\mu s$ • WIDE BANDWIDTH 8MHz • LOW DRIFT $2\mu V/^\circ C$ • FAST SETTLING (0.01%, 10V STEP) 4.2μs • LOW POWER CONSUMPTION 35mW/AMP • SUPPLY RANGE $\pm 5V$ TO $\pm 20V$ 	<p>The HA-4602 and HA-4605 are high performance dielectrically isolated monolithic quad operational amplifiers with superior specifications not previously available in a quad amplifier. These amplifiers offer excellent dynamic performance coupled with low values for offset voltage and drift, input noise voltage and power consumption.</p> <p>A wide range of applications can be achieved by using the features made available by the HA-4602/4605. With wide bandwidth (8MHz), low power (35mW/amp), and internal compensation, these devices are ideally suited for precision active filter designs. For audio applications these amplifiers offer low noise ($8nV/\sqrt{Hz}$) and excellent full power bandwidth (50kHz). The HA-4602/4605 is particularly useful in designs requiring low offset voltage (0.3mV) and drift ($2\mu V/^\circ C$), such as instrumentation and signal conditioning circuits. The high slew rate ($4V/\mu s$) and fast settling time (4.2μs to 0.01%, 10V step) makes these amplifiers useful components in fast, accurate data acquisition systems.</p> <p>The HA-4602 and 4605's are available in 14 pin CERDIP packages which are interchangeable with most other quad op. amps. HA-4602 is specified from $-55^\circ C$ to $+125^\circ C$, and HA-4605 is specified over $0^\circ C$ to $+75^\circ C$ range.</p>
<p>APPLICATIONS</p> <ul style="list-style-type: none"> • HIGH Q, WIDE BAND FILTERS • INSTRUMENTATION AMPLIFIERS • AUDIO AMPLIFIERS • DATA ACQUISITION SYSTEMS • INTEGRATORS • ABSOLUTE VALUE CIRCUITS • TONE DETECTORS 	
<p>PINOUT</p> <p style="text-align: center;">Package Code 4U</p> <p style="text-align: center;">TOP VIEW</p>	<p>SCHEMATIC</p> <p style="text-align: center;">ONE FOURTH ONLY (HA-4602/4605)</p>

ABSOLUTE MAXIMUM RATINGS (Note 1)

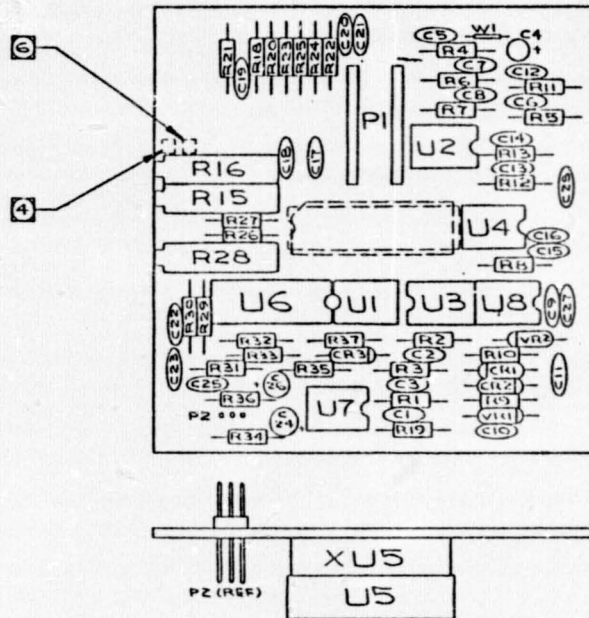
Temperature (Note 1)	+25°C Unless Otherwise Stated	Power Dissipation (Note 4)	880mW
Voltage Between V+ and V- Terminals	40.0V	Operating Temperature Range	-55°C ≤ T _A ≤ +125°C
Differential Input Voltage	±7V	HA-4602-2	0°C ≤ T _A ≤ +75°C
Output Voltage (Note 2)	±15.0V	HA-4605-5	-65°C ≤ T _A ≤ +150°C
Output Short Circuit Duration (Note 3)	Indefinite	Storage Temperature Range	

ELECTRICAL CHARACTERISTICS

PARAMETER	TEMP.	HA-4602-2 -56°C to +125°C			HA-4605-5 0°C to +75°C			UNITS
		MIN.	TYP.	MAX.	MIN.	TYP.	MAX.	
INPUT CHARACTERISTICS								
* Offset Voltage	+25°C		0.3	2.5		0.5	3.5	mV
	Full			3.0			4.0	mV
Δ _o Offset Voltage Drift	Full		2			2		μV/°C
* Bias Current	+25°C		130	200		130	300	nA
	Full			325			400	nA
* Offset Current	+25°C		30	75		30	100	nA
	Full			125			120	nA
Common Mode Range	Full	±12			±12			V
Input Noise Voltage (f = 1KHz)	+25°C		6			6		nV/√Hz
Input Resistance			500			500		KΩ
TRANSFER CHARACTERISTICS								
* Large Signal Voltage Gain (Note 5)	Full	100K	250K		75K	250K		V/V
* Common Mode Rejection Ratio (Note 6)	Full	80			80			dB
Channel Separation (Note 6)	+25°C		-100			100		dB
Small Signal Bandwidth	+25°C		8			8		MHz
OUTPUT CHARACTERISTICS								
* Output Voltage Swing (R _L = 10K)	Full	±12	±13		±12	±13		V
(R _L = 2K)	Full	±10	±12		±10	±12		V
Full Power Bandwidth (Note 5)	+25°C		80			80		KHz
Output Current (Note 7)	Full	±10	±15		±8	±15		mA
Output Resistance	+25°C		200			200		Ω
TRANSIENT RESPONSE (Note 8)								
Rise Time	+25°C		50			50		ns
Overhoot	+25°C		30			30		%
Slew Rate	+25°C		±4			±4		V/μs
Settling Time (Note 10)			4.2			4.2		μs
POWER SUPPLY CHARACTERISTICS								
* Supply Current (I ⁺ or I ⁻)	+25°C		4.8	5.5		5.0	5.5	mA
* Power Supply Rejection Ratio (Note 9)	Full	80			80			dB

*100% tested for HA-4602-2

APPENDIX 3



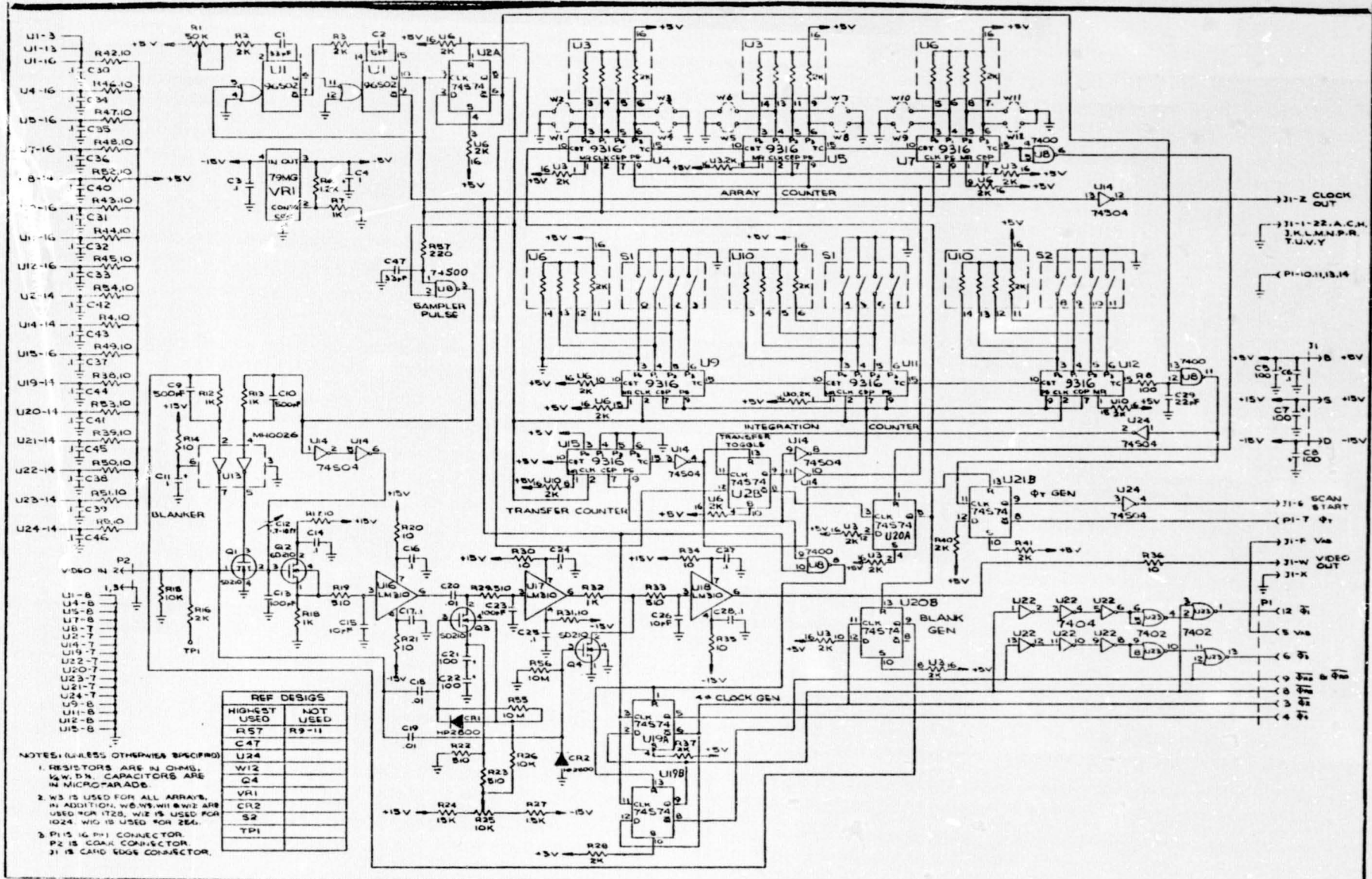
NOTES: (UNLESS OTHERWISE SPECIFIED)

1. COMPONENT HEIGHT SHALL BE .50 MAX.
2. LEAD PROTRUSION SHALL BE .06 MAX.
3. FOR SCHEMATIC SEE DWG O11-0275.
4. INKSTAMP ASSY REV LETTER IN LOCATION SHOWN USING BLACK INK. COVER WITH ONE COAT OF CLEAR KRYLON N21303.
5. TAPE HOLES FOR 22 PIN SOCKET, CIRCUIT SIDE, INSTALL SOCKET AT TOUCH-UP.
6. INKSTAMP APPROPRIATE DASH NR ACCORDING TO FOLLOWING TABLE:

DEVICE	DASH NR
CCPD256	-01
CCPD1024	-02
CCPD1728	-03

7. BEND C1 OVER APPROX 45° FROM VERTICAL IN DIRECTION TOWARD EDGE OF THE BOARD AND C17, 18 & 19 TOWARD P1 PRIOR TO SOLDERING.

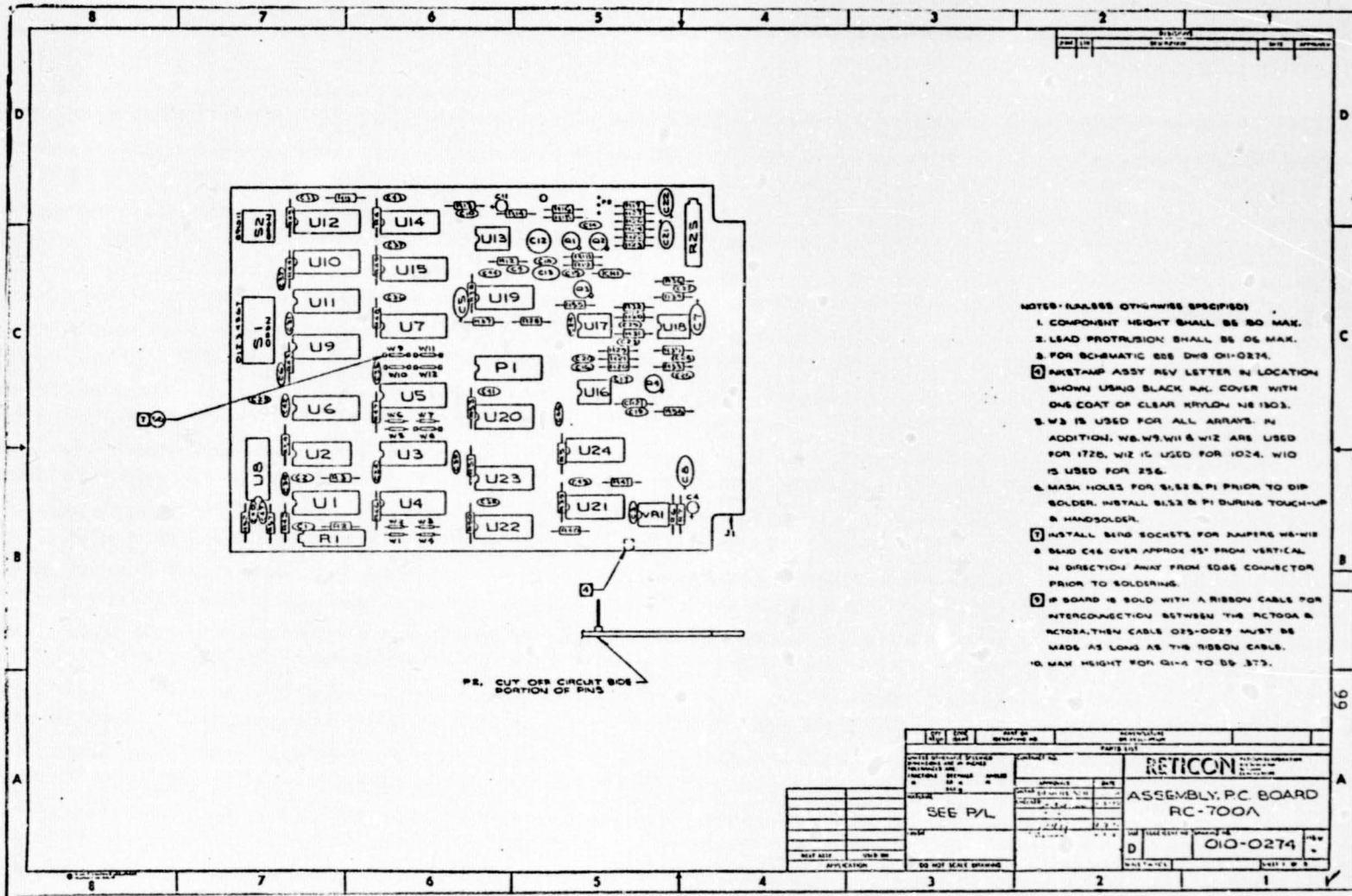
QTY REQD	CODE IDENT	PART OR IDENTIFYING NO.	NOMENCLATURE OR DESCRIPTION
PARTS LIST			
UNLESS OTHERWISE SPECIFIED DIMENSIONS ARE IN INCHES TOLERANCES ARE: FRACTIONS DECIMALS ANGLES ± .010 ± .005 ± .010		CONTRACT NO.	RETICON CORPORATION 2500 UNIVERSITY AVENUE SANTA CLARA, CALIF. 95050
MATERIAL		APPROVALS	DATE
SEE P/L		DRAWN DENNIS YGH	1-1-77
FINISH		CHECKED BY D. G. ...	1-2-77
NEXT ASSY USED ON		APPROVED [Signature]	1-2-77
APPLICATION		ASSEMBLY, P.C. BOARD RC-702A	
DO NOT SCALE DRAWING		SIZE	CODE IDENT NO
		C	010-0275
		DRAWING NO.	REV
			-
		SCALE TWICB	SHEET 1 OF 2



REF DESIGNS

HIGHEST USED	NOT USED
R57	R9-11
C47	
U24	
W12	
Q4	
VRI	
CR2	
S2	
TPI	

NOTES: (UNLESS OTHERWISE SPECIFIED)
 1. RESISTORS ARE IN OHMS, 1/4W.D.M. CAPACITORS ARE IN MICROFARADS.
 2. W3 IS USED FOR ALL ARRAYS. IN ADDITION, W6, W8, W11 & W12 ARE USED FOR U728, W12 IS USED FOR U24. W10 IS USED FOR 254.
 3. P1 IS 16 PIN CONNECTOR. P2 IS COAX CONNECTOR. P3 IS CARD EDGE CONNECTOR.



- NOTES: UNLESS OTHERWISE SPECIFIED:
1. COMPONENT HEIGHT SHALL BE 50 MAX.
 2. LEAD PROTRUSION SHALL BE 06 MAX.
 3. FOR SCHEMATIC SEE DWG 010-0274.
 4. PARTSTAMP ASSY REV LETTER IN LOCATION SHOWN USING BLACK INK. COVER WITH ONE COAT OF CLEAR KRYLON NE 1303.
 5. W3 IS USED FOR ALL ARRAYS. IN ADDITION, W6, W9, W11 & W12 ARE USED FOR 1726. W12 IS USED FOR 1024. W10 IS USED FOR 256.
 6. MASK HOLES FOR S1, S2 & P1 PRIOR TO DIP SOLDER. INSTALL S1, S2 & P1 DURING TOUCH-UP & HANDSOLDER.
 7. INSTALL BIND SOCKETS FOR JAMPIERS W6-W12 & BAND C46 OVER APPROX 45° FROM VERTICAL IN DIRECTION AWAY FROM EDGE CONNECTOR PRIOR TO SOLDERING.
 8. IF BOARD IS SOLD WITH A RIBBON CABLE FOR INTERCONNECTION BETWEEN THE RC700A & RC702A, THEN CABLE 025-0029 MUST BE MADE AS LONG AS THE RIBBON CABLE.
 9. MAX HEIGHT FOR Q1-6 TO BE 373.

RC700A/RC702A CCPD INTERFACE SYSTEMGENERAL

The RC700A/RC702A interface system provides the timing, video processing, and blanking requirements for the Reticon CCPD series photodiode arrays. A simplified block diagram is shown in Figure 1. Each system consists of two boards, a 4.5 x 6.5 inch (11.4 x 16.5 cm) "motherboard" (RC700A) and a 3.0 x 3.0 inch (7.6 x 7.6 cm) satellite "array board" with design to match each particular type of array. The two boards are interconnected, either directly or by means of a 16-conductor 30-inch (max) ribbon interconnect cable, to form a complete evaluation processing package for one of the Reticon Charge Coupled Photo Diode (CCPD) arrays. A coaxial interconnect cable for the video signals is also required. The various satellite boards are identified by dash numbers in accordance with Table I.

TABLE I BOARD-ARRAY MATCH

<u>Board Description</u>	<u>Array Description</u>	<u>C15-C16 Capacitor Value</u>
RC702A-01	CCPD-256	1000 pf
RC702A-02	CCPD-1024	680 pf
RC702A-03	CCPD-1728	none

The interface system, comprised of one RC-700A motherboard and one RC702A satellite board, is intended for use in evaluating the performance of one of the CCPD series of photodiode arrays. For some applications, the interface system may be used directly as a portion of a larger system such as a complete camera for a scanning controller.

- o Accepts all CCPD series arrays.
- o Operates at sampling rates from less than 100 KHz to 5 MHz.
- o Sampled and held box-car video output.
- o Output blanking provided between scans.
- o Dynamic range more than 200:1.

FUNCTIONAL DESCRIPTION

The system functions are separated into three major sections: (1) the sensor and its immediate interface, (2) the logic control, and (3) the analog signal processing circuit. Figure 2 is a block diagram which shows the organization of the circuits and their interrelations.

The logic control section includes the basic trigger generator, the four-phase clock circuits, and the transfer control circuits for the array, along with the

ICON	RETICON CORPORATION	SIZE	DRAWING NO.	C	SHEET 2 of 1
	910 Benicia Ave. Sunnyvale California 94086	A	045-0042		

generation of the sampling and dc restoration pulses for the signal processing circuits.

The signal processing circuits comprise the preamplifier (physically located on the satellite board), the sampling switch and the sample-and-hold capacitor, the switch-edge-cancellation (SEC) capacitor, a simple filter, and the buffer amplifier for the output. The odd and even pixels from the array are summed at the preamplifier via the gain-balancing potentiometer. The combined samples are then resampled and held on the holding capacitor for the duration of a single pixel, then processed with dc restoration, filtering, blanking, and buffering.

In the resampling process, sampling switch energy induces extraneous charge on the capacitor. The switch-edge cancellation (SEC) trimmer capacitor is adjusted to minimize or cancel the extraneous charge by coupling charge from a negative-going version of the sampling pulse.

The dc restoration circuit restores a ground reference to the sampled-and-held video during the retrace or blanking time of the array.

The simple RC low-pass filter is used to minimize residual switching spikes and to maintain minimum noise bandwidth consistent with the array switching speed.

Normally, the filter is fixed, but in some situations it may be desirable to change the value of C23 to change the corner frequency of the filter to more closely match an unusual sampling rate.

CIRCUIT DESCRIPTION

The array requires four-phase clocks, a transfer pulse, and complementary re-set clocks. Please refer to the device data sheet for the detailed requirements. As specified in the data sheet, the clock waveforms have crossing-point and edge-control requirements, and the transfer pulse must occur at the proper time while the four-phase clocks are held stationary. The logic section provides the required sequencing and shaping, with all timing controlled by a basic trigger oscillator operating at twice the desired sample rate or four times the four-phase clock rate. The trigger oscillator is composed of U1, an edge triggered one-shot with regenerative feedback. The frequency is controlled by R₁, R₂ and C₁. With values as given on the schematic, the trigger frequency may be varied from approximately 1.5 to 8 MHz, giving sample rates of 750 KHz to 4 MHz. By changing C₁ to 500 pf, the frequencies may be reduced to cover sample rates of 75 KHz to 1.25 MHz. With C₁ deleted, the upper sample-rate limit becomes approximately 5 MHz. The trigger pulse may be monitored at connector pin J1-Z.

The four-phase clocks receive basic sequencing by U19, a dual D flip-flop connected in a twisted-ring configuration. Each flip-flop produces comple-

ICON	RETICON CORPORATION	SIZE	DRAWING NO.	C	SHEET 3 OF
	910 Benicia Ave. Sunnyvale California 94086	A	045-0042		

mentary square waves at one fourth the trigger period, with one trigger period of shift between the two flip flops to give the sequence $\phi_1, \phi_2, \phi_3, \phi_4, \phi_1$ -----

The ϕ_1/ϕ_3 flip flop also supplies the reset gates ϕ_{RE} and ϕ_{RO} , and the CCD receiving gate ϕ_{RG} . Clock shaping is desired for ϕ_1 and ϕ_3 to increase the overlap; for this purpose direct and delayed waveforms are combined in NOR U23 to give high-crossing clocks at the outputs of the translator U4 (RC702). Compensation for the lesser capacitances of the shorter arrays, CCPD1024 and CCPD256, is provided by additional capacitors C15 and C16 at the array's clock input terminals. The values are as listed in Table I.

Clocks $\phi_2, \phi_4, * \phi_{RE}$ and $* \phi_{RO}$ require no such clock shaping so that the appropriate generator outputs are directly translated through the MH0026 voltage translators and applied to the array. The clock swing must conform to value specified by CCPD Data Sheet.

The transfer pulse is required once per scan. It is sequenced at U21B by a combination of a transfer toggle from the transfer counter U15 and a clock pulse from the trigger divider U2A. Translator U3 (RC702A) converts the level to the range -4 to +5 volts for application to the array.

A dc restoration pulse and blanking pulse are similarly generated at U20B, translated by U13, and applied to switches Q3 and Q4.

The sampling pulse is generated once per signal sample by combination of the direct and divided trigger at U8-3. After translation, the inverted pulse is applied to sampler switch Q1 and a complementary pulse for switch-edge cancelling coupled through SEC capacitor C12. The sampling-switch pulse is nominally 75 nanoseconds wide.

ANALOG CIRCUIT

Odd and even outputs are balanced by R28 and applied to combiner-amplifier U6 followed by a unity gain buffer U7 (RC702A). The video signal from each output of the array is alternately reset at a high level of approximately +6 volts and released to carry the information at a lower level of approximately +2.5 volts. After combination and buffering, the saturated video signal has an amplitude of approximately 2.5 volts peak to peak, riding on a (dark) bias level of approximately +4.5 volts.

The sample-and-hold circuit consists of an FET switch, Q1, hold capacitor C13, SEC capacitor C12, and buffer source follower Q2. The dc (ground level) restoration circuit is isolated by two unity-gain buffers, U16 and U17. The dc bias level for dark conditions is shifted to ground by clamping C20 during the

*(Called ϕ_1 and ϕ_2 respectively on the 702A board.)

RETICON	RETICON CORPORATION	SIZE	DRAWING NO.		
	910 Benicia Ave. Sunnyvale	A	045-0042	C	SHEET 4

transfer period. At other times, charge does not change on C20 so that relative signal levels are transmitted with the proper ground reference. The reference level is adjustable at R25. Leakage may cause a shift in the reference, so C20 must have low leakage and for integration times longer than approximately 4 msec the value of C20 should be increased to 0.1 μ f so that input current of U17 will not upset the reference.

BIAS CIRCUITS

The system operates with the array substrate at -5 volts, supplied by regulator VR1. Fixed voltages for V_{OG} , V_{RD} , and V_{DD} in accordance with the device data sheet are obtained by means of resistive dividers and filters from the +15 volt supply. Biases for V_{IG} odd and even are balanced to equal values by adjustment of R16, and their levels (approx. 10 volts) set by R15 to give a (dark) video output level from U5 pin 2 Or 21 of 2.0 ± 0.1 volts. Later, the balance adjustment is further trimmed to minimize the dark signal odd-even unbalance (see set-up procedure).

VAB is nominally connected to ground with the jumper W_1 provided on the board (see assembly drawing).

If desired, this jumper may be removed and a voltage from -3 to +5 volts applied to connector J1-F. Such a change will vary the level of saturation and so change the maximum output; however, antiblooming properties are affected and may be lost if VAB is taken more negative than approximately -3 volts.

COUNTERS

There are three counters in the system: 1.) an array counter set to match the length of the particular array, 2.) an integration counter which determines the scan period, and 3.) a transfer counter which controls the transfer and flyback times independent of the other counters. The control sequence is as given in Figure 3.

The terminal count of the transfer counter controls the start of both the array and integration counters. This same control stops the transfer counter. The array counter runs at twice the rate of the other two, and has a preset number matched to twice the length of the array in use plus 4. This preset number is determined by jumper links on the RC700A board as shown in Figure 4. The selected number as chosen by links W8-W12 must match twice the number of elements in the array. The clocking rate and number sequence of the links result in the weighting of Table II. Links are installed to add weights to give the number chosen. For example, for a CCPD1024, only link W12 is selected from this group. Link W3 is permanently installed to account for internal timing.

RETICON	RETICON CORPORATION	SIZE	DRAWING NO.	C	SHEET 5 OF
	910 Benedic Ave. Sunnyvale	A	045-0042		

TABLE II
WEIGHTING FOR ARRAY COUNTER
(See Figure 4)

<u>Link Designation</u>	<u>(Binary No.)</u>	<u>Equivalent Element Count</u>
W-12	(2048)	1024
W-11	(1024)	512
W-10	(512)	256
W-9	(256)	128
W-8	(128)	64

The integration counter determines the scan period and hence the integration time. The count is selected by rocker switches S1 and S2 on the edge of the RC700A board with the appropriate binary weighting designated on the board. The count as selected by the weighting must be not less than the number of elements in the array in use plus seventeen counts. The RC700A board's counter has an inherent count of one. In addition, the transfer timer adds an additional count of fourteen. Therefore, to calculate the proper switch settings this formula must be used for minimum count:

$$[\text{S2 setting (selects element count)}] + \text{Inherent count} + \text{Transfer Timer} + 2$$

For example: The minimum count for a CCPD 1024 array would be achieved as follows: $[\text{S2-10 closed } (2^{10})] + [\text{Inherent count } (1)] + [\text{Transfer Timer } (14)] + [\text{S1-1 closed } (2^1)] = 1041$. Larger numbers are permissible. (Note: The smallest count position (2^0) is actually permanently shorted so that this switch position is immaterial.

TABLE III
INTEGRATION COUNTER SWITCH SETTINGS (For Minimum Count)

<u>CCPD</u>	<u>S1</u>	<u>S2</u>
256	4 closed (2^4)	8 closed (2^8)
1024	4 closed (2^4)	10 closed (2^{10})
1728	4, 6, 7 closed ($2^4, 2^6, 2^7$)	9, 10 closed ($2^9, 2^{10}$)

The termination of the integration count starts the transfer counter, initiates transfer of stored array data into the CCD output register, and stops the four-phase clocks for the duration of the transfer period. The end of the transfer count then reinitiates the entire sequence above. A timing diagram showing the interrelationships is given in Figure 5.

Complete schematic diagrams are attached for the RC700A and the RC702A. Location of adjustment is shown in the assembly drawings. For power supply connections see the schematics and assembly drawings.

Specifications

<u>Inputs</u>	1. Power	+15 volts at approximately 150ma d.c. -15 volts at approximately 70ma d.c.
	2. V _{AB}	+5 volts at approximately 600ma d.c. This terminal is normally at ground (see test)
<u>Outputs</u>	1. Video Output Terminal:	a) Approximately 2.4 volts for saturated light output; b) Output impedance < 10 ohm
	2. Scan Start Sync	A negative TTL level pulse synchronous with the start of scan is provided for system updating.
	3. Trigger Out	A negative TTL-level pulse synchronous with the internal trigger generator.

SETUP PROCEDURE

There are six controls: 1.) Clock Frequency Control R1, 2.) Dark Level Adjust R25, 3.) Sec Trimmer Capacitor C12, *4.) V_{IC} Odd/Even Balance R16, *5.) V_{IG} level R15, *6.) Gain Balance Potentiometer R28.

*(Note: The items so marked are found on the RC702A array board.)

The light source must be uniform and must be perpendicular to the array, because any parallax will cause odd-even patterns and will interfere with the adjustment procedure.

Select the array and adjust the integration time with the long counter as described under "counters" in the Logic Control section.

When the array is selected, the corresponding clock line capacitors must be selected. The proper capacitance value for each array is listed in Table 1.

ICON	RETICON CORPORATION	SIZE	DRAWING NO.	C	SHEET 7 OF
	910 Benecis Ave. Sunnyvale California 94086	A	045-0042		

<u>Alignment Steps</u>		<u>Caution!</u>			
For power supply connection see P. C. Assembly Drawing.		<u>DO NOT SHORT OUTPUT OF U7 TO GROUND.</u>			
Operation	Control	Operational Steps			
Clock Frequency	Frequency Control R1 (RC700A)	<ol style="list-style-type: none"> 1.) Synchronize oscilloscope from clock output terminal, J1-Z. 2.) Monitor Pin 12 of the array; adjust β_1 clock frequency to the desired data rate. Note: Data rate = $2 \times \beta_1$ rate. 			
Odd-Even Adjustment and dc level set in the dark.	V_{IG} odd/even R16 (RC702A) V_{IG} level R15 (RC702A)	<ol style="list-style-type: none"> 1.) With an oscilloscope monitor pins 9 and 14 of the array and set the dc levels to equality with R16 and R15 (Note: the level is approx. +10 volt $R_{15} \text{ CC} \downarrow \text{ voltage}$) 2.) With an oscilloscope, monitor the video out (array in dark) at P2-2. Adjust R15 to bring the output dc level to a 2.0 ± 0.1 volt peak to peak signal. 			
	Gain balance, R28 (RC702A)	3.) Mechanically adjust R28 to approximately midposition.			
	V_{IG} Odd/Even, R16 (RC702A)	4.) With an oscilloscope, monitor video out at P2-2 and set the array in dark and adjust odd-even to a minimum by trimming R16.			
Gain Balance Adjustment	Gain Balance, R28 (RC702A)	<ol style="list-style-type: none"> 1.) Monitor video output at J1-W. 2.) Partially cover the array to obtain a gradient in the signal output from dark to approx. 90% saturation. 3.) Adjust R28 to obtain a uniform gradient in video response at the 90% saturation level by minimizing the differential gain. 4.) In making this adjustment, R16 may also need to be trimmed to remove the Odd-even patterns in the dark. 5.) Repeat Steps 3 and 4 until uniform gradient in the video is obtained. 			
 TICON RETICON CORPORATION 910 Benicia Ave. Sunnyvale California 94086		SIZE A	DRAWING NO. 045-0042	C	SHEET 8 OF

Alignment Steps (Continued)

Operation	Control	Operational Steps
SEC Adjustment	SEC, C ₁₂ (RC700A)	<ol style="list-style-type: none"> 1.) Monitor the video output at J1-W with an oscilloscope. 2.) Set the array in the dark. 3.) Adjust C₁₂ while observing the switch spikes. Minimize these spikes by trimming C₁₂.
	VIG Odd/Even, R16 (RC702A)	<ol style="list-style-type: none"> 4.) When these spikes are minimized, the odd-even pattern may require trimming. Use R16 to trim out the odd-even pattern.

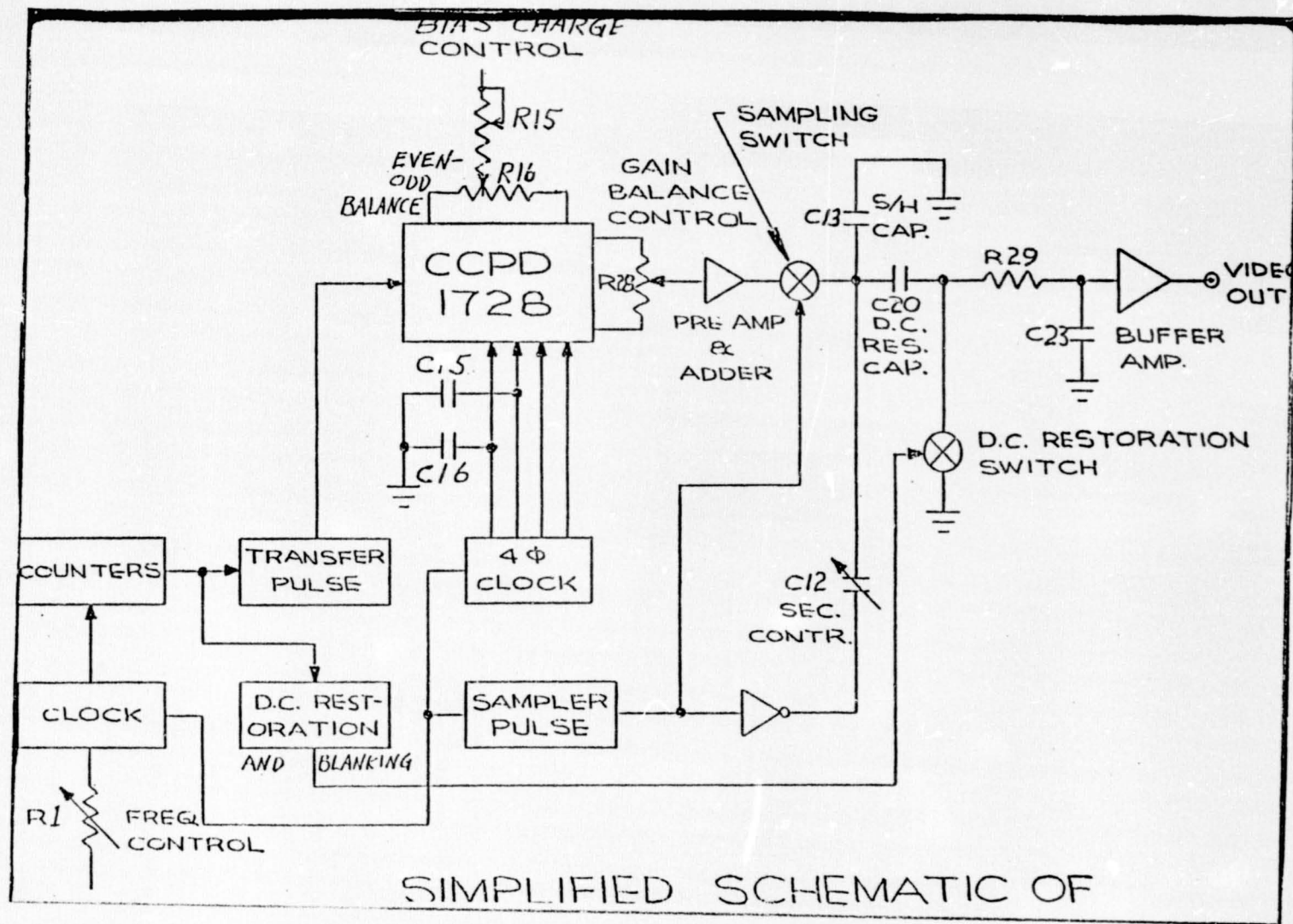
RETICON
 RETICON CORPORATION
 910 Benicia Ave.
 Sunnyvale
 California 94086

 SIZE
 A

 DRAWING NO.
 . 045-0042

C

SHEET 9



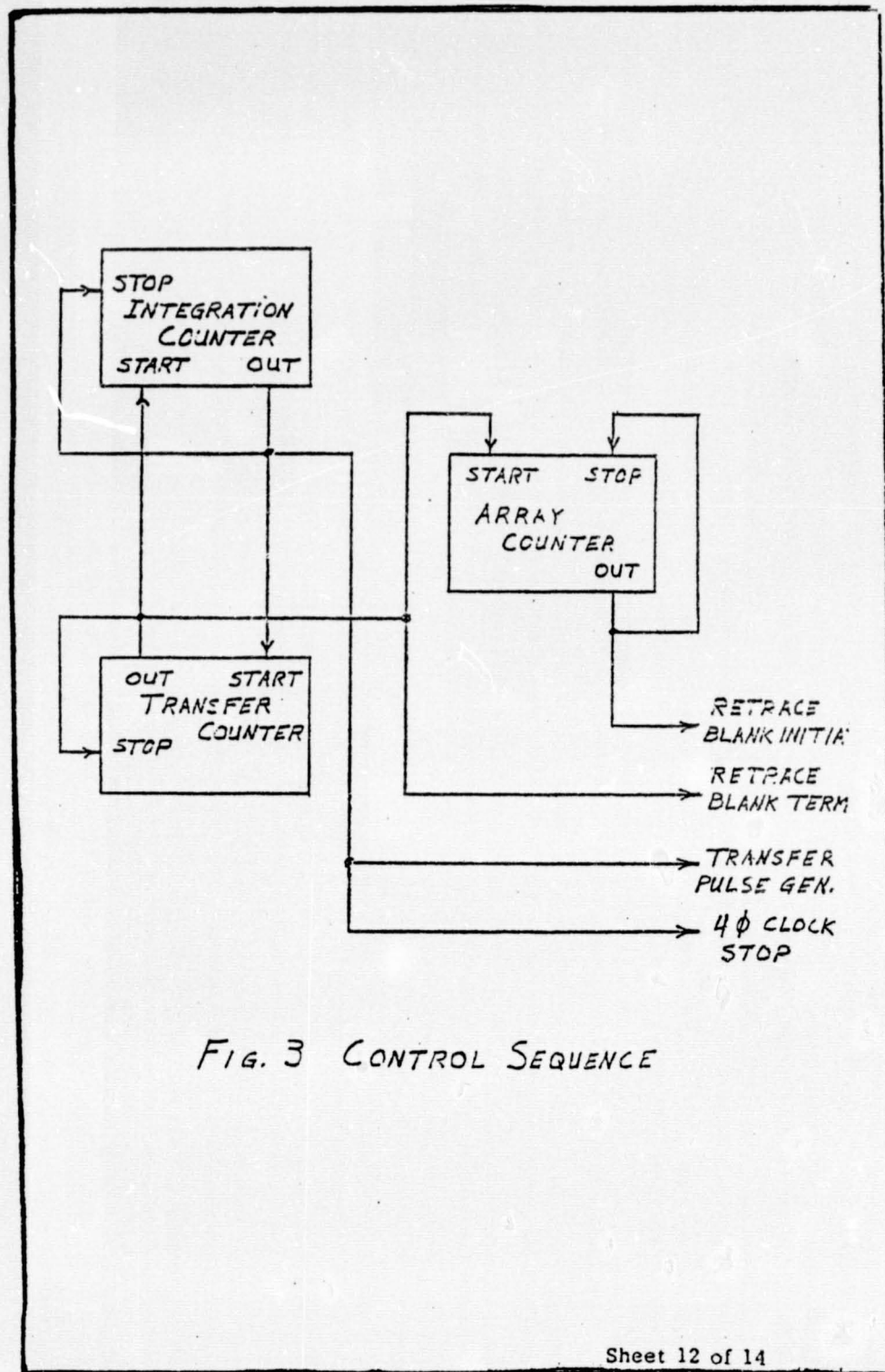


FIG. 3 CONTROL SEQUENCE

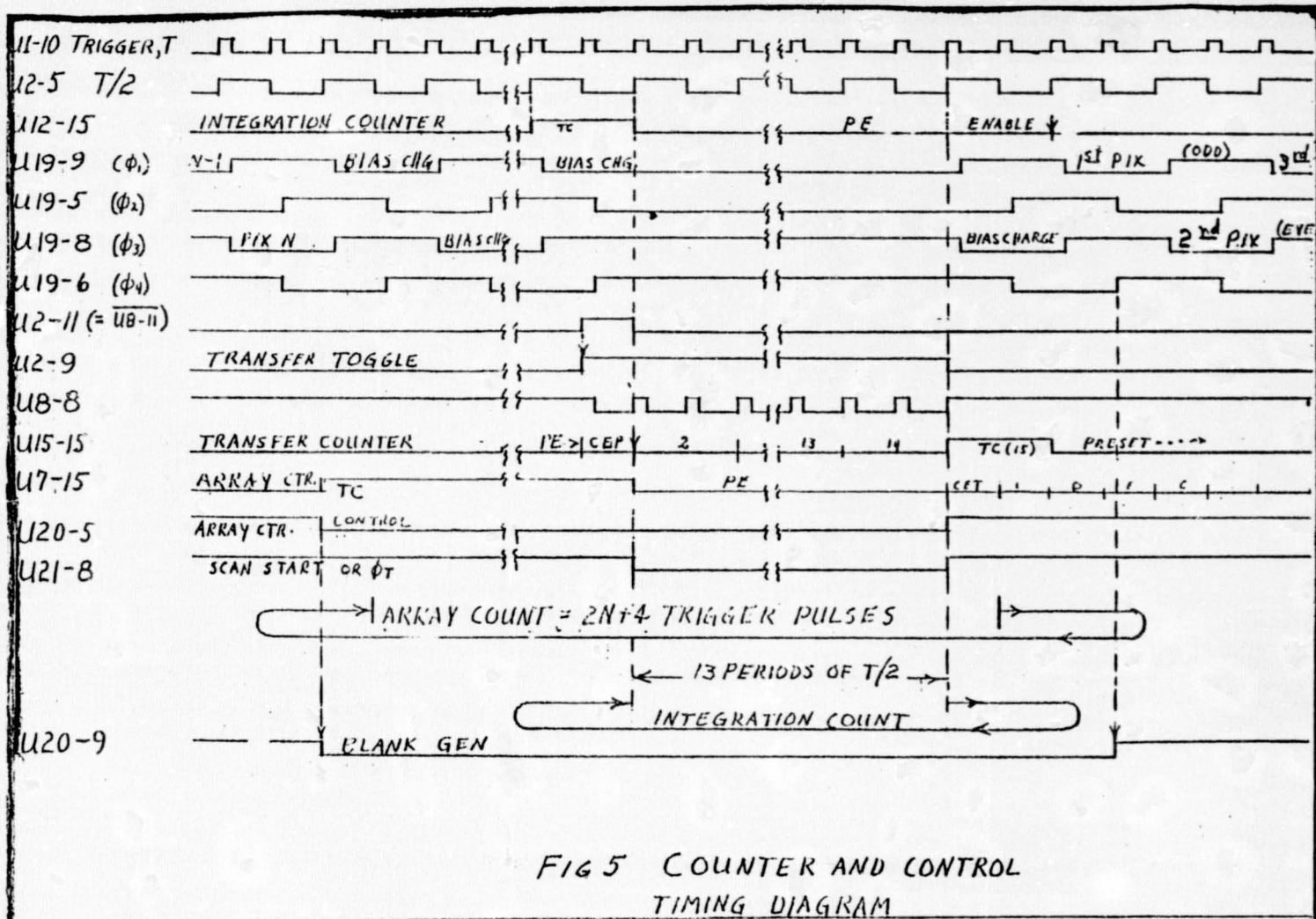


FIG 5 COUNTER AND CONTROL TIMING DIAGRAM

**MMH0026
MMH0026C**

MOS CLOCK DRIVER

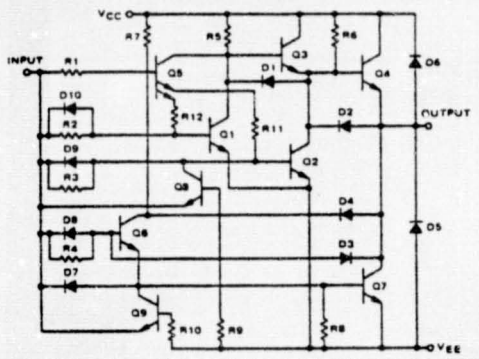
Specifications and Applications Information

DUAL MOS CLOCK DRIVER

... designed for high-speed driving of highly capacitive loads in a MOS system.

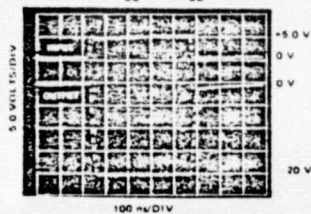
- Fast Transition Times - 20 ns with 1000 pF Load
- High Output Swing - 20 Volts
- High Output Current Drive - ± 1.5 Amperes
- High Repetition Rate - 5.0 to 10 MHz Depending on Load
- M TTL and MDTL Compatible Inputs
- Low Power Consumption when in MOS "0" State - 2.0 mW
- +5.0-Volt Operation for N-Channel MOS Compatibility

FIGURE 1 - CIRCUIT SCHEMATIC (1/2 CIRCUIT SHOWN)



TYPICAL OPERATION

$R_s = 10 \Omega$, $C_L = C_{in} = 1000 \text{ pF}$, $f = 1.0 \text{ MHz}$
 $PW = 500 \text{ ns}$, $V_{CC} = 0 \text{ V}$, $V_{EE} = -20 \text{ V}$

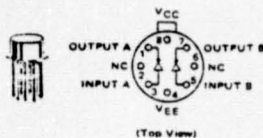


See Packaging Information Section for outline dimensions.

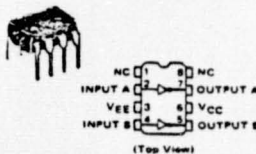
**DUAL MOS
CLOCK DRIVER**

**MONOLITHIC
SILICON INTEGRATED CIRCUIT**

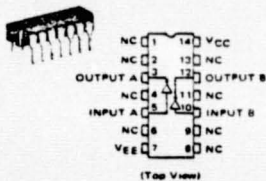
**G SUFFIX
METAL PACKAGE
CASE 601**



**P1 SUFFIX
PLASTIC PACKAGE
CASE 676
(MMH0026C Only)**



**L SUFFIX
CERAMIC PACKAGE
CASE 632
TO-118**



High-Frequency N-P-N Transistor Array

For Low Power Applications at Frequencies up to 500 MHz

- Features:**
- Gain-Bandwidth Product $f_{\beta} > 1$ GHz
 - Power Gain = 20 dB (typ.) at 100 MHz
 - Noise Figure = 3.3 dB (typ.) at 100 MHz
 - All independent transistors on a common substrate

The CA3127E consists of four general-purpose silicon n-p-n transistors on a common insulating substrate. Each of the independent transistors exhibits low 1/f noise and a f_{β} of up to 500 MHz, making the CA3127E useful up to 500 MHz. Access is provided to each of the terminals for the individual transistors and a separate substrate connection has been provided for maximum suppression of parasitic oscillations. The packaging construction of the CA3127E provides low inductance and thermal matching of the four transistors. The CA3127E is designed as a 16-lead dual-in-line package and operates over the full military temperature range of -55 to +125°C.

CHARACTERISTICS CURVES COMMON-EMITTER CONFIGURATION

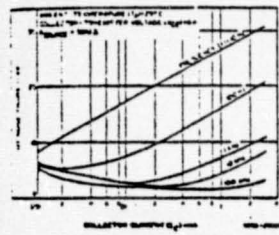


Fig. 1 - 16-lead figure 1 collector current of f_{β} SOURCE = 500 Ω.

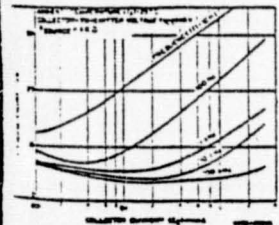


Fig. 2 - 16-lead figure 2 collector current of f_{β} SOURCE = 10 Ω.

- Applications:**
- VHF amplifier
 - VHF mixer
 - Modulation-demodulation - RF mixer/rectifier
 - IF amplifier
 - Superheterodyne
 - Switching
 - Switching detectors
 - Composite amplifiers

CA3127E

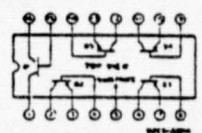


Fig. 1 - Schematic diagram of CA3127E.

MAXIMUM RATINGS, Absolute-Maximum Values, at $T_A = 25^\circ\text{C}$

POWER DISSIPATION, P_D

Any one transistor 80 mW

Transistor array 475 mW

For $T_A > 25^\circ\text{C}$ 475 mW

For $T_A > 25^\circ\text{C}$ (Derate Linearly at) 8.61 mW/°C

AMBIENT TEMPERATURE RANGE

Operating -55 to +125°C

Storage -65 to +150°C

LEAD TEMPERATURE (During Soldering):

All electrodes 617.5 to 620 over 11.20 to 19.75 mm lead span for 10 seconds max. 170°C

The temperature ranges apply for each transistor in the device.

Collector-emitter Voltage, V_{CE0} 15 V

Collector-base Voltage, V_{CB0} 30 V

Collector-Substrate Voltage, V_{CS0} 30 V

Collector Current, I_C 30 mA

The substrate of each transistor of the CA3127E is bonded to the substrate by an array of leads. The substrate terminal \bar{S} must be connected to the most negative point in the external circuit to maintain maximum common-mode rejection and is provided for normal transistor operation.

STATIC ELECTRICAL CHARACTERISTICS at $T_A = 25^\circ\text{C}$

CHARACTERISTICS	SYMBOL	TEST CONDITIONS	LIMITS			UNITS
			Min.	Typ.	Max.	
For Each Transistor						
Collector-emitter Breakdown Voltage	$V_{(BR)CEO}$	$I_C = 10 \text{ mA}, I_B = 0$	30	22	-	V
Collector-base Breakdown Voltage	$V_{(BR)CBO}$	$I_C = 1 \text{ mA}, I_E = 0$	15	24	-	V
Collector-substrate Breakdown Voltage	$V_{(BR)CSO}$	$I_C = 10 \text{ mA}, I_B = 0, I_E = 0$	30	80	-	V
Emitter-emitter Breakdown Voltage*	$V_{(BR)EE0}$	$I_C = 10 \text{ mA}, I_E = 0$	4	5.7	-	V
Collector Current Gain	β_{DC}	$V_{CE} = 10 \text{ V}, I_B = 0$	-	-	85	dB
Collector Current Gain	β_{CB}	$V_{CB} = 10 \text{ V}, I_E = 0$	-	-	80	dB
DC Forward Current Transfer Ratio	β_{FE}	$V_{CE} = 5 \text{ V}$	$I_C = 5 \text{ mA}$	20	84	-
			$I_C = 1 \text{ mA}$	40	90	-
			$I_C = 0.1 \text{ mA}$	30	95	-
Base-emitter Voltage	V_{BE}	$V_{CE} = 5 \text{ V}, I_C = 1 \text{ mA}$	$I_B = 5 \text{ mA}$	0.71	0.81	0.91
			$I_B = 1 \text{ mA}$	0.66	0.76	0.85
			$I_B = 0.1 \text{ mA}$	0.60	0.70	0.80
Collector-base Breakdown Voltage	$V_{(BR)CB0}$	$I_C = 10 \text{ mA}, I_E = 1 \text{ mA}$	-	0.25	0.50	V
Magnitude of Difference in V_{BE}	$ \Delta V_{BE} $	I_C & I_B identical	-	0.5	5	mV
Magnitude of Difference in β_{FE}	$ \Delta \beta_{FE} $	$V_{CE} = 5 \text{ V}, I_C = 1 \text{ mA}$	-	0.3	3	dB

*When used as a diode for rectifier or voltage regulator, the device must not be subjected to more than 0.1 milliwatt of average power per junction. Maximum diode current should be limited to 10 mA. If a diode array using emitter current should be less than 10 mA.

DYNAMIC CHARACTERISTICS at $T_A = 25^\circ\text{C}$

CHARACTERISTICS	SYMBOL	TEST CONDITIONS	Fig. No.	LIMITS			UNITS
				Min.	Typ.	Max.	
1/f Noise Figure	NF	$f = 100 \text{ kHz}, R_{\theta} = 50 \Omega, I_C = 1 \text{ mA}$	2	-	1.8	-	dB
Gain-Bandwidth Product	f_{β}	$V_{CE} = 5 \text{ V}, I_C = 5 \text{ mA}$	4	-	1.95	-	GHz
Collector-emitter Capacitance	C_{CE}	$V_{CE} = 5 \text{ V}, f = 1 \text{ MHz}$	5	-	340	-	pF
Collector-substrate Capacitance	C_{CS}	$V_{CS} = 5 \text{ V}, f = 1 \text{ MHz}$	5	-	740	-	pF
Emitter-emitter Capacitance	C_{EE}	$V_{EE} = 5 \text{ V}, f = 1 \text{ MHz}$	5	-	5	-	pF
Voltage Gain	A	$V_{CE} = 5 \text{ V}, f = 10 \text{ MHz}, R_{\theta} = 1 \text{ k}\Omega, I_C = 1 \text{ mA}$	6, 18	-	20	-	dB
Power Gain	G_p	Constant Collector current $f = 100 \text{ MHz}, V^* = 12 \text{ V}$	10, 20	27	30	-	dB
Noise Figure	NF	$I_C = 1 \text{ mA}$	19, 20	-	3.3	-	dB
Input Resistance	Z_{i1}	Common emitter	18	-	400	-	Ω
Output Resistance	Z_{o2}	Common emitter	12	-	4.8	-	Ω
Input Capacitance	C_{i1}	$V_{CE} = 5 \text{ V}$	10	-	3.1	-	pF
Output Capacitance	C_{o2}	$I_C = 1 \text{ mA}$	13	-	7	-	pF
Magnitude of Forward Transmittance	$ T_{21} $	$f = 100 \text{ MHz}$	14, 15	-	24	-	dB

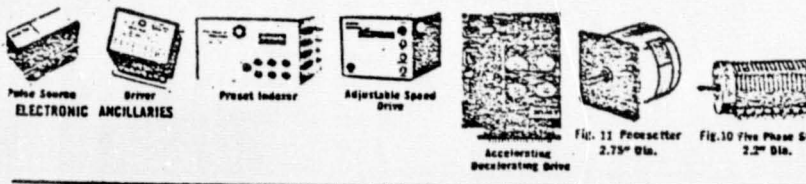
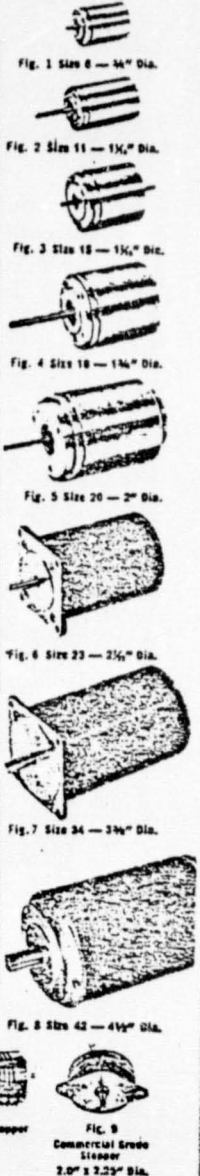


INCREASE PRODUCT RELIABILITY — REDUCE COSTS!

Choose Steppers and Controls from the broad, flexible line of Rapsidsyn Company, and be assured of top quality at prices you can live with. Check our widest range of step angles in 2, 3, 4 and 5 phase units — all designed to operate from a wide variety of solid state logics which are stock items. Also available, RAPID SYN Synchronous 72, 200, 300, 450 and 600 RPM motors. You'll like our service on your special requirements.

RAPID-SYN STEPPERS... RATINGS AND CHARACTERISTICS*

Step Angle	Size	*Model Number	Type	Res./p (Ohms)	Rated Voltage (VDC)	Static Stall Torque (Oz. In.)	Defeat Torque (Oz. In.)	Dynamic Torque (Oz. In.)	Response (PPS)	Induct. mh	Motor Inertia (gm. cm. ²)	Weight (Oz.)	Length Max. (In.)	FIG. No.
1.8°	23	23F-160	VR/5p	0.4	2.0	50	0	25	2000	1.00	350	66	4.938	10
	23	23D-6102	PM/4p	5.1	5.1	53	5	35	700	6.80	87	20	2.0	6
	23	23D-6108	PM/4p	0.63	1.3	53	5	35	1100	.88	87	20	2.0	6
	23	23D-6204	PM/4p	2.6	4.3	100	8	65	900	6.30	200	32	3.25	6
	23	23D-6209	PM/4p	0.37	1.7	100	8	65	1350	.80	200	32	3.25	6
	23	23D-6306	PM/4p	1.16	3.4	150	10	100	1050	3.90	320	44	4.0	6
	23	23D-6309	PM/4p	0.48	2.2	150	10	100	1150	1.43	320	44	4.0	6
	23	23M-07	PM/4p	80	28	30.0	1.0	20.0	700	73.00	30.0	17.0	2.000	6
	23	23M-05	PM/4p	1	6	30.0	1.0	20.0	1000	5.10	30.0	17.0	2.000	6
	23	23M-501	PM/4p	5	6	60.0	2.0	40.0	450	4.5	120.0	20.0	2.250	6
	23	23M-502	PM/4p	20	12	60.0	2.0	40.0	425	16.30	120.0	20.0	2.250	6
	23	23M-503	PM/4p	80	24	60.0	2.0	40.0	425	66.50	120.0	20.0	2.250	6
	23	23M-700	PM/4p	3	6	90.0	4.0	65.0	480	11.50	200.0	30.0	3.250	6
	34	34D-9106	PM/4p	0.95	2.9	150	5	110	750	3.8	643	5.2	2.45	7
	34	34D-9109	PM/4p	0.39	1.8	150	5	115	875	1.83	643	5.2	2.45	7
	34	34D-9209	PM/4p	0.55	2.9	300	10	200	750	2.71	1200	88	5.31	7
	34	34D-9311	PM/4p	0.52	2.8	450	15	300	650	1.90	1850	124	5.31	7
	34	34D-9314	PM/4p	0.31	2.2	450	15	300	750	1.0	1850	124	5.31	7
	34	34H-02	PM/4p	0.50	2	125.0	4.0	90.0	1100	1.76	375.0	45.0	2.500	7
	34	34H-501	PM/4p	20	14	140.0	6.0	100.0	500	65.00	550.0	50.0	2.437	7
	34	34H-507	PM/4p	150	35	140.0	6.0	100.0	500	1.25	550.0	50.0	2.437	7
	34	34H-508	PM/4p	10	8	140.0	6.0	100.0	500	27.00	550.0	50.0	2.437	7
	34	34H-509	PM/4p	4.50	5.5	140.0	6.0	100.0	500	20.00	550.0	50.0	2.437	7
	34	34H-510	PM/4p	0.50	2.0	140.0	6.0	100.0	550	1.50	550.0	50.0	2.437	7
34	34H-700	PM/4p	0.70	3.0	280.0	10.0	200.0	800	4.00	1100.0	76.0	3.687	7	
34	34H-901	PM/4p	1.1	4.5	500.0	15.0	250.0	600	6.13	1800.0	150.0	5.312	7	
42	42D-111-112	PM/4p	.37	2.3	625	15	425	500	2.4	3900	125	4.74	8	
42	42D-112-112	PM/4p	.60	3.6	1125	30	840	300	5.3	8150	232	6.99	8	
42	42D-113-1	PM/4p	.4	3V	1392	81	1104	475	2.8	11.996	352	9.60	8	
2.25°	23	23F-215	VR/5p	0.4	2.0	50	0	25	2000	1.76	350	66	4.938	10
5°	23	23M-300	PM/4p	4.4	6	45.0	8.0	30.0	350	5.80	120.0	30.0	3.25	6
	23	23V-300	VR/4p	3.0	6	40.0	0	22.0	420	7.50	120.0	30.0	3.25	6
	34	34M-300	PM/4p	0.75	3	90.0	7	60.0	400	3.4	1200.0	75.0	3.687	7
7.5°	11	11RS-01	VR/4p	100	28	2.3	0	1.20	750	45.00	2.5	5.0	1.400	2
	15	15RS-03	VR/4p	55	28	8.0	0	5.0	1100	47.0	3.0	6.5	1.500	3
	20	20RS-01	VR/4p	20.0	28	30.0	0	10.0	700	47.0	10.0	20.0	2.500	5
	23	23PS-01A	PM/4p	70.0	28	13	1.2	8	425	66.5	30	8	1.062	9
	28	28PS-05-24	PM/4p	175	24	18.5	3.0	12.5	140	160.0	93	24	2.25	11
15°	8	08R-01	VR/4p	100	28	1.0	0	0.6	1400	65.0	0.18	1.8	1.000	1
	8	08V-01	VR/3p	60	28	1.3	0	0.50	1100	30.0	0.18	1.8	1.000	1
	11	11R-01	VR/4p	55	28	5.8	0	3.25	1040	45.0	1.0	4.7	1.625	2
	11	11V-01	VR/3p	80	28	2.75	0	1.75	630	56.0	1.0	4.7	1.625	2
	15	15R-01	VR/4p	35	28	8.0	0	4.50	1170	60.00	0.7	6.5	1.500	3
	15	15V-01	VR/3p	16	28	5.8	0	2.25	1000	14.0	0.6	6.5	1.500	3
	18	18R-01	VR/4p	55	28	11.5	0	8.0	670	140.0	5.0	13.0	1.875	4
	20	20R-03	VR/4p	35	28	18.0	0	6.6	525	75.0	3.5	20.0	2.500	5
	20	20R-07	VR/4p	20	28	38.0	0	25.0	400	51.0	10.0	20.0	2.500	5
	20	20R-17	VR/4p	10	28	40.0	0	30.0	700	24.0	10.0	20.0	2.500	5
	20	20V-01	VR/3p	10	28	50.0	0	13.8	475	30.0	10.0	20.0	2.500	5
	20	20V-03	VR/3p	20	28	40.0	0	10.0	400	54.0	10.0	20.0	2.500	5
	28	28RF-06-24	PM/4p	175	24	17.5	1.5	12.0	130	260.0	93	24	2.25	11
	45°	8	08M-01	PM/4p	65	28	1.0	0.10	0.35	700	25.0	0.2	1.75	1.000
11		11M-01	PM/4p	45	28	2.5	0.20	1.50	425	14.0	1.2	4.5	1.625	2
15		15M-01	PM/4p	30	28	8.1	0.30	4.80	300	17.9	5.0	10.0	2.100	3
18		18M-01	PM/4p	40	28	6.0	0.25	3.5	350	14.0	4.0	13.0	1.875	4
20		20M-01	PM/4p	12	28	15.0	0.40	8.7	200	13.0	15.0	26.0	2.500	5
30°	8	08P-02	PM/4p	100	28	0.8	0.10	0.25	350	18.0	0.3	1.75	1.000	1
	11	11P-01	PM/4p	60	28	2.5	0.20	1.10	240	22.0	1.2	4.3	1.625	2
	15	15P-03	PM/4p	20	28	11.0	0.30	7.0	175	14.1	5.0	10.0	2.100	3
	18	18P-01	PM/4p	20	28	8.0	0.25	6.0	260	20.0	4.0	13.0	1.875	4
	20	20P-03	PM/4p	12	28	20.0	0.40	9.0	180	13.0	10.0	20.0	2.500	5



DANA INDUSTRIAL
 Rapidsyn Company
 Dept. EM, 11901 Burke Street
 Santa Fe Springs, Calif. 90670
 Tel. (213) 698-2595 Telex: 69-6352

SIGMA

MOTION CONTROL DIVISION
BRAINTRUST, MASSACHUSETTS 01907 (617) 843-5000

STEPPING MOTORS

200 STEPS/REVOLUTION (1.8°/STEP) ±3% ACCURACY MOTORS • FOR USE WITH LOW COST UNIPOLAR DRIVERS



UNIPOLAR RESISTANCE LIMITED (R/L) DRIVE CARDS



The Motion Control Division of Sigma Instruments, Inc. introduced its first patented stepping motor, the Cyclonome®, in 1952. It was an invention ahead of its time, and the beginning for what, today, has become the broadest line in the industry. Therefore, these specifications represent the tip of the iceberg, and serve as an indication of the wide range of stepping motor systems Sigma can provide. If what you need is not described here, our Sales Department will be pleased to provide more information.

Typical Torque, oz-in		Max. Speed sps	Unipolar amp/phase	Motor Dia. x Length inches	Sigma Model No.
50 sps	500 sps				
22	20	1,500	1.5	2.2 x 1.5	20-22150200E1.5
48	30	825	0.9	2.2 x 2.0	20-22200200E5.1
120	15	600	1.5	2.2 x 3.5	20-22350200E3.7
115	80	900	3.4	3.4 x 2.4	20-34240200E05
265	150	600	4.0	3.4 x 3.7	20-34370200E075
300	—	450	3.5	3.4 x 5.0	20-34500200E1.2

Data indicates typical performance on 24 VDC unipolar R/L drive.

UNIPOLAR RESISTANCE LIMITED (R/L) DRIVE CARD

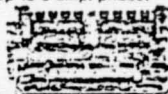
For general applications where high speed/torque requirements are not demanding, the unipolar R/L drive card offers an uncomplicated, low cost solution.

200 STEPS/REVOLUTION (1.8°/STEP) ±3% ACCURACY HIGH PERFORMANCE, HIGH SPEED MOTORS • FOR USE WITH BIPOLAR CHOPPER DRIVERS



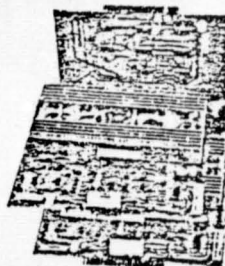
BIPOLAR CHOPPER DRIVES CARDS AND DRIVE SYSTEMS

SINGLE CARD BIPOLAR CHOPPER*
This is a simple, economical, space-saving package because all the electronics — logic with half- and full-step capability; both phase drivers — are on one card. The single card bipolar chopper delivers up to 5 amp/phase.



Typical Torque, oz-in		Max. Speed sps	Bipolar amp/phase	Motor Dia. x Length inches	Sigma Model No.
50 sps	1,000 sps				
165	150	10,000	4.5	3.4 x 2.4	21-34240200B025
420	300	15,000	10.0	3.4 x 3.7	21-34370200B009
600	510	15,000	10.0	3.4 x 5.0	21-34500200B015
1,000	800	10,000	10.0	4.2 x 7.0	21-42700200F03
1,500	900	10,000	10.0	4.2 x 8.8	21-42880200F03

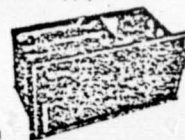
Data indicates typical performance on Sigma patented bipolar chopper drive.



3-CARD BIPOLAR CHOPPER* SET
Three-card set delivers up to 10 amp/phase. Half- and full-step logic card, and two drive cards offer flexibility for users preferring to provide the power supply.

BIPOLAR CHOPPER DRIVE* WITH POWER SUPPLY

For those who prefer one compact package, the stepping motor driver incorporates the 3-card bipolar chopper (delivering 10 amp/phase) and appropriate power supply.



*Patented

APPENDIX C

APPENDIX C
LASER DIODE POWER SUPPLY

Laser diode

Laser Diode Laboratory, Inc.
Metuchen, New Jersey 08840
(201) 549-7700

Model #	LD-167/0.04% duty factor
peak power	100-105 watts
number of diodes	5
emitting area	16 x 16 mils
peak forward current	75 amps
duty factor	.04% (selected)
wavelength	904 nm
spectral width	3.5 nm
rise time	0.5 ms
max. pulse width	200 ns
max. operating temp.	75°C
package type	LDL-8
beam spread	50% 17°
	100% 19°
price	\$175.00

Pulser

Power Technology, Inc.
Mablevale, Arkansas 72204
(501) 568-1995

Model #	IL75C
pulse current	40-80 amps
pulse width	30-200 nsec
rise time	8-24 nsec
fall time	10-28 nsec
pulse rate (max.)	10 KHz
current input a	300 ma
input voltage	26-70 volts
size	1 1/4 x 2 1/2
price	\$1,250.00

Slip Rings

CAY110 Capsule Slip Ring
Airflyte Electronics Company
New Hook Road
Bayonne, New Jersey 07002
(201) 436-2230

Mechanical

- | | |
|-------------|---------------------------|
| 1. rings | gold alloy, 24 |
| 2. brushes | gold alloy spring tapered |
| 3. speed | 500 rpm |
| 4. lifetime | 10 ⁸ revoluts. |
| 5. rotation | bi directional |

Electrical

- | | |
|---------------|-----------|
| 1. current | 1 amp |
| 2. voltage | 150 VDC |
| 3. resistance | 5 million |
| 4. 24 rings | |

Signals

- | | |
|----------|-----------------------------|
| 1 | laser fire |
| 1 | mirror motor drive |
| 1 | elevation encoder CW pulse |
| 1 | elevation encoder zero ref. |
| <u>8</u> | detector output |
| 12 | |



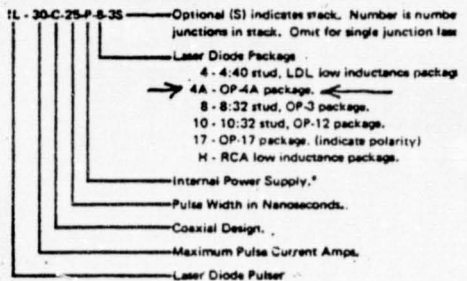
Power Technology Incorporated

Address correspondence to: Box 4403 Little Rock, Arkansas 72204
 Plant location: 7925 Mabelvale Cutoff Mabelvale, Arkansas 72103 501-568-11

ILC SERIES Laser Diode Pulsers



ORDERING INFORMATION



*Add X to internal power supply models if temperature compensation is to be omitted.

Note: All standard models are for use with diodes having cathode (neg.) connected to case and stud except OP-17, and H package which are reverse polarity. All models available with reverse-polarity on special order.

	IL1C-IL9C	IL10C	IL20C	IL25C	IL30C	IL40C	IL60C	IL75C	IL100C	
Minimum range of pulse current adjustment	1-9 (1)	6-11	11-22	14-27.5	16-33	22-44	33-66	41-82.5	55-110	Amps
Range of pulse width available	7-500	7-500	10-200	10-200	10-200	15-200	20-200	30-200	40-200	ns
Typical rise time 7-50ns P.W.	2	2	3	4	4	5	5	8	10	ns
Typical rise time 51-200ns P.W.	12	14	16	18	18	20	22	24	26	ns
Typical fall time 7-50ns P.W.	2	3	5	6	6	7	8	10	12	ns
Typical fall time 51-200ns P.W.	14	16	18	20	20	22	26	28	30	ns
Maximum pulse rate, external P.S. (2) (6) (7)	100-1000	100	100	100	100	75	50	40	30	k PPS
Maximum pulse rate, internal P.S. (2) (7)	50	40	30	20	20	20	15	10	10	k PPS
Maximum pulse rate, internal clock (2) (3)	20	20	20	20	20	20	20	20	8	k PPS
Current required at 24V for 0 PPS	20	20	20	20	20	20	20	20	20	mA
Current required at 100ns and 24V for 10k PPS	35	40	75	100	150	200	300	-	-	mA
Minimum supply voltage for 10k PPS at 100ns (4)	14	14	18	18	20	24	24	-	-	volts
Voltage required from external power supply (5)	4-30	6-30	10-40	15-50	15-50	20-55	20-60	26-70	30-80	volts
Size:										
Internal power supply	1x4"				1x4"	1½x4"	1½x4"	1½x4"	1½x4"	inches
External power supply	1x2"				1x2"	1½x2"	1½x2"	1½x2"	1½x2"	inches

- 1) 40% to 110% of any specified current between 1 and 9 amps.
- 2) May exceed maximum duty factor of commercially available diodes. Consult diode manufacturer's specification sheet before operating.
- 3) Rate specified is for 50ns pulse width. For 100ns divide by 2, for 200ns divide by 4. Pulse rate limited to help prevent damage to laser diode.
- 4) 2k PPS at 200ns on IL100C only.
- 5) Range of regulated voltage required from external power supply. Maximum current will not exceed 250mA at maximum pulse rate and maximum pulse width. Most applications require less than 25mA. (External power supply models only)
- 6) Requires external clock for high rates.

ORIGINAL PAGE IS
OF POOR QUALITY



Power Technology Incorporated

Address correspondence to: Box 4403 Little Rock, Arkansas 72204
Plant location: 7925 Mabelvale Cutoff Mabelvale, Arkansas 72103

Specifications Applicable to all Mode

Pulse Voltage - Suitable for one diode, 2 to 6 diode stacks on special order.

Pulse Current Stability - $\pm 1/2\%$ for $\pm 10\%$ battery voltage variation.

Pulse Current Metering - 50 ohm coax connector. Amphenol 27-9

0.1 volt per 1.0A for nominal pulse currents of one through 9 amps.

0.1 volt per 10A for nominal pulse currents of 10 through 40 amps.

0.1 volt per 20A for nominal pulse currents of 41 through 100 amps.

Metering jack must be terminated in 50 ohm non-inductive resistor for correct pulse current reading. 51 ohm 5% composition resistor is generally suitable. Termination is necessary only while metering.

Temperature Compensation - Pulse current is reduced by approximately 10% for each 25°C. below 27°C.

Internal Clock Stability - $\pm 2\%$

Internal Clock Programming - Internal clock enabled by a jumper, clock rate set by one external resistor or potentiometer.

Internal Clock Limitations - Operation with battery voltage less than 9 volts may be unsatisfactory. Internal clock requires separate 9 to 28 volt clock power supply on pulsers designed for external power supply.

External Triggering - Terminals are provided. May be trig-

gered by TTL circuitry. Approximately 3 volt pulse 500 ohm required. Rise time should be less than 1us.

Sync. Output - Use External Trigger Leads. Isolate ^{Pulse width} 1K min.

Operating Voltage Range of Internal Power Supply - 6- at low pulse rates, 14-24V at maximum pulse rates, 9V inum for operation with internal clock.

Variable Pulse Width - Available as option. Consult fact

Controls - Pulse current adjust potentiometer located adjacent to connector.

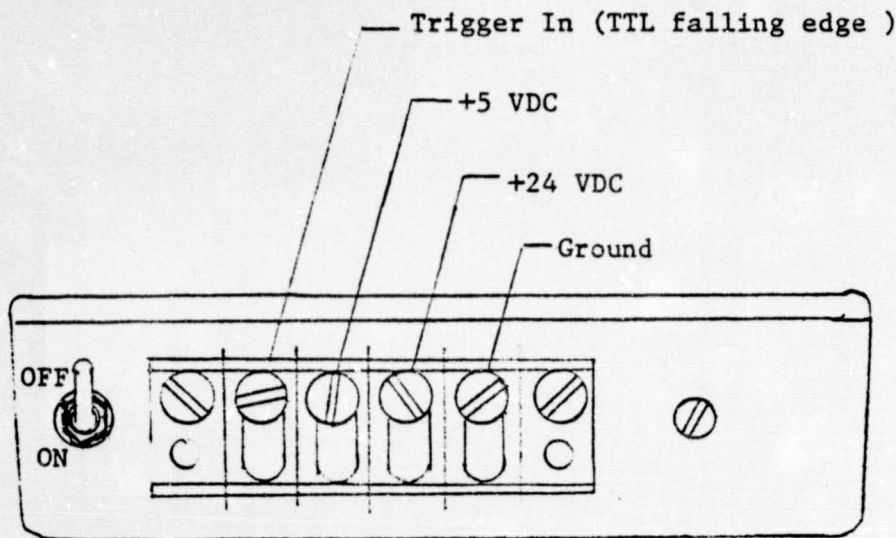
Connectors - Power connector located on end opp diode. Mating connector provided for power. Pulse cur metering, Amphenol 27-9, located adjacent to p connector.

Weight - 1" x 2 1/4" - 75 gr., 1" x 4 1/2" - 95 gr., 1 1/4" x 2 100 gr., 1 1/4" x 4 1/2" - 125 gr.

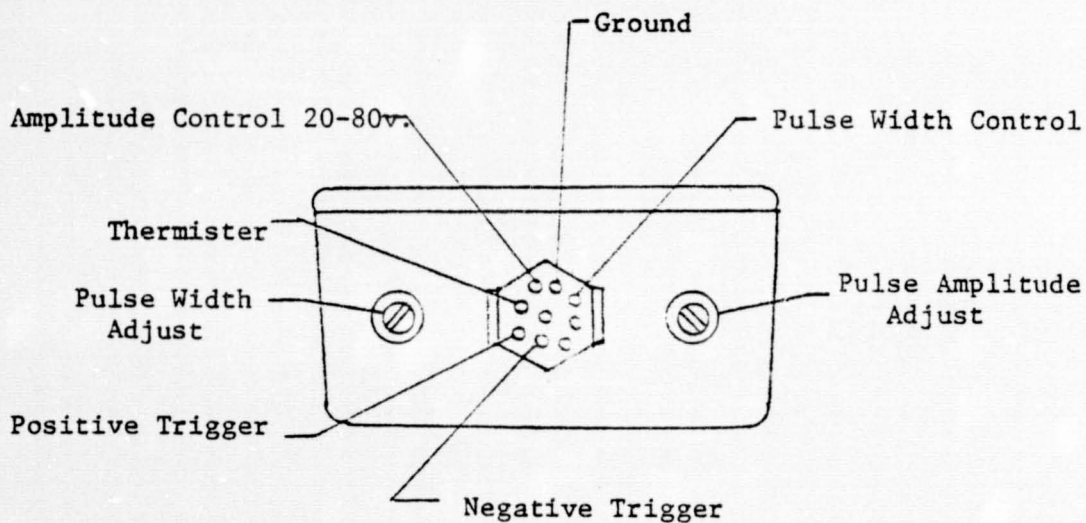
WARNING - PERSONAL SAFETY PRECAUTIONS

Laser Radiation - Diode lasers in operation emit invisible infrared radiation which may be harmful to the human eye. Appropriate safety precautions must be taken to avoid the possibility of eye damage.

Electrical Shock - Operating voltages applied to some of these products present a shock hazard. Appropriate precautions should be taken.

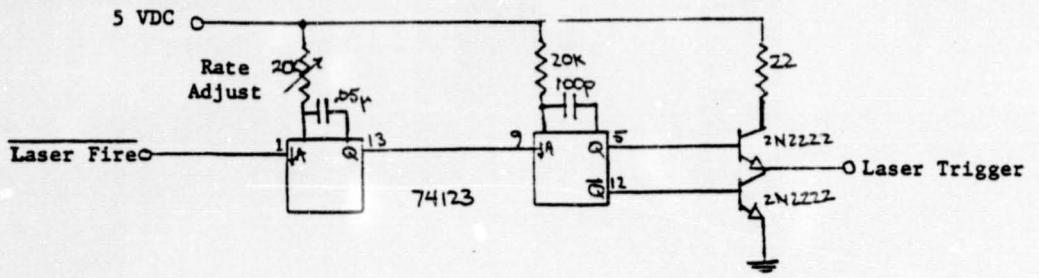


Power Supply Inputs

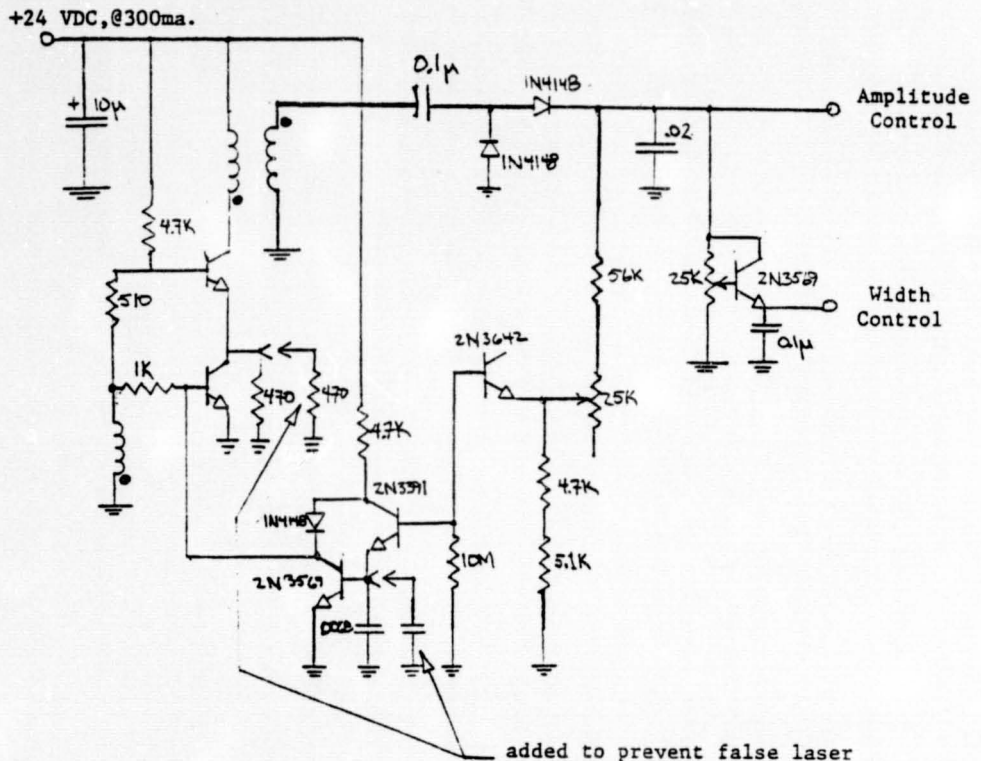


Power Supply Outputs

LASER POWER SUPPLY

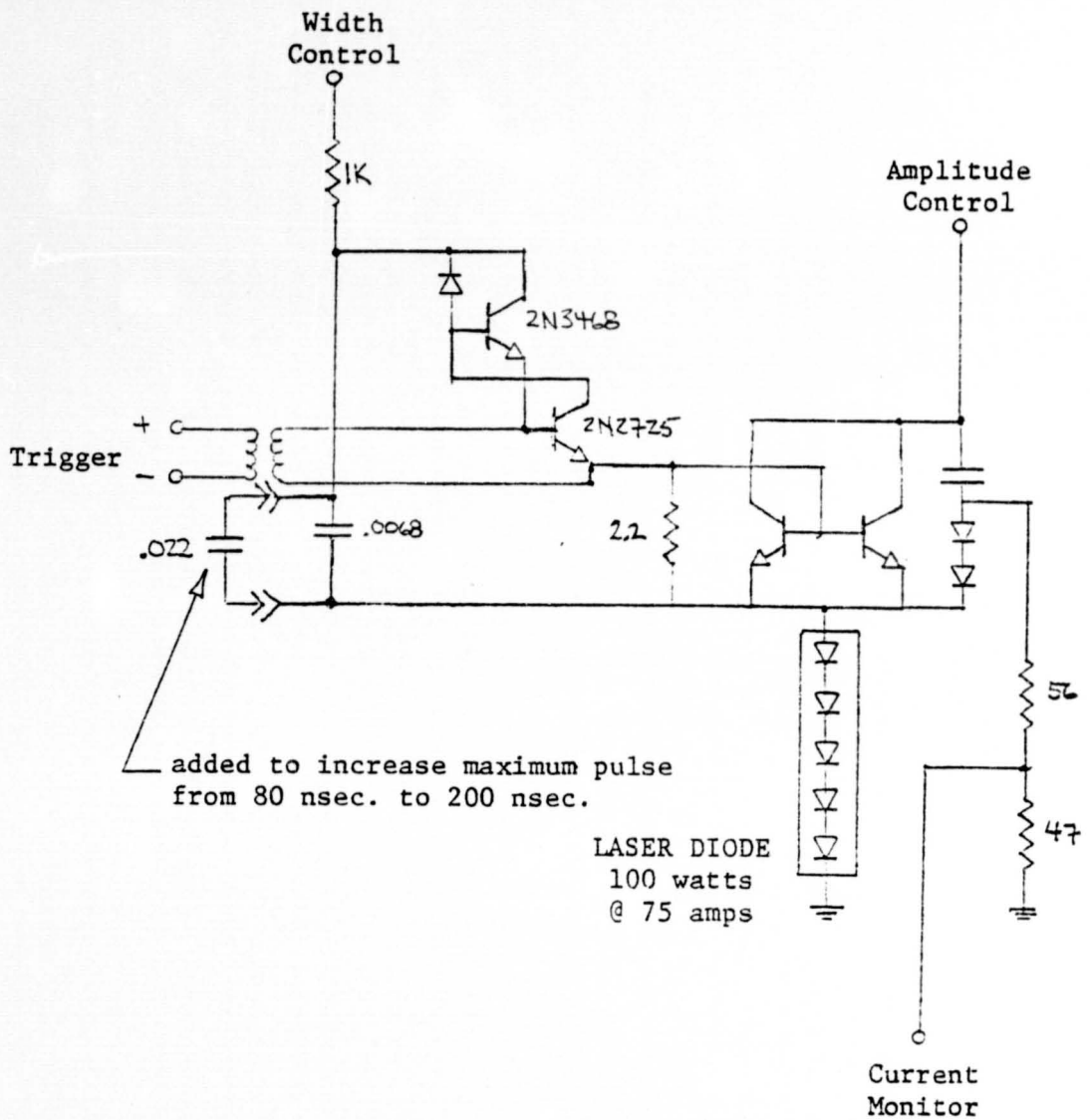


1. Limits laser firing rate
2. Produces 500nsec. laser trigger pulse



added to prevent false laser triggering caused by large ripple at output

LASER POWER SUPPLY CIRCUIT



CIRCUIT WITHIN PULSER HEAD